# Investigation of the Amyloid Properties of Winter Flounder Antifreeze Protein (AFP6) and the Application of Aqueous Curcumin in the Detection of this Protein

by

Dane Carlyle Sands

Submitted in partial fulfilment of the requirements
for the degree of Master of Science

at

Dalhousie University
Halifax, Nova Scotia
March 2020

**TABLE OF CONTENTS**

# LIST OF TABLES

## LIST OF FIGURES

# ABSTRACT

A *Pseudopleuronectes americanus* antifreeze protein, AFP6, has previously been shown to form amyloid upon specific interaction with an ice surface. In this work, an *in situ* real-time assay for amyloid formation by amyloid beta was implemented in order to evaluate potential cross-seeding of amyloid formation by synthetic AFP6. However, insufficient AFP6 amyloid was produced to continue with the assay. Through this work, AFP6 was found to be easily separated from other proteins due to its solubility in acetone. Furthermore, although AFP6 is undetectable using common positive protein stains, aqueous curcumin allowed fluorescence-based detection of AFP6. The absorbance and fluorescence spectra of curcumin are both altered in the presence of AFP6, with more marked changes following 70 °C incubation. However, the melting point and secondary structure of AFP6 determined by circular dichroism were unchanged by curcumin. Thus, single-reagent methods for purifying and detecting this unusual protein were found to be effective.

# LIST OF ABBREVIATIONS AND SYMBOLS USED

| | |
|---|---|
| aβ | amyloid beta |
| AFGP | antifreeze glycoprotein |
| AFP | antifreeze protein |
| Asx | aspartic acid or asparagine |
| C | Celsius |
| Da | Dalton |
| DEAE | diethylaminoethyl |
| EGCG | (−)-epigallocatechin-3-gallate |
| HPLC | high performance liquid chromatography |
| IBPs | ice binding proteins |
| INP | ice nucleating protein |
| PAGE | polyacrylamide gel electrophoresis |
| RFU | relative fluorescence unit |
| RT | room temperature |
| SDS | sodium dodecyl sulphate |
| TEM | transmission electron microscopy |
| ThT | Thioflavin T |
| UV | ultraviolet |
| X | any amino acid |

## ACKNOWLEDGEMNTS

I would firstly like to thank my supervisor Dr. Vanya Ewart. I could not have wished for a more thorough, patient, and supportive, supervisor. Dr. Ewart's optimism and love for her work is outstanding and made working in her lab a true joy. Thank you Dr. Ewart for accepting me into your lab and guiding me through these years.

I would also like to thank my supervisory committee: Dr. Barbara Karten and Dr. Paul Liu. Your advice throughout the program was invaluable and helped me become a better scientist.

Thank you to all the previous and current members of the Ewart lab, you were a pleasure to work with and I'm sure you'll all go on to do great things. I am particularly grateful to undergraduate students Melissa Carsky and Erin Donovan, who worked with me to produce data, as shown in this thesis.

Thank you to the lab groups in the Biochemistry and Molecular Biology department, as well as many other labs in the Tupper, who were so forthcoming in letting me use their equipment or borrow reagents. I would especially like to thank the Bedard lab, the Karten lab and the Waisman lab, and I am grateful to Mary-Ann Trevors, Victoria Miller, Joyce Chew, and Jeff Simmons for their generous training in the use of specialized lab equipment. Thank you also to all the labs who donated dry ice to the Ewart lab.

Finally, I would like to thank my family and friends. This was possible because of your support.

# CHAPTER 1: INTRODUCTION

The world's oceans cover approximately 71% of the earth's surface. Approximately 90% of that water is below 5 ºC (De Maayer, Anderson, Cary, & Cowan, 2014; Dubé, Leggiadro, & Ewart, 2016). Many terrestrial regions of the world also reach temperatures below the freezing point during winter months (Rodrigues & Tiedje, 2008). In the cells of living organisms, cold stress can have effects on enzymatic reactions, gene expression, protein folding, and metabolism (De Maayer et al., 2014). At temperatures below the freezing point, ice may form which can cause cellular dehydration and, in some cases, pierce membranes leading to cell death (Bredow, Vanderbeld, & Walker, 2016). Despite the danger that cold temperatures bring, many species have adapted and survive under these conditions.

## 1.1 Ice Binding Proteins

In the 1950's, researchers noticed that fish at temperatures below their freezing points in marine (salt) water avoided freezing (Scholander, Flagg, Walters, & Irving, 1953; Yeh & Feeney, 1996). Further work showed that the fish avoided freezing as a result of proteins that non-colligatively lowered the freezing point of the blood plasma, and these proteins were named antifreeze proteins (AFPs) (DeVries & Wohlschlag, 1969). Further investigation showed that AFPs were not limited to Antarctic species, but could also be found in north Atlantic fishes (Duman & Devries, 1974). The discovered AFPs inhibited the growth of ice within the organisms that had them. Further research has shown that not all proteins that bind to ice play the role of inhibiting ice growth, leading to the more general term ice-binding proteins (IBPs) to describe the greater variety of proteins including AFP and others. Following their first discovery in fish, IBPs

were identified in insects, plants, bacteria and fungi (Bar-Dolev, Celik, Wettlaufer, Davies, & Braslavsky, 2012). The IBPs of different species differ drastically in structure, but all share an ice-binding role.

### 1.1.1 Ice Binding Protein Mechanism

IBPs are defined by their ability to bind to ice. The best-known IBPs are the AFPs, which inhibit ice crystal growth by adsorption to the ice surface. As AFPs bind to ice, the ice front must grow between the proteins, starting from a flat surface and eventually growing into a convex curve. Growth of ice on the highly curved front is not as energetically favourable as it would be with less curvature or a flat surface, thus arresting ice crystal growth within a certain temperature interval. This results in a substantial non-colligative depression of the freezing point from the equilibrium freezing point, causing a freezing point depression (Knight, Cheng, & DeVries, 1991). In addition, bound AFPs also slightly elevate the melting point of ice crystals (Celik et al., 2010). As shown in Figure 1, the difference between the elevated melting point and depressed freezing point is known as thermal hysteresis (Davies, 2014). Ice crystals with bound AFPs will not grow until the temperature is lowered below the thermal hysteresis temperature interval. If the temperature drops below the AFP-lowered freezing point the effect of AFPs will be overcome and the ice front will burst through the gaps between the proteins, eventually growing over them (Davies, 2014). Research suggests that the adsorption of IBPs to ice is irreversible (Meister, DeVries, Bakker, & Drori, 2018; Pertaya et al., 2007) and covering of the bound AFPs by growing ice suggests why this may be.

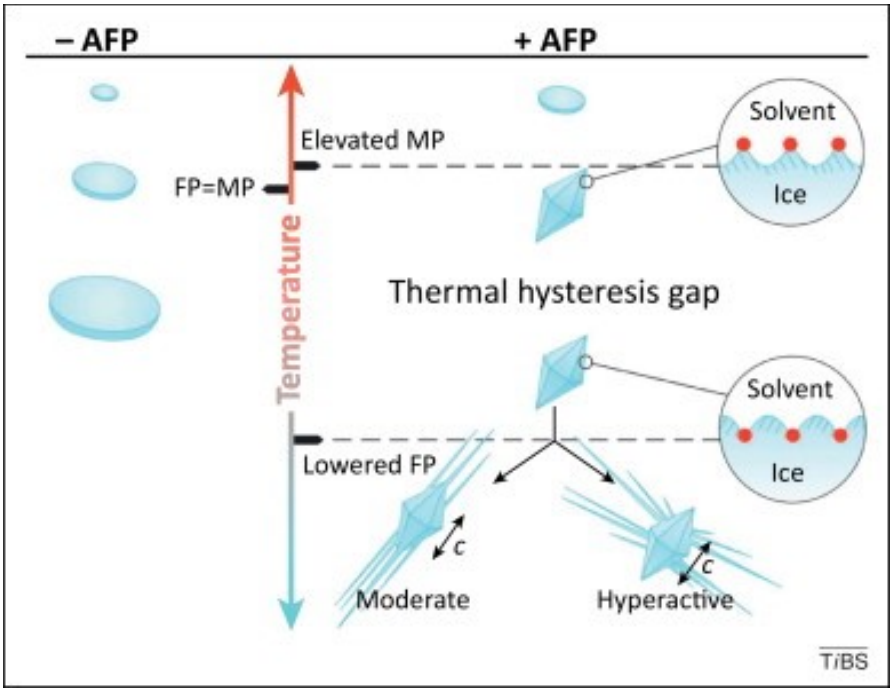


Figure 1: Ice growth in the absence and presence of antifreeze proteins as temperature decreases. Left: In the absence of antifreeze proteins, the melting point is equal to the melting point and ice continually grows as a flat disk as temperature drops. Right: Antifreeze proteins bind along the ice surface, inhibiting ice growth through elevating the melting point while depressing the freezing point. This separation is known as the thermal hysteresis gap. If the temperature drops below the depressed freezing point, the ice will overcome the inhibition effect of the protein and burst out in the form of spicules. (Image from Davies, 2014).

While the first IBPs identified were mainly AFPs, the IBPs are known to be more diverse, with a variety of functions. While the majority of known IBPs are AFPs that inhibit ice growth, others have additional or separate functions including inhibition of recrystallisation, initiation of ice nucleation, ice structuring and adhesion to ice surfaces (Griffith & Yaish, 2004; Guo, Garnham, Whitney, Graham, & Davies, 2012; Gupta & Deswal, 2014; Lindow, Arny, & Upper, 1982; Raymond, Fritsen, & Shen, 2007; Raymond, Janech, & Fritsen, 2009; Yu et al., 2010). This work will focus specifically on the AFPs.

### 1.1.2 Types of Ice Binding Proteins

Type 1 AFPs were first discovered in in winter flounder (*Pseudopleuronectes americanus*) caught of the coast of Nova Scotia (Duman & Devries, 1974). Since that time, they have been discovered in several other species, such as the shortfin sculpin and the Atlantic snailfish among others, but the type 1 AFPs of the winter flounder are the best understood to date (Fletcher, Hew, & Davies, 2001).

Most type I AFP proteins are relatively small, ranging in size from approximately 3-4 kDa, alpha helical, and having a high percentage of alanine residues (Patel & Graether, 2010). These proteins have a repeated sequence motif represented by T-A-A-X-A-X-X-A-A-X-X (in which T refers to Thr, A is most often Ala, and X is any amino acid residue) is also found to occur periodically within the sequences of type I AFPs and mutation based studies have implied that the threonine methyl group along with alanine groups are important for ice binding activity (Patel & Graether, 2010). The most studied

type 1 AFP is the winter flounder liver antifreeze protein 6 (AFP6) will be discussed in depth later in this work.

Recently a “hyperactive” type I AFP has been found in some right eyed flounders. The term “hyperactive” in this context simply means it exhibits a far greater thermal hysteresis. This hyperactive type I AFP exhibits 10-fold greater thermal hysteresis on a molar concentration basis than the more typical shorter type 1 AFPs at equivalent concentrations (Marshall, Chakrabartty, & Davies, 2005). This novel AFP, termed “Maxi”, was found to be a dimer of two alpha helical monomers arranged antiparallel that overlap to give a four helix bundle. (Sun, Lin, Campbell, Allingham, & Davies, 2014). Maxi is much larger than other type I AFPs with a size of approximately 16.7 kDa and its sequence is primarily in the form of repeats of T/I-X-X-X-A-X-X-X-A-X-X, where X is any amino acid (Sun et al., 2014).

The type II AFPs are the largest known AFPs, from about 14-24 kDa and can be found in several species, including Atlantic herring (*Clupea harengus*), Japanese smelt (*Hypomesus nipponensis*), and sea raven (*Hemitripterus americanus*) (Liu et al., 2007; Yamashita et al., 2003). This class of AFPs are cystine and disulfide bond-rich, being homologous to C-type lectins (Gronwald et al., 1998). Type II AFPs can be further differentiated into two subclasses, $Ca^{2+}$ dependent type II AFPs such as those found in herring and that found in sea raven that do not bind $Ca^{2+}$ (Liu et al., 2007).

Type III AFPs tend to be moderately sized when compared to the prior two classes of fish proteins with an average size around 7 kDa. These proteins are produced by eelpouts, including the ocean pout (*Marcrozoarces americanus*), Atlantic wolffish (*Anarhichas lupus*) and several Antarctic species. The proteins exhibit beta sandwich

motifs with alpha helical turns and are homologous to the C-terminus of mammalian sialic acid synthase (Baardsnes & Davies, 2001; Bar Dolev, Braslavsky, & Davies, 2016; Venketesh & Dayananda, 2008; Yeh & Feeney, 1996). Type III AFPs ice-binding surface is believed to be flat, and binding is thought to involve both polar and apolar groups. (Antson et al., 2001; Siemer & McDermott, 2008)

The type IV AFPs were discovered in the longhorn sculpin (*Myoxocephalus octodecimspinosis*) (Deng, Andrews, & Laursen, 1997). The protein, termed SL-1, had a thermal hysteresis similar to type 1 AFPs at equal molar concentration (Deng et al., 1997). It was found to be roughly 12.3 kDa, glutamine-rich, and highly alpha helical (Zhao, Deng, Lui, & Laursen, 1998). The protein was characterized as a four-helix bundle, and had a primary structure similarity to several apolipoproteins (Gauthier et al., 2008). Type IV AFPs were made even more interesting by the discovery that sequence homologs were found in warm water fish that shouldn't require AFPs (Gauthier et al., 2008; Lee et al., 2011). Further studies have noted that the protein is involved in embryogenesis, leading some to suggest that the protein could have had multiple functions throughout evolution (Gauthier et al., 2008; Liu, Zhai, & Gui, 2009; Mao et al., 2018; Xiao et al., 2014).

Antifreeze (glyco)proteins were the first IBPs to be discovered, and are found in Antarctic fishes (Devries, 1971). They were found after the realization that the freezing point depression in some fish plasma was too large to be from salt concentrations alone (Devries, 1971). There are 8 types of AFGPs identified thus far and they rang from 2.2 in type 1 AFGPs to 36 kDa in type 8 (Feeney, 1974; Harding, Anderberg, & Haymet, 2003). All types however share the same basic trait of a repeating unit of (Ala-Ala-Thr),

with the sugar β-d-galactosyl-(1→3)-α-N-acetyl-d-galactosamine bound to the threonine's hydroxyl group, though in some larger AFGPs the first alanine is sometimes replaced by a proline (Devries, 1971; DeVries, Vandenheede, & Feeney, 1971; Geoghegan, Osuga, Ahmed, Yeh, & Feeney, 1980; Hew, Slaughter, Fletcher, & Joshi, 1981). While the thermal hysteresis values for AFGPs are similar to those of AFP type I proteins, their structures are vary depending on their size and the temperature (Urbańczyk, Góra, Latajka, & Sewald, 2017).

Ice binding proteins have also been found in many other organisms, including plants, bacteria, fungi, and arthropods. These non-fish AFPs commonly have a beta solenoid like-fold, with some differences in structure, but ice binding sites differ throughout (Graether et al., 2000; Hakim et al., 2013; Hanada, Nishimiya, Miura, Tsuda, & Kondo, 2014; Kondo et al., 2012; Middleton et al., 2012). Many of these proteins, like those of insects, are hyperactive antifreeze proteins, as terrestrial insects, plants, and microbes surrounded by ice and snow can face significantly colder temperatures on land than fish do in the ocean. The exact mechanism of ice binding has been difficult to define in part due to the wide range structures and motifs found in ice binding proteins (Sharp, 2011).

### 1.1.3 Novel Uses of Ice Binding Proteins

The ice growth inhibition ability of ice binding protein has led to many intriguing potential applications in biotechnology. One area in which it is commonly considered is the food industry. Freezing and thawing cycles during transport may cause the growth of large ice crystals by recrystallization, which negatively impacts texture of foods; AFPs

have been used to prevent this phenomenon, thereby improving both the texture and quality of refrozen ice creams, meats, and dough (Feeney & Yeh, 1998; Yeh, Kao, & Peng, 2009). AFPs also show potential for agricultural purposes. Transgenic lines of plants producing AFPs may lead to increased food quality by preventing ice crystal growth and resulting drip loss in produce as well as reduced crop loss during frosts (Bar Dolev et al., 2016; Venketesh & Dayananda, 2008). An AFP from *Daucus carota*, a type of wild carrot, has been expressed in the apoplast of tobacco (*Nicotiana tabacum)* and *Arabidopsis thaliana*, but in some cases the expressed AFPs have not imparted any frost resistance and work remains to be done (Kenward, Brandle, McPherson, & Davies, 1999; Meyer, Keil, & Naldrett, 1999; Worrall et al., 1998).

AFPs have also been investigated for their potential as a biomedical cryoprotectant. Several studies have shown AFPs can be effective in preserving various mammalian tissues under different forms of freezing (Amir et al., 2003; Hirano et al., 2008; Kim et al., 2017; Kim, Shim, Lee, Kang, & Hur, 2015; Lee et al., 2015; Lee et al., 2015). In contrast, other studies have shown AFP-induced damage to cells from, perhaps from the sharp, needle-like ice spicules that can form when they are frozen (Wang, Zhu, Yang, Layne, & Devries, 1994). AFP-induced spicule formation can be also be utilized for medical purposes such as adjuvants for cryosurgery. The sharp spicules induced by frozen AFPs can pierce cells and damage unwanted tissue such as tumors (Koushafar, Pham, Lee, & Rubinsky, 1997; Muldrew et al., 2001; Pham, Dahiya, & Rubinsky, 1999).

## 1.2 Winter Flounder (*P. americanus*)

### 1.2.1 Winter Flounder Biology and Habitat

The winter flounder is a right eyed flatfish that inhabits the Atlantic costal waters off North America (Bigelow & Schroeder, 1953). The range of this species stretches from the waters off Labrador, Canada to the coast of Georgia in the United States. Flounder up to 63.5 cm and weighing up to 3.6 kg have been caught on George's Bank, an offshore fishing ground between the coast of the United States and southern Nova Scotia (Bigelow & Schroeder, 1953). The winter flounder was once a common commercial and recreational fishing target; however, the stocks have dropped in the past century after many years of overfishing (Frisk et al., 2018; Ziegler, Zacharias, & Frisk, 2019).

### 1.2.2 Ice Binding Proteins of the Winter Flounder

The most thoroughly studied AFPs are small, alanine-rich, helical type I AFPs of winter flounder, noted above (Patel & Graether, 2010; Yang, Sax, Chakrabartty, & Hew, 1988; Yeh & Feeney, 1996). The initial hypothesis for the recognition of ice by these peptides was that hydrogen bonding mediated their binding to the ice lattice; however, this offered no explanation for the preferential binding of the AFP to ice crystals when surrounded by excess liquid water (Knight et al., 1991; Raymond & DeVries, 1977; Yang et al., 1988). Site-directed mutagenesis studies of the ice binding surface, as well as identification of putative ice binding sites from structurally diverse AFPs then lead to the hypothesis that the hydrophobic groups were important in the specificity for ice (Chao et

al., 1997; Jorov, Zhorov, & Yang, 2004; W. Zhang & Laursen, 1998). This hypothesis was supported theoretically by proposing that binding of AFP to ice was driven by the increase in entropy resulting from the release of bound water molecules into solution when the hydrophobic ice binding site recognized the ice lattice (Davies, 2014).

Molecular dynamics experiments as well as recent NMR studies suggest that both hydrophobic and hydrophilic groups are important for binding to ice. Currently the most likely proposed mechanism suggests that water molecules form clathrate-like cages around the apolar residues that are anchored by hydrogen bonding from polar residues (Figure 2). In this way, the ice binding proteins may arrange the water molecules into an ice-like arrangement within the binding site before adsorption to the ice front (Chakraborty & Jana, 2017, 2018; Garnham, Campbell, & Davies, 2011).

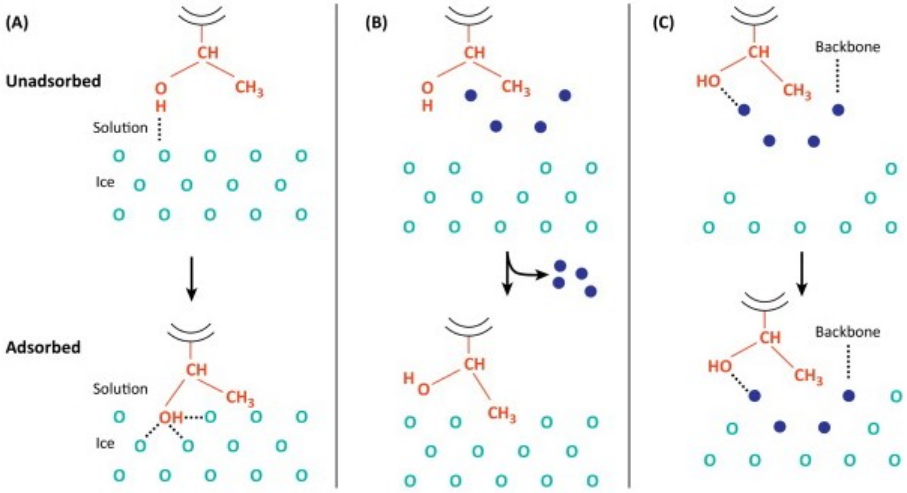


Figure 2:The three proposed binding mechanisms of antifreeze protein ice binding. Threonine is shown in red, the light blue "O"s represent ice and the filled in circles represent free water molecules. Panel A: The hydrogen bond mechanism. Panel B: the hydrophobic force mechanism. Panel C: the anchored-clathrate mechanism. (Image modified from Davies, 2014).

Winter flounder produce a variety of type I AFPs. The AFP genes expressed in liver and secreted into the blood are produced on a seasonal basis, with AFPs being expressed from November to May, with the flounder to concentrations of 1-10 mg/ml (0.3 mM – 3 mM) in the coldest months and 0 mg/ml in the warmest (Gong, King, Fletcher, & Hew, 1995). The production of these AFPs, which are the most abundant in the fish, is regulated by the photoperiod through growth hormone. Growth hormone, released in the summer, inhibits transcription of the genes encoding these proteins. In the winter months, when days are shorter, growth hormone levels diminish and AFPs are produced (Fletcher, Idler, Vaisius, & Hew, 1989; Gong et al., 1995). There are also a set of related AFPs expressed in skin and other tissues at lower levels; these are not seasonally regulated and they do not appear in the blood plasma (Gong, Ewart, Hu, Fletcher, & Hew, 1996; Z. Y. Gong et al., 1995; Miao, Chan, Hew, & Gong, 1998).

Resolution of plasma AFPs preparations with high performance liquid chromatography (HPLC) yields 9 peaks, with only peaks 3-9 showing thermal hysteresis. (Fourney, Joshi, Kao, & Hew, 1984). Peaks 6 and 8, referred to originally as HPLC6 and HPLC8, make up the majority of AFPs in the plasma (Fourney et al., 1984; Hew, Joshi, & Wang, 1984; Miao, 2001). The two proteins, now termed winter flounder liver protein 6 (AFP6) and winter flounder liver protein 8 (AFP8), are both 37 residues in length, and differ in sequence at only three positions (Figure 3). The 9$^{th}$ HPLC peak (AFP9) consists of 51 residues, and produces a higher thermal hysteresis on a molar basis than AFP6 or AFP8 (Chao, Hodges, Kay, Gauthier, & Davies, 1996).

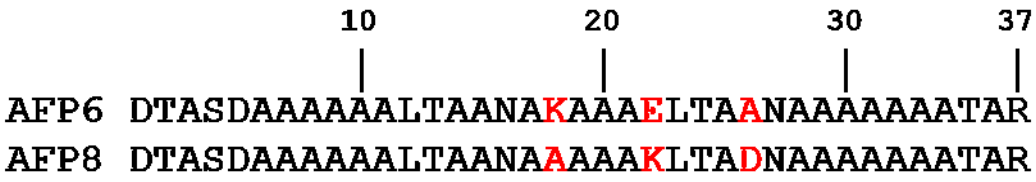


Figure 3: The aligned sequences of AFP6 and AFP8. The three amino acids that differ between the isoforms are indicated in red.

### 1.2.3 AFP6 Structure and Function

AFP6, like all type 1 AFPs, is an alpha-helical monomer as shown in Figure 4. This has been shown through circular dichroism (CD) and X-ray crystallography (Gronwald et al., 1996; Sicheri & Yang, 1995; Yang et al., 1988). As noted above, it is comprised of 37 amino acid residues, with 23 (62%) Ala. The alanines occur as part of the 11-amino acid residue repeat featuring the Thr residues noted above (Patel & Graether, 2010)**.** AFP6 is an amphipathic helix, with a stabilizing salt bridge between Lys18 and Gln22 (Wen & Laursen, 1993). The first 36 residues are all in alpha-helical conformation, with the final arginine residue (Arg37) in a $3_{10}$ helical confirmation (Sicheri & Yang, 1995). When visualized from the end of the alpha helix, AFP6 has 3 distinct faces. As depicted in Figure 5, a hydrophilic face is formed by residues such as asparagine, glutamic acid and serine, a hydrophobic face is formed by the methyl groups of threonine and alanine, and another hydrophilic face, hereby called the threonine face, consisting of the hydroxyl groups of threonine and either asparagine or aspartic acid (Jorov et al., 2004).

Early studies of AFP6 suggested that the peptide would bind to the ice face via hydrogen bonding provided by the threonine face of the peptide (Brooke-Taylor, Grant, Elcock, & Graham Richards, 1996; Knight et al., 1991; Raymond & DeVries, 1977; Yang et al., 1988). That proposed mechanism was challenged by mutation studies showing that replacing threonine with non-polar valine residues incapable of forming hydrogen bonds resulted in only a minor loss of activity, while replacing threonine with polar serine eliminated all activity. (Chao et al., 1997; Haymet, Ward, & Harding, 1999; Zhang & Laursen, 1998). Further study showed that mutation of Ala17 or Ala 21 to Leu on the

hydrophobic face of the peptide eliminated and greatly reduced thermal hysteresis (Baardsnes et al., 1999). Mutations of Ala19 and Ala20, located on the hydrophobic face of the peptide, to Leu had not effect (Baardsnes et al., 1999).

This led to a the proposal of a distinct binding mechanism involving hydrophobic and van der Waals forces (Chao et al., 1997; Haymet et al., 1999; Jorov et al., 2004; Sicheri & Yang, 1995; W. Zhang & Laursen, 1998). As noted previously in this chapter, more recent research has also suggested the "anchored clathrate water" mechanism, in which a combination of hydrophilic, hydrophobic, and Van der Waals forces are required for ice binding (Chakraborty & Jana, 2017, 2018; Garnham et al., 2011). This appears consistent with the proposal of multiple modes of interaction of AFP6 with ice.

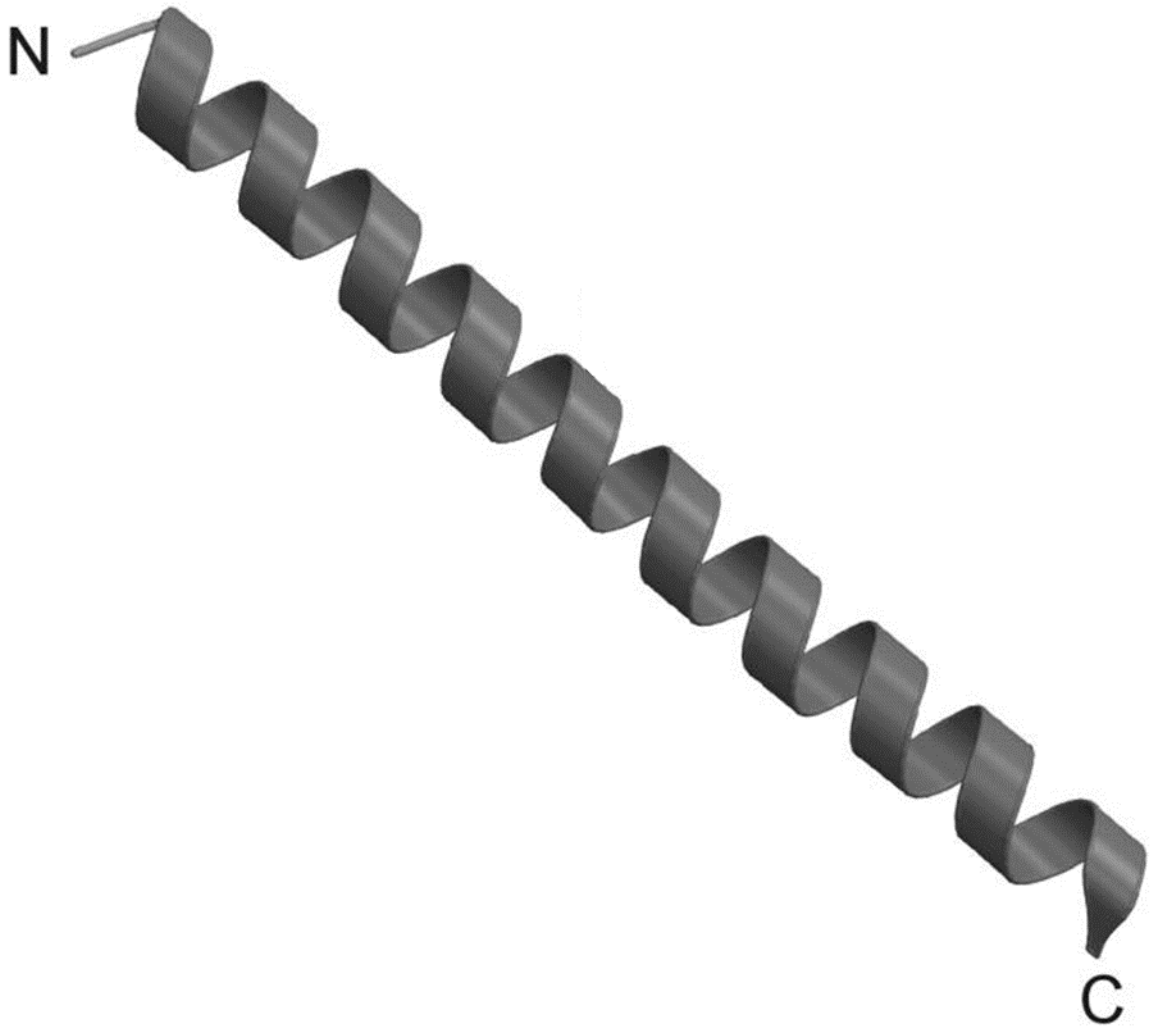


Figure 4: Alpha helical structure of AFP6 represented as a ribbon model. (Modified from (Graether, Slupsky, & Sykes, 2003)).

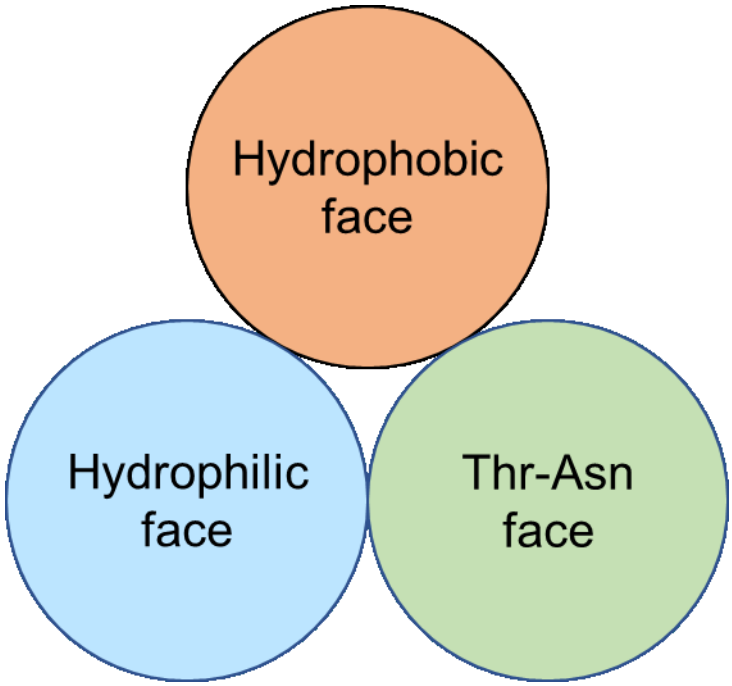


Figure 5: Diagram of the view down the axis of the AFP6 helix showing distinct faces. One face is primarily hydrophobic, one is relatively hydrophilic, and one has a preponderance of threonine and asparagine.

### 1.2.4 AFP6 Ice Interaction

While most of AFP6 research has specifically focused on its structure and function of binding to ice resulting in thermal hysteresis, recent work has led to another avenue of research. While studying the solution structure and ice binding mechanism of AFP6, Graether et al. (2003) found that repeated freezing and thawing of the protein resulted in amyloid formation. Although the capacity to convert to an amyloid fold has been proposed to be intrinsic to all peptides, most experiments show that few proteins will readily transition and even those that do often require harsh treatments such as low pH or chaotropic agents (Bucciantini et al., 2002; Chiti & Dobson, 2006; Dorta-Estremera, Li, & Cao, 2013; Iñaki Guijarro, Sunde, Jones, Campbelli, & Dobson, 1998).

Graether et al. (2003) achieved amyloid transition of AFP6 at neutral pH and physiological salt concentrations, just by freezing and thawing a high concentration of protein (75 mg/mL or 23 mM). Further research by the group found that even brief freezing was sufficient to trigger the transition of AFP6 to an amyloid form, and that, once present, the fibrils continued to grow at 20 ºC. They suggested that this implied the unfolding process occured upon melting, when a large number of protein molecules are uniformly aligned in close proximity along the ice surface (Graether & Sykes, 2009). In contrast to the freezing-induced amyloid formation, the incubation of AFP6 at 4 ºC for several days resulted in a distinct non-amyloid gel (Graether et al., 2003). There was a relationship between pH and the type of gel formed, where at pH 4 amyloid was consistently formed, whereas the formation of the distinct amorphous gel was favoured at

pH 8 (Graether & Sykes, 2009). The amyloid and gel formation are both interesting as it appears that, under different conditions, the AFP6 will form different types of aggregates.

After the discovery of freezing and thawing-induced amyloid transition in AFP6, there was the question of what exactly was causing the transition. Dubé, Leggiadro, & Ewart (2016) investigated this by evaluating the three aspects of freeze-thaw process individually: sub-zero temperature, the phase change from water to ice, and the interaction of the AFP6 with the ice surface. This was done by setting up experiments which included supercooling to -2.0 ºC, flash freezing in a dry ice-ethanol bath, or transfer of a liquid sample directly onto an ice surface. Fluorescence-based assays and transmission electron microscopy confirmed that amyloid transition of AFP6 required interaction with the ice surface (Dubé et al., 2016) . Fibrils formed by AFP6 are shown in Figure 6.

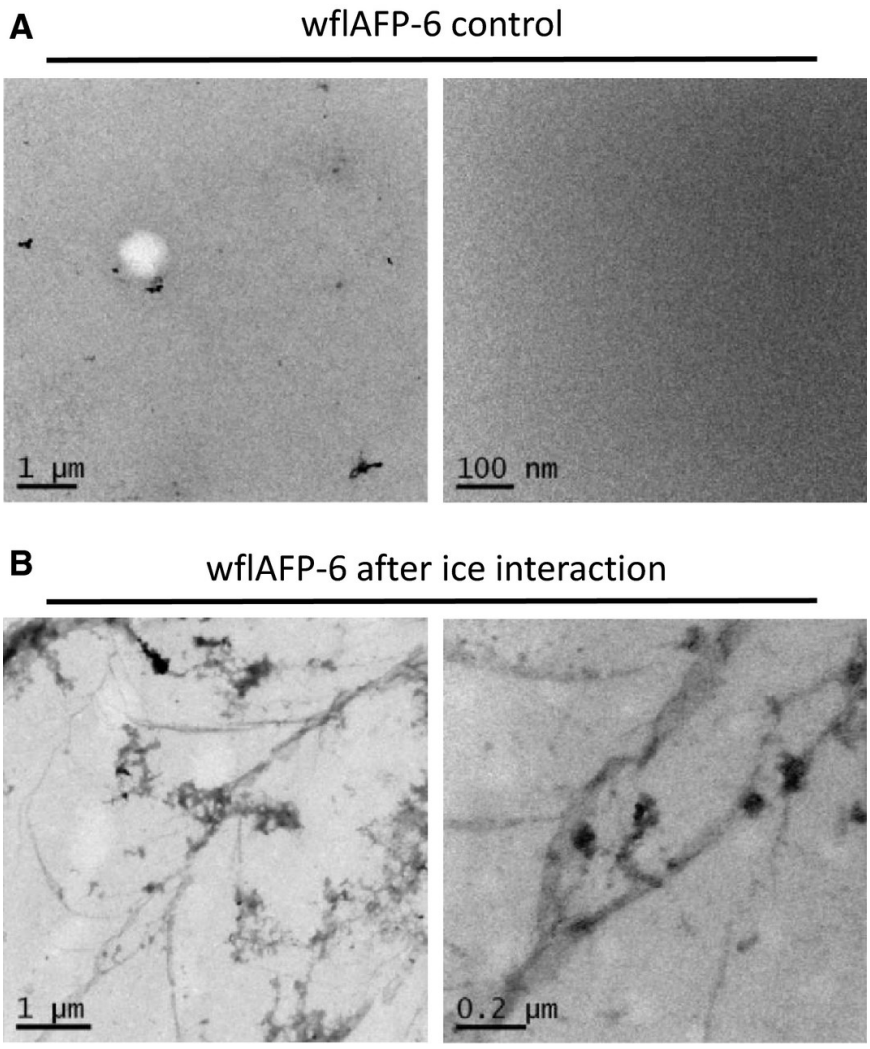


Figure 6: Formation of amyloid by AFP6 upon specific interaction with ice. Panel A: No amyloid fibrils apparent with a sample of AFP6 kept at 4ºC. Panel B: Amyloid formation after AFP6 interaction with ice surface. (Image from (Dubé et al., 2016))

## 1.3 Amyloid

### 1.3.1 Protein Folding and Misfolding

Given the propensity of AFP6 for amyloid formation, amyloids will be considered more thoroughly in this section. Proteins include macromolecular machines and structures that fulfill a wide variety of roles within living organisms. The three-dimensional structures, or folds, that proteins adopt are essential to their functions. As a protein is synthesized, it will collapse on itself due to hydrophobic effects, with the nonpolar residues interacting with each other in a way that minimizes their contact with the aqueous solvent. The folding process is thermodynamically driven (Li, Fooksa, Heinze, & Meiler, 2018). The nascent protein will be in a high energy state, and will adapt many partially folded and transition states until the low energy, native fold is achieved (Englander & Mayne, 2014). The native state is the folded state in which the protein can carry out its normal function in the organism. The energy change can be visualized as a funnel shape, where the nascent unfolded protein starts at the top, and ideally reaches the native state at the bottom. In some cases, proteins adopt their native fold spontaneously. In other cases, a class of proteins known as chaperone proteins, direct the nascent protein toward its native structure.

Protein misfolding occurs when a protein does not adopt its native structure. This may occur from non-native interactions between the amino acid residues (which may result from mutations in the protein sequence), from protein folding stress taxing the chaperone system or from the direct effect of biological or physical factors. As structure

is paramount to protein function, an unfolded or incorrectly folded (misfolded) protein is not likely to be able to fulfill its role within the organism. This can have serious consequences, depending on the protein in question. In some cases, misfolded proteins may interact with one another, thereby aggregating in denatured form. Alternatively, they may refold, forming a highly stable beta-rich amyloid structure.

### 1.3.2 Amyloid Structure and Transition

The world amyloid comes from Latin word for starch, amylum. The term amyloid was originally used by Rudolph Virchow in 1854 to describe waxy deposits found in organs that stained with iodine, just as starch did (Kyle, 2001). It was later discovered that the deposits were not starch, but proteinaceous in nature; however the name "amyloid" was already in use and so it was left unchanged (Kyle, 2001).

In tissues, amyloid deposits, sometimes given other names such as plaques, are comprised of insoluble fibrils of aggregated proteins. These fibrils are characteristically rod shaped with diameters ranging between 7-13 nm (Chiti & Dobson, 2006). They are usually unbranched and several micrometers in length, but can exhibit polymorphism (Xue, Homans, & Radford, 2009). They are usually comprised of multiple interacting protofibrils that are on the scale of 2-7 nm (Chiti & Dobson, 2017). The protofibrils are formed by oligomers of the misfolded parent protein, which are in turn assembled from monomers (Chiti & Dobson, 2017; Jackson & Hewitt, 2017).

The defining characteristic of amyloid fibrils comes from the molecular structure. While proteins may form other kinds of aggregates, most are amorphous and without a defined folded structure. In contrast, amyloid has a characteristic beta sheet-rich

structure, making it a structurally organized aggregate. The beta sheets of amyloid fibrils run perpendicular to the fibril length, with the sandwiched beta sheets being 10 Å apart and each strand being 4.7 Å apart (Jackson & Hewitt, 2017). Although amyloid is formed of beta sheet, it is not formed more readily by proteins with beta sheet-rich native structures, except for unusual cases in which amyloid is the native fold of the protein (Chuang, Hori, Hesketh, & Shorter, 2018). In the vast majority of cases, unfolded proteins with other native folds transition to an amyloid fold by a molecular rearrangement, resulting initially in oligomers of beta-sheet rich amyloid structure regardless of the structure of the parent monomer (Chiti & Dobson, 2017). As illustrated in Figure 7, these oligomers have templating action and can therefore induce the same transition in adjacent unfolded monomers of the native protein, leading to a growing self-assembly of the amyloid form. Amyloid fibrils are extremely stable, often even more so than their monomer components, resulting in a characteristic resistance to proteinase K and to other treatments and conditions that would normally unfold proteins (Chiti & Dobson, 2017).

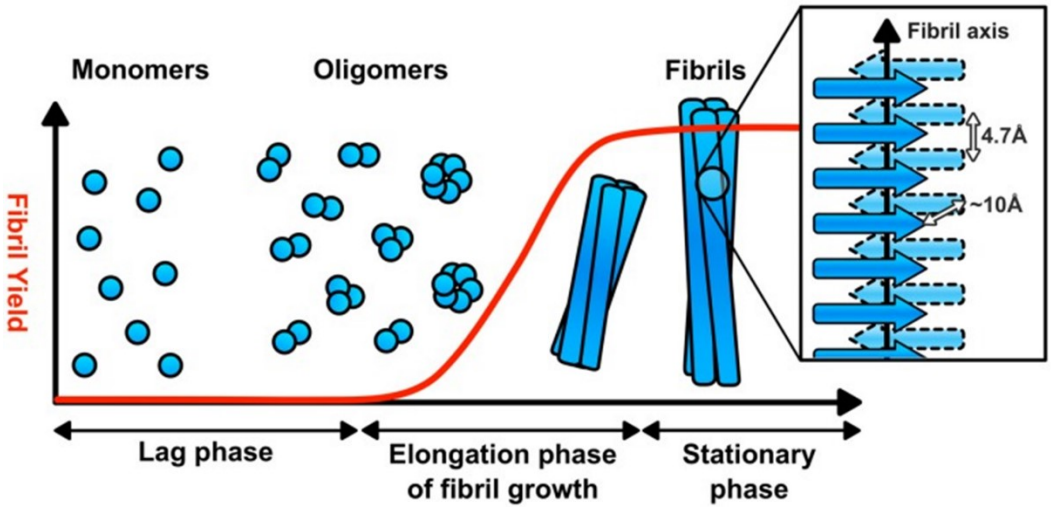


Figure 7: Schematic representation of the formation of amyloid fibrils. Amyloid transition begins with native monomers in the lag phase. After nucleation, the monomers interact with one another to become oligomers, beginning the elongation phase. Oligomers aggregate and undergo remodelling to form beta-sheet rich fibrils. Image from (Jackson & Hewitt, 2017).

### 1.3.3 Amyloid-Forming Proteins

There are greater than 30 known amyloid forming proteins, with many of them being related to human disease (Sipe et al., 2010). However, there are also some amyloid-forming proteins that are not cytotoxic. These are known as functional amyloids. As noted above, there is also evidence that the ability to form amyloid might be intrinsic to all proteins (Chiti & Dobson, 2006). Some examples of common disease and functional amyloid forming proteins are discussed below.

Perhaps the best-known amyloid forming protein is amyloid beta (aß), a small peptide that forms the characteristic amyloid plaques in patients with Alzheimer's disease. The aß is cleaved from the aß precursor protein into a 40 or 42-residue peptide that can take on several different conformations (Agrawal & Skelton, 2019). With the growing number of Alzheimer's disease cases, soluble aß and resulting plaques have been the target of much research.

Alpha-synuclein is a 140-residue protein was long thought to be intrinsically disordered, but it has recently been shown to form alpha helical multimers and it also adopts a helical structure when bound to lipids (Bartels, Choi, & Selkoe, 2011; Dettmer et al., 2017). It is primarily found in the brain but is produced at lower levels in other tissues as well. Alpha synuclein is known for its involvement in Parkinson's disease. Aggregated alpha synuclein deposits in nerve cells, known as Lewy bodies, are a pathological hallmark of Parkinson's disease (Goedert, Jakes, & Spillantini, 2017)

Huntingtin is an approximately 350-kDa protein that was recently found to be primarily alpha helical in its native form (Guo et al., 2018). Its exact size depends on the number of glutamine-rich repeats it contains. The protein has several functions, including acting as a transcriptional regulator, a protein scaffold, and as a vital part of neurogenesis (Jimenez-Sanchez, Licitra, Underwood, & Rubinsztein, 2017). Mutations in the huntingtin gene result in a string of glutamine repeats in the protein, which aggregate and form amyloid within the brains of affected patients, leading to Huntington's disease (Drombosky et al., 2018).

Islet amyloid polypeptide (IAPP), or amylin, is 37-residue peptide that is produced by beta cells in the pancreas. It has a mostly disordered structure, but does show a transient helix at the amino terminal (Westermark, Andersson, & Westermark, 2011). IAPP functions alongside insulin to modulate glucose homeostasis (Bhowmick, Singh, Trikha, & Jeremic, 2018). Patients suffering from type 2 diabetes develop amyloid deposits of IAPP in their pancreas, and these aggregates of IAPP are toxic through membrane disruption (Bhowmick et al., 2018).

Some bacteria utilize proteinaceous filaments within their extracellular matrix. These fibrils may be used in biofilms or for adhesion. One such example of this is the functional amyloid protein "curli" which is produced by enteric bacteria such as *Escherichia coli* and *Salmonella enterica*. These curli filaments exhibit the same biophysical properties as amyloid, such as the organized beta sheet rich structure, protease resistance and tinctorial properties. However, curli fibrils are not formed by protein misfolding, instead the amyloid is formed through a well coordinated biogenesis

pathway (Barnhart & Chapman, 2006; Blanco, Evans, Smith, Badtke, & Chapman, 2012; Evans & Chapman, 2014).

### 1.3.4 Seeding of Amyloid

Amyloid aggregation is a complex process and not entirely understood, but it can be broken down into smaller components for study. These include (1) the lag phase, in which monomers are in solution and before aggregation has begun, (2) primary nucleation, in which the monomers unfold (if applicable) and misfold into amyloid oligomers, (3) elongation, in which further aggregation of the oligomers occurs along with rearrangement into fibril structure, and (4) secondary nucleation, in which fibrils may induce misfolding of soluble monomers (Giorgetti, Greco, Tortora, & Aprile, 2018).

When monomeric amyloid is "seeded" with existing fibrils, it can reach its primary nucleation phase more quickly. This is also a general feature shared by several proteins, in which the addition of an amyloid form of a protein will seed the formation of amyloid by other molecules of the same protein. This can set off the chain reaction, leading to even more rapid formation of mature amyloid fibrils and continued propagation of the amyloid form of the protein. Seeding by the amyloid form of the same protein is called homologous seeding, and it has been understood this to occur for quite some time. Based on the scheme outlined in Figure 7, seeding shortens the lag phase step, otherwise the pathway continues as normal.

In heterologous seeding, a protein in its amyloid form may induce amyloid formation in a distinct protein. This heterologous seeding between different proteins may suggest that common amyloid structures or amyloid forming mechanisms are shared

between these proteins. The idea of this being possible had been postulated before, but only recently have its consequences been understood. For example, the presence in an animal of one amyloid-related disease, such as type 2 diabetes, with the misfolding of amylin, can lead to Alzheimer's disease through amyloid formation from aβ (Oskarsson et al., 2015; Zhang et al., 2015). Similarly, aβ has also shown the capability to act as a seed for alpha-synuclein and tau in mouse models (Bassil et al., 2020).

### 1.3.5 Detection of Amyloid

To detect seeding, the amount of fibril growth over time must be tracked. The most common way to observe fibril formation, as well as possibly the best way to track it, is through amyloid-staining dyes. While iodine may have led to the term amyloid, perhaps the dye most uniquely tied to amyloid throughout history is Congo Red. Like many historical dyes, Congo Red was originally a textile dye. In the early 1900s, however, many textile dyes were examined for use in pathology (Steensma, 2001). A physician first showed that Congo Red bound to amyloid when he injected a patient with it and then observed by microscopy that their liver and spleen sections had been dyed (reviewed by Fernandez-Flores, 2011). Congo red staining of amyloid is most commonly known for "apple-green birefringence under polarized light" (Yakupova, Bobyleva, Vikhlyantsev, & Bobylev, 2019). In practice there may be several colours seen depending on how the polariser or analyzer is rotated (Howie, 2015; Howie & Brewer, 2009; Yakupova et al., 2019).

Thioflavin-T (ThT) is another dye useful in amyloid detection, well known for its higher sensitivity compared to other dyes such as Congo Red (Fernandez-Flores, 2011)

and its lower background than thioflavin S (LeVine, 1999). This sensitivity comes in part as it is a fluorogenic stain as opposed to the direct-dye of Congo red (Biancalana & Koide, 2010). ThT was presented by Vassar and Culling to be a stain that would only fluoresce when bound to amyloid (Biancalana & Koide, 2010; Vassar & Culling, 1959). They discussed the viability of using ThT as a general amyloid dye in 1959, but it was over 30 years later when the biophysical properties of the dye were fully explored and ThT grew from a histological stain into the common amyloid fibril detection agent that it is today (Biancalana & Koide, 2010; LeVine, 1993; Naiki, Higuchi, Hosokawa, & Takeda, 1989).

The structure of ThT can bee seen in figure 8. ThT is comprised of two planar segments, benzylamine and benzathiole, linked by a single carbon bond, around which there can be movement in solution (Biancalana & Koide, 2010). Binding of the dye to grooves along the amyloid fibrils "locks" the molecule in place, restricting the movement around the carbon-carbon bond and allowing the dye to be detected (Gade Malmos et al., 2017; LeVine, 1999). ThT is especially useful as even with a constant concentration of dye, the fluorescence increases linearly with the concentration of fibrils in the sample. Since it does not affect fibril formation kinetics *in vitro*, it does not interfere appreciably with the amyloid formation it is used to measure, which has made it a powerful tool for observing amyloid formation (Naiki, 2017). There are however some considerations with the use of ThT, as with all dyes, such as the issue of specificity to fibrils. Although ThT is a sensitive reporter dye for fibril formation, it also binds ta few other protein with β-sheet rich structures(Harel, Sonoda, Silman, Sussman, & Rosenberry, 2008; Rovnyagina et al., 2018). Thus, care must be taken in the interpretation of results.

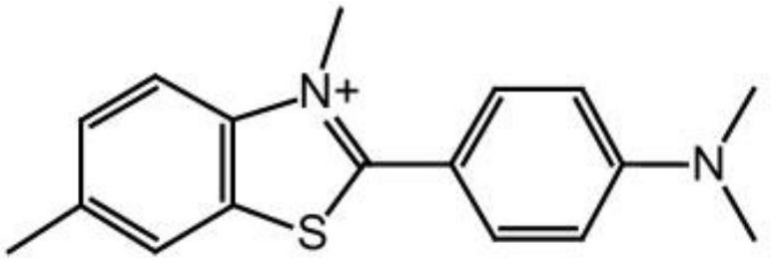


Figure 8: Structure of Thioflavin T. Rotation occurs around the carbon-carbon bond linking the benzylamine and benzathiole segments. This rotation is restricted upon binding to fibrils. (Modified from (Biancalana & Koide, 2010))

ThT may also compete for binding to amyloid fibrils when used as an assay for anti amyloid drugs, resulting in false negatives (Naiki, 2017). Finally it does not bind all fibril polymorphs equally (Naiki, 2017). These issues can be addressed by careful experimental design, ensuring that the proper controls are chosen and by further examining samples subject to ThT assays with other experiments to determine whether the fluorescence change was due to fibril formation. Analysis by electron microscopy is particularly useful, as fibrils can be viewed and measured if present. The natural product curcumin has also been investigated as an amyloid stain and will be discussed in more depth later in this chapter.

### 1.3.6 Anti-Amyloid Compounds

With protein misfolding to amyloid is involved in many diseases, there has been substantial research into compounds that can either inhibit or modulate fibril growth. In most cases, the mechanism by which the compound inhibits or modulates amyloid transition is not well understood. In many cases these compounds are polyphenol natural products or derivatives of them, leading to suggestions that the aromatic groups may be key to this interaction by both covalent and noncovalent interactions that inhibit aggregation (Bu, Rao, & Wang, 2016; Phan et al., 2019; Porzoor et al., 2015; Velander et al., 2017). Some of the most studied of these anti-amyloid compounds include (−)-epigallocatechin-3-gallate (EGCG), resveratrol, and curcumin (Cheng et al., 2013).

EGCG is a major bioactive in green tea. Green tea is produced from the leaves of the *Camellia sinensis* plant and it has been brewed in Asian cultures for thousands of years. EGCG has been investigated in several studies involving neurodegenerative

diseases and amyloid due to its antioxidant and anti-inflammatory properties (Pervin et al., 2018).EGCG can bind to monomer aß and alpha synuclein and modulate mature fibrils, reducing them to non-toxic aggregates (Bieschke et al., 2010; Ehrnhoefer et al., 2008; Jha et al., 2017; Palhano, Lee, Grimster, & Kelly, 2013) . EGCG has also been suggested to inhibit aggregation of a mutant form of the huntingtin protein (Ehrnhoefer et al., 2006). More recent studies have found that EGCG treatment resulted in a reduced fibril intensity i*n vivo* in heterozygous (wt/tg) mice overexpressing human IAPP, although not in diabetic homozygous mice (tg/tg) (Franko et al., 2018).

Resveratrol, (3,5,4'-trihydroxy-trans-stilbene), is a compound found in several different plant species, but most notably in red grapes, and thus, red wine. Like EGCG, it is a polyphenol that has been implicated as a possible neuroprotectant and a modulator of amyloid formation (Ge, Qiao, Qi, Wang, & Zhou, 2012). It has been shown to reduce amyloid plaques *in vivo* in mice (Karuppagounder et al., 2009). Resveratrol has also been shown to directly degrade aß monomers, therefore acting pre-emptively as an antiamyloidogenic compound (Marambaud, Zhao, & Davies, 2005).

Curcumin is the final example of an anti amyloid protein covered in this introduction, but due to its importance to this thesis it is the subject of the section below.

## 1.4 Curcumin

### 1.4.1 *Curcumin Longa*

*Curcumin longa*, more commonly referred to as turmeric, is a rhizomatous plant native to India and southeast Asia. The rhizomes are often dried and ground into a powder and used in a variety of different ways (Ammon & Wahl, 1991). The first note of turmeric in the western world was by Marco Polo in the 13$^{th}$ century, but it has been used in eastern cultures for much longer (Trujillo et al., 2013). Turmeric has traditionally been used as a spice, a dye, and as a form of natural medicine. The compounds curcumin, dimethoxy curcumin and bis-demethoxycurcumin give turmeric its characteristic colour and are the main secondary metabolites of *C. longa* (Nelson et al., 2017).

### 1.4.2 Curcumin

Curcumin, or diferuloylmethane, is a secondary metabolite, or a compound produced by an organism that is not essential to growth or development (Kroymann, 2011). The structure was elucidated in 1910 (Ghosh, Banerjee, & Sil, 2015; Gupta, Patchva, Koh, & Aggarwal, 2012; Kunnumakkara et al., 2017). Three years later, the same group successfully synthesized the compound (Gupta et al., 2012).

Curcumin is a bis-α,β-unsaturated β-diketone which exhibits keto-enol tautomerism dependent on the pH of the solution (Anand, Sundaram, Jhurani, Kunnumakkara, & Aggarwal, 2008). Structures are shown in Figure 8. The bis keto form is seen in acidic to neutral aqueous solutions while the enol form is dominant at alkaline

pH (Sharma, Gescher, & Steward, 2005). Curcumin is poorly water-soluble, but readily dissolves in organic solvents (Sharma et al., 2005).

Curcumin is the most well-known and studied of the linear diarylheptanoid compounds known as curcuminoids, but *C. longa* also produces the derivatives demethoycurcumin and bisdemethoxycurcumin as well (Anand et al., 2008; Siviero et al., 2015). Commercially available curcumin is a mixture of the above curcuminoids, with a extracts containing approximately 80% curcumin, 15% demethoxycurcumin and 5% bisdemethoxycurcumin (Anand et al., 2008; Siviero et al., 2015). Considering curcumin's role in traditional medicine, its biological effects are of interest. The first clinical trial using curcumin took place in 1937 to evaluate its effectiveness as a treatment of biliary disease (Oppenheimer, 1937). Just over a decade later, curcumin showed promise as an antibacterial against *Mycobacterium tuberculosis*, *Salmonella paratyphi*, *Staphylococcus aureus*, and *Trichophyton gypseum* (Schraufstatter & Bernt, 1949). In the 1970s, interest in the biological functions of curcumin began to grow and research into use of curcumin as a natural sourced medicine began to take off (Gupta et al., 2012). .

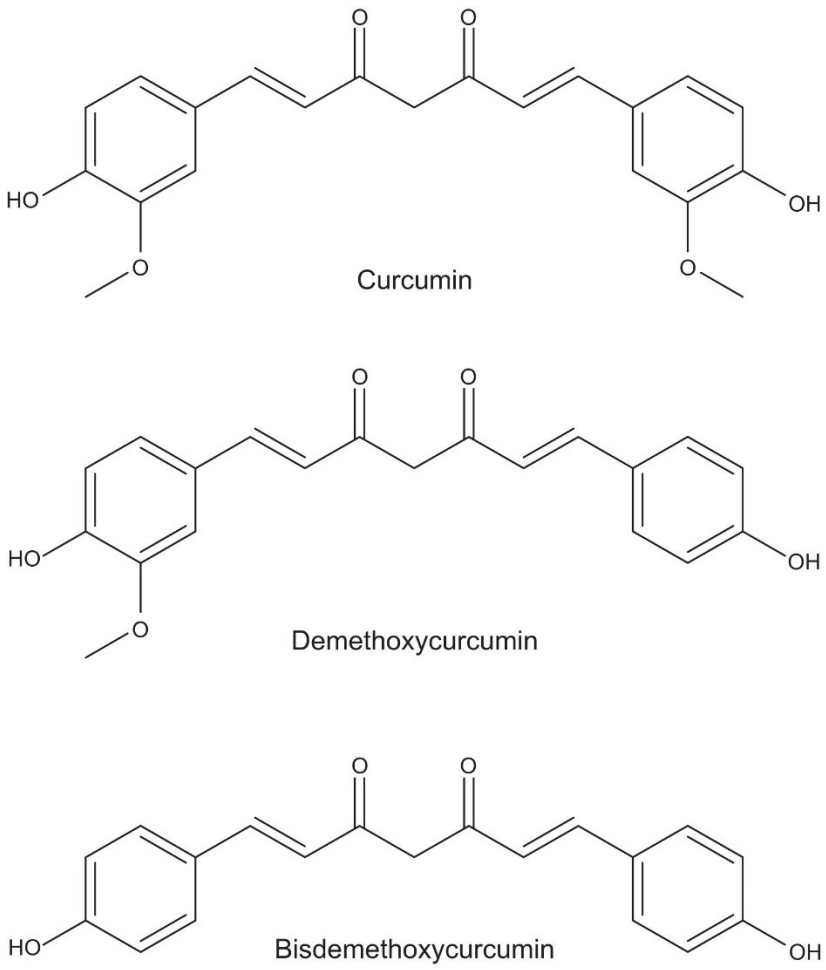


Figure 9: Structures of the curcuminoids found in a commercially prepared sample of curcumin (Images from (Darvesh et al., 2012).

### 1.4.3 Curcumin as a Medicine

The end of the 20th century saw a huge increase in published research pertaining to curcumin, suggesting an increasing number of biological roles (Aggarwal & Sung, 2009). Curcumin has been reported to have exhibited anti-inflammatory, anti-diabetic, anti-carcinogenic and wound healing properties among others (Kunnumakkara et al., 2017). These diverse reported effects may stem from the wide range of molecular targets not limited to DNA, RNA, cytokines, enzymes, transcription factors, cell receptors, and even aß. (Siviero et al., 2015).

Curcumin has such a wide range of molecular targets due to its ability to bind many different compounds. It is a hydrophobic compound, and its two phenyl groups can interact with other hydrophobic molecules such as hydrophobic pockets in proteins (Gupta et al., 2011;Liu et al., 2018). Carbonyl and phenolic groups are found in both the centre and each end of curcumin allows for hydrogen bonding as well (Gupta et al., 2011; Liu et al., 2018).

Several studies have addressed curcumin's potential benefit in neurodegenerative diseases, especially in relation to the protein misfolding involved in Alzheimer's disease (Darvesh et al., 2012; Pandey, Strider, Nolan, Yan, & Galvin, 2008). Curcumin binds to aβ *in vitro* and in certain model systems (Reddy et al., 2018). In cultured cells and mouse models curcumin inhibits amyloid fibril formation, as well as reduce plaques (Reddy et

al., 2018). Early studies suggested that curcumin inhibits formation of aß oligomers and fibrils, binds plaques, and reduces amyloid *in vitro* and when injected into transgenic mice (F. Yang et al., 2005). One study reported that curcumin reduced the toxicity of aß fibrils and oligomers in SH-SY5Y cells (Thapa, Jett, & Chi, 2016). Another group found similar results with alpha synuclein, noting that curcumin seemed to alter fibril formation, to a less toxic form (Singh et al., 2013).

### 1.4.4 Curcumin as a Protein Stain

Curcumin's interaction with amyloid has also been utilized for visualization purposes. Curcumin fluoresces when bound to aß plaques and this was used to visualize amyloid in tissue sections of various brains (Garcia-Alloza, Borrelli, Rozkalne, Hyman, & Bacskai, 2007; Mutsuga et al., 2012; Yang et al., 2005). It was subsequently reported that curcumin binds alpha synuclein oligomers, but not monomers (Singh et al., 2013). It has been proposed that curcumin could be utilized as a form of diagnostic agent and find use in subsequent treatment for amyloid diseases (Koronyo, Salumbides, Black, & Koronyo-Hamaoui, 2012).

In addition to its fluorescence when bound to amyloid, curcumin has been reported to fluoresce when bound to non-amyloid proteins under specific conditions (Kurien & Scofield, 2009; Kurien, Singh, Matsumoto, & Scofield, 2007). Research has only recently shown that the solubility of curcumin in aqueous solution could be greatly increased through heating, thereby making it amenable to use as a protein stain (Kurien & Scofield, 2009; Kurien et al., 2007).

## 1.5 Visualizing Proteins

### 1.5.1 Sodium Dodecyl Sulfate–Polyacrylamide Gel Electrophoresis

When attempting to purify or enrich a molecule from a given solution, it is important to understand the methods being used as well as the means to detect it. One of the most common techniques used in the separation and visualization of molecules is polyacrylamide gel electrophoresis (PAGE). The most common form of this method used in protein analysis includes the denaturation of proteins with the detergent sodium dodecyl sulfate before separation on the polyacrylamide gel (SDS-PAGE).

In SDS-PAGE, proteins are denatured by boiling in the presence of SDS, a detergent which is made up of a carbon tail attached to a polar sulfate group. The SDS molecules interact with proteins, imparting a negative charge that is relative to size of the protein. When these uniformly negatively charged proteins are subject to an electric current, they migrate toward the positive electrode and their speed of movement is determined by the sieving of the polyacrylamide matrix. Following separation, the proteins must be detected by staining or by other means. To visualize proteins that have been separated via electrophoresis within the gel, stains are used.

### 1.5.2 Use of Protein Stains

Detection of proteins is necessary for designing and carrying out experiments. Quantification of proteins before an assay or visualization of proteins after separation by SDS-PAGE are quantitative and qualitative examples of this, respectively. Protein can be detected or visualized in many ways, but not all are applicable for proteins in a gel after

SDS-PAGE separation. Some methods are not applicable to proteins that have been separated by SDS-PAGE as the proteins are embedded in the gel matrix. For analysis of proteins after gel electrophoresis, protein stains are utilized. These stains, also commonly referred to as dyes, are small molecules that bind to proteins and have properties that allow for visualization. Some stains produce a visible colour, while others fluoresce when exposed to a certain wavelength of light. Some commonly used stains for protein detection in SDS-PAGE gels are discussed below.

Coomassie Brilliant Blue was originally used as a textile dye; however, beginning in 1963, it was used to stain proteins following electrophoresis (Fazekas de St Groth, Webster, & Datyner, 1963). Coomassie Brilliant Blue is a triphenolmethane-like dye available in two forms, G-250 and R-250, with the difference being two additional methyl groups in the R-250 dye (Georgiou, Grintzalis, Zervoudakis, & Papapostolou, 2008). The molecule interacts primarily with basic amino acids such as lysine, arginine and histidine and the complex is further stabilized by aromatic amino acids such as tryptophan and phenylalanine. (Georgiou et al., 2008). It was originally believed that only the anionic form of the molecule bound protein, but recent research has suggested that the neutral form binds as well (Georgiou et al., 2008). This stain allows the detection of 0.3-1.0 μg of protein in a PAGE gel band (Ren, Okerberg, & Mathews, 2012). The protein-dye complex has a maximal absorbance between 595 to 620 nm (depending on the solution/form of the molecule) and appears blue, as the name suggests (Sapan, Lundblad, & Price, 1999)

The use of silver staining as a means of detection proteins following SDS-PAGE was first noted in 1979 by Switzer et al. (Rabilloud, Vuillard, Gilly, & Lawrence, 1994;

Ren et al., 2012). In this staining process, ionic silver binds to proteins, and it is then reduced to elemental silver, which results in a dark grey colour. The process is akin to silver photography (Hempelmann & Krafts, 2017). The exact mechanism of protein staining by silver is not known, but it does appear to depend on protein structure (Merril, 1986). Silver staining is up to 100 times more sensitive than Coomassie staining with a detection level in the low nanogram range, but it is also more time-consuming (Rabilloud et al., 1994).

Fluorescent stains are also very sensitive and often require less gel handling than silver staining procedures. One of the earlier rapid, general, fluorescence-based stains was Nile Red, a hydrophobic dye that came into use in the 1990s. Unfortunately, the dye was relatively insoluble, forming precipitates on gels during staining and its low photostability made it impractical (Steinberg, 2009). Molecular Probes then presented the SYPRO Orange and SYPRO Red dyes in 1996 (Steinberg, Jones, Haugland, & Singer, 1996). These stains required only a single step staining process that only took up to 60 minutes post SDS-PAGE and allowed the detection of 1-2 ng (SYPRO Orange) or 4-8 ng (SYPRO Red) of protein. The stains worked as general protein stains and were more sensitive than the colloidal Coomassie blue stain while being photostable enough to take several photos (Steinberg, 2009). There are now a wide variety of commercially available fluorescent stains for SDS-PAGE and they are commonly used for protein visualisation in the lab.

### 1.5.3 Limitations of Common Protein Stains

Despite the common usage of the three types of stains described above, there are still limitations to their use. For example, although Coomassie Blue is the most common general stain used, it may not bind well to peptides that are missing basic and aromatic groups. Silver staining requires many steps and requires toxic compounds. Even the fluorescent stains, while usually utilizing safer solvents than silver staining, are not completely biosafe and they have the added disadvantage of being relatively expensive. Although there are many viable dyes commercially available for lab usage, it is relevant to continue considering more versatile, economical and environmentally responsible staining agents.

## 1.6 Research Objectives

Despite many years of research there are still new properties of amyloid or new pathogenic amyloid proteins being found today. As the number of people with amyloid-based diseases continues to grow, it is imperative that we better understand how proteins transition from their soluble native state to amyloid forms capable of cytotoxicity. Understanding how a natively helical molecule such as AFP6 can undergo rapid transition to amyloid upon freeze-thaw could lead to the development of a model system for amyloid formation. Further understanding of the properties of AFP6 that cause it to have the capability for such a transition would also be valuable. Therefore, the development of a model system for amyloid formation utilizing the uniquely inducible amyloid formation by AFP6 was the primary research objective.

### 1.6.1 Examination of Amyloid Formation by aß and AFP6

Previous research has shown that AFP6 can form amyloid under specific conditions, and that ice interaction is required for this transition. Fluorescence assays and transmission electron microscopy have been utilized to examine this. While common amyloidogenic proteins studied in labs require agitation or harsh conditions to study, AFP6 transition to amyloid is readily inducible. Along with the potential for an excellent model for amyloid transition, AFP6 amyloid could potentially be applied for use in high throughput anti- amyloid screening. However, the relevance of AFP6 as a model for amyloid formation by human proteins such as aβ is unknown. One way in which to begin examining this is to evaluate the cross-seeding capability of AFP6 for aβ, which has not yet been investigated. An intrinsic property of amyloid is the capability for homologous seeding (Chiti & Dobson, 2017).Recent research has suggested that closely related pathogenic amyloids have the capability for cross-seeding, as noted above (Bassil et al., 2020; Oskarsson et al., 2015). Therefore, this is a property that could be directly evaluated for the AFP6, in order to evaluate the similarity of its amyloid to the aβ amyloid and eventually others. The goal of the current investigation was to investigate the heterologous seeding properties of AFP6, thereby providing a first measure of its relevance as a more general model for amyloid research. This was done through implementing ice induced amyloid formation assays based on those described by Dubé al. (2016). An *in-situ* assay for tracking heterologous and homologous amyloid seeding through ThT fluorescence was developed. This has set the framework for the continuation of this research.

### 1.6.2 Interaction of AFP6 with Curcumin

As noted above, AFP6 consists of only 37 residues with a skewed Ala-rich amino acid composition. It is consequently difficult to visualize with many common stains, including Coomassie Blue. The staining of AFP6 with curcumin as well as the interaction between the two was investigated. Aqueous solubilized curcumin was used following SDS-PAGE to test for successful staining of the peptide. The effect of AFP6 on curcumin was investigated through monitoring absorbance and fluorescence of the curcumin with and without AFP6 at differing temperatures. Likewise, the effect that curcumin had on AFP6 was observed using circular dichroism. These experiments may help understand the binding interaction between the two molecules, and perhaps can lead to the common laboratory use of curcumin as a biosafe dye.

# CHAPTER 2: EXMANINATION OF AMYLOID FORMATION BY aβ AND AFP6

## 2.1 Introduction

The most prevalent cause of dementia is Alzheimer's disease, a neurodegenerative disease characterized by the formation of extracellular amyloid plaques consisting of fibrillar aß and the intracellular aggregation of tau protein (Bloom, 2014). As noted earlier in this work, Alzheimer's is one of many diseases that stem from the formation of amyloid by proteins. Furthermore, recent studies have indicated that amyloidogenic proteins are able to induce amyloid formation in a different protein, such as aß aggregation-induced misfolding of IAPP (Oskarsson et al., 2015; M. Zhang et al., 2015). For these reasons, understanding the basis for the conversion of proteins to an amyloid form is a healthcare priority. However, the study of amyloid-forming proteins can be challenging due to background amyloid formation in samples prior to experimentation and to the long and difficult procedures required to trigger amyloid formation by some proteins (Arslan & Chakrabartty, 2009; Herva et al., 2014). Therefore, a model protein that can convert to an amyloid form in a reliable user-determined fashion could find use in screening for anti-amyloidogenic compounds.

While the potential for conversion from a native fold to amyloid fibrils is believed to be intrinsic to all proteins, it most often requires harsh treatment that would not occur under physiological conditions (Chiti & Dobson, 2006; Dorta-Estremera et al., 2013). This makes the study of amyloid transition using proteins with low amyloid propensity interesting, but not ideal as a model of how the transition would occur under natural conditions. Several methods including agitation, amplification steps or other measures

have been used to generate and amplify amyloid from amyloid-forming proteins (Atarashi et al., 2007; Herva et al., 2014; Holmes et al., 2014; Qiang, Yau, & Tycko, 2011; Soto, Estrada, & Castilla, 2006). These vary in expense, applicability and reproducibility.

AFP6 transitions from a stable, alpha-helical conformation to a beta sheet structure with clear amyloid characteristics under mild and even physiological conditions (Dubé et al., 2016; Graether et al., 2003). This transition is unique among known proteins, as the amyloid formation is induced upon melting after specific interaction with ice (Dubé et al., 2016). Furthermore, the formation of amyloid in this manner is rapid, with fibrils forming after just 15 minutes at -20 ºC and fibril growth continuing with incubation at 20 ºC (Graether & Sykes, 2009).

The rapid and inducible formation of amyloid by AFP6 could make it a potentially useful model for the study of the amyloid transition. In order to assess the relevance of AFP6 as a general amyloid model, the similarity of the amyloid formed by AFP6 and one or more human amyloids must be investigated. Research has already shown that AFP6 amyloid binds to amyloid specific dyes, exhibits a beta sheet conformation, forms insoluble fibrils, and can self propagate amyloid formation among AFP6 monomer (Dubé et al., 2016; Graether et al., 2003; Graether & Sykes, 2009).

The ability of AFP6 to cross template other known amylogenic proteins and the effect that known anti-amyloid compounds may have on AFP6 fibrils is also yet to be investigated. These investigations can be carried out through the design and implementation of *in-vitro* seeding assays by monitoring amyloid formation through ThT fluorescence in native AFP6 alone and when treated with AFP6 fibrils. Cross-seeding

assays could be designed by treating known amylogenic proteins such as native Aß with AFP6 fibrils and vice versa, observing potential fibril growth through ThT fluorescence. The effectiveness of known anti amyloid compounds such as EGCG against AFP6 amyloid formation could also be investigated with the same ThT-based assay.

The goal of this project was to evaluate the potential of AFP6 to be a relevant model for amyloid formation through understanding its heterologous seeding capabilities as well as its reaction to anti-amyloid compounds.

## 2.2 Materials and Methods

### 2.2.1 Preparation of aβ Samples

Lyophilized synthetic amyloid beta 1-42 manufactured by rPeptide was obtained from Cedarlane. Mass spectrometry and HPLC analysis data were provided by the supplier. The peptide was reconstituted in 0.1 % ammonium hydroxide (v/v) at 4 ºC. The sample was sonicated using a bath sonicator (Cole-Parmer 8890) for 1 minute in ice water before quantification by measuring UV absorbance at 215 nm and 225 nm with a Molecular Devices SpectraMax M3 and using the method developed by Waddell (Brand et al., 2019; Chaudhary, Singh, & Nagaraj, 2011; Waddell, 1956; Wolf, 1983). Samples were then aliquoted and stored at -20 ºC until their use.

### 2.2.2 Preparation of AFP6 Samples

Preliminary studies were done using serum samples prepared from the winter flounder, *P.americanus*. Blood plasma from Newfoundland winter flounder was provided

by Dr. Garth Fletcher (Memorial University of Newfoundland). This plasma was diluted 1:1 with phosphate-buffered saline prepared from tablets (Bioshop, 137 mM NaCl, 2.7 mM KCl, 10 mM $Na_2HPO_4$, 1.8 mM $KH_2PO_4$), filtered through a 0.20 µm filter, aliquoted and stored at -20 ºC.

AFP was isolated by gel filtration and DEAE ion exchange chromatography of the plasma and the resulting material was lyophilized. This lyophilized preparation was solubilized in 10 mM ammonium acetate, pH 6 before use.

Lyophilized synthetic AFP6 was obtained from three suppliers: BioBasic, Genscript, and Biomatik. All three provided yield data (mg), reverse phase HPLC analysis and mass spectrometry analysis. Protein was solubilized in 10 mM ammonium acetate, pH 6 and then quantified by measuring UV absorbance at 215 nm and 225 nm using the method previously described in the preparation of aβ. Solubilized AFP6 was then aliquoted and flash frozen in a dry ice-ethanol bath before being stored at -20 ºC until their use.

In cases where the concentration of AFP6 in solution was lower than required, the samples were concentrated by centrifugal filtration through 3 kDa filters (GE Healthcare, VivaSpin 500) that were pre-washed beforehand with 10 mM ammonium acetate buffer to remove glycerol.

### 2.2.3 Endpoint Thioflavin T Assay

ThT endpoint assays followed standard procedures (LeVine, 1999), with modifications. As ThT is light-sensitive, its preparation and use took place under low light conditions. Fifty mM ThT was solubilized in $H_2O$ and filtered through a 0.45 µm filter. One µL of the solution was diluted into 1 ml of 50 mM glycine, pH 8.5 to give a working solution of 50 µM ThT. The solution was wrapped in foil and stored at 4 °C until use.

Two hundred forty µL of working ThT solution was mixed with 10 µL of 5 mM AFP6 (5 µL of 10 mM stock with 5 µL of water) from the ice interaction assays (described in following sections) in a black 96 well plate (Greiner). A negative control of 240 µL of ThT solution with 10 µL of water was used. The fluorescence of the plated samples was then measured as described above.

### 2.2.4 Generation and Detection of Ice-Binding Induced Amyloid Formation by AFP6

The assay followed the method published by Dubé et al. (2016). This assay was originally designed to determine which aspect of freezing caused amyloid formation seen upon the repeated freezing and thawing of AFP6; the phase change (ice formation), the low temperature, or the specific interaction of the protein with an ice surface. Samples termed “cold” control were kept at 4 °C during all incubation steps of the assay. The supercooled samples were incubated at – 2 °C during the experiment while staying unfrozen in the liquid phase. The phase change samples were flash frozen before

incubation at – 2 °C to preclude ice interaction, and the ice interaction samples were incubated at – 2 °C along with a small (5 µL) quantity of ice formed from distilled $H_2O$.

In the cases of the cold control and supercooling, 5 µL of 10 mM AFP6 was added to a fresh microcentrifuge tube. In the case of phase change, 5 µL of 10 mM AFP6 was added to a fresh microcentrifuge tube then flash frozen in a dry-ice ethanol bath. In the case of ice interaction, 5 µL of $H_2O$ was added to a clean microcentrifuge tube and frozen in a dry ice-ethanol bath and then 5 µL of 10 mM AFP6 was added. The cold control sample was removed to a 4 °C refrigerator while the remaining samples were transferred to a circulating refrigeration unit held at -2 °C. After 2 hours, the samples were removed to 20 °C for 10 minutes. Following freeze-thaw, 5 µL of water were added to all samples other than the ice interaction ones in order to make all sample volumes equal.

Optimization attempts with this assay included the evaluation of several parameters in order to increase the chance for amyloid formation. Over several separate iterations of the experiment, the concentration of AFP6 was raised from 10 mM to 15 mM, the volume of sample added to the ice seed was increased from 5 µL to 10 µL, the volume of the ice crystal was adjusted from 5 µL to 10 µL, the temperature of the circulating chiller was adjusted, and samples were run through the assay more than once These series of experiments were undertaken in order to minimize the background fibril formation and maximize fibril induction by seeding, if it were to occur.

In the final version of this assay, each sample of 5 µL of 17.5 mM synthetic AFP6 (Biomatik) was pipetted onto a 5 µL ice seed of distilled $H_2O$ incubated at -2 °C for 2 hours. These samples were then allowed to melt, and all 10 µL of the resulting 8.75 mM

AFP6 samples was pipetted onto a 3 µL ice seed of distilled $H_2O$ and incubated at -3.0 °C for 20 minutes, then dropped to -5 °C for 30 minutes.

In the same assay, control samples consisted of 5 µL of 17.5 mM synthetic AFP6 (Biomatik) incubated at 4 °C for 2 hours. Five µL of distilled $H_2O$ was added after 2 hours to equalize sample volumes with the above ice-containing sample. These control samples were then incubated at 4 °C for 50 minutes. After this another 3 µL of distilled $H_2O$ was added to equalize sample volumes.

A blank solution of 240 µL of working ThT solution, 10 µL of 10 mM ammonium acetate, pH 6 were also plated. The fluorescence of the plated samples was recorded on a SpectraMax M3 microplate reader (Molecular Devices) with an excitation wavelength of 450 nm and emission detection at 482 nm.

A method was also implemented to combine the approaches of Graether & Sykes and Dubé et al. in order to maximize the possibility of fibril formation (Dubé et al., 2016; Graether et al., 2003; Graether & Sykes, 2009). Five µL of distilled $H_2O$ was added to a 500 µL microcentrifuge tube and frozen at – 20 °C . Samples of 13 mM of 77% pure synthetic AFP6 in 10 mM ammonium acetate, pH 6 were pipetted onto this ice surface and, then placed at – 20 °C for 12 hours. As a control, 13 mM the same AFP preparation was incubated at 4 °C for 12 hours. Following this incubation, 5 µL of distilled $H_2O$ was added to the samples that had been at 4 °C to make the volume between all samples equal. After this samples from both – 20 °C and 4 °C conditions were incubated at room temperature on the bench top for 1 hour. The samples were then centrifuged briefly at 7000 rpm (D1008, Scilogex) before being removed to -20 °C or 4 °C for another 12-hour incubation respectively. This process was repeated 5 times.

To further favour amyloid formation, these samples were then prepared much like the amyloid beta *in-situ* assay described in the following section. A stock of 200 mM ThT in distilled $H_2O$ was prepared and diluted to 200 µM in 50 mM glycine, pH 8.5. 10X PBS stock (1370 mM NaCl, 27 mM KCl, 100 mM $Na_2HPO_4$, 18 mM $KH_2PO_4$, pH 7.5), This was combined with the frozen-thawed AFP6 samples to give a final in-well concentration of 270 µM AFP6, 20 µM ThT, 137 mM NaCl, 2.7 mM KCl, 10 mM $Na_2HPO_4$, 1.8 mM $KH_2PO_4$. The corresponding negative control had a final concentration of 20 µM ThT, 137 mM NaCl, 2.7 mM KCl, 10 mM $Na_2HPO_4$, 1.8 mM $KH_2PO_4$. The plate was sealed with transparent QPCR seal (FroggaBio) and then shaken at 37 °C at 600 rpm (Orbit P2, Labnet) for 139 hours as ThT fluorescence was measured. Samples were then removed from the plate and flash frozen in a dry ice-ethanol bath until transmission electron microscopy (TEM) experiments.

### 2.2.5 In-Situ aβ Homologous Seeding Assay

Solutions of 10X (200 mM ThT stock) was prepared and diluted to 200 µM in 50 mM glycine, pH 8.5. 10X PBS stock (1370 mM NaCl, 27 mM KCl, 100 mM $Na_2HPO_4$, 18 mM $KH_2PO_4$, pH 7.5) was prepared.

Solutions of aß monomer were thawed on ice and then sonicated for 1 minute in ice water as described above. Samples were then briefly centrifuged in a tabletop centrifuge (D1008, SciLogex) at 7000 rpm. The aß stock was then diluted with 10X PBS, $H_2O$, and ThT solution to give a final assay solution of 8 µM aß, 20 µM ThT, 137 mM

NaCl, 2.7 mM KCl, 10 mM $Na_2HPO_4$, 1.8 mM $KH_2PO_4$. The corresponding negative control was the same solution, but with the absence of aß.

A fibril solution was produced by shaking 16 µM aß monomer, 20 µM ThT, 137 mM NaCl, 2.7 mM KCl, 10 mM $Na_2HPO_4$, 1.8 mM $KH_2PO_4$ at 600 rpm (Orbit P2, Labnet) at 37 °C for at least 200 hours. The growth of fibrils was monitored through observation of ThT fluorescence at 482 nm throughout the shaking. The presence of aß fibrils was further confirmed by TEM analysis, as described below. The volume of fibril stock added was varied over the optimization process of the assay and is described in further depth in the Results section. In each case the volume of $H_2O$ added was replaced with the volume of fibrils added to give a final concentration of 107 nM to 1.4 µM fibrils.

Samples testing the effect of EGCG on amyloid formation were prepared such that each sample had a final concentration of 8 µM aß, 16 µM EGCG, 20 µM ThT, 137 mM NaCl, 2.7 mM KCl, 10 mM $Na_2HPO_4$, and 1.8 mM $KH_2PO_4$. The corresponding negative control had a final concentration of 16 µM EGCG, 20 µM ThT, 137 mM NaCl, 2.7 mM KCl, 10 mM $Na_2HPO_4$, and 1.8 mM $KH_2PO_4$. The plates were then sealed with QPCR adhesive plate seals (FroggaBio) and shaken at 400 rpm (Orbit P2, Lab at 37 °C in between taking ThT fluorescence measurements.

### 2.2.6 Silver Iodide-Induced AFP6 Amyloid Formation

The experimental set up is listed in Table 1. Samples were subject to temperature regimens expected to allow antifreeze protein binding to the AgI crystal surface. They were then subject to a temperature regimen expected to favour seeding of further amyloid by any that might have formed (Graether et al., 2009).

Table 1: Preparation of samples for AgI induced AFP6 amyloid formation.

| Sample shorthand | Sample |
|---|---|
| A | 500 mg AgI + 5 μL 10 mM AFP6 |
| B | 500 mg AgI + 5 μL 10 mM AFP6 |
| C | 5 μL 10 mM AFP6 |
| D | 5 μL 10 mM AFP6 |
| E | 500 mg AgI + 5 μL of 10 mM ammonium acetate, pH 6 |
| F | 500 mg AgI + 5 μL of 10 mM ammonium acetate, pH 6 |

All samples were prepared in duplicate. Ten mM synthetic AFP6 in 10 mM ammonium acetate, pH 6 was chilled on wet ice (0 °C) for 10 minutes. Five µL of 10 mM AFP6 was added to each of tubes A-D, 5 µL of 10 mM ammonium acetate was added to tubes E and F to act as a control. All samples were then incubated at 4 °C for 4 hours, then transferred to wet ice (0 °C) for 2 hours, to – 20 °C for 12 hours, to 4 °C for 2 hours, wet ice for 2 hours, then transferred to -20 °C for 12 hours.

Following this, samples were incubated at room temperature for 30 minutes, then at 37 °C for 30 minutes. All samples were briefly centrifuged at 7000 rpm (D1008, Scilogex) then the liquid sample was carefully transferred to a fresh microtube, taking care to avoid AgI granules. The liquid samples were then incubated at room temperature for a further 20 minutes before being mixed with 245 µL working ThT solution described above. These samples were transferred to an opaque black 96 well plate (Greiner) and sealed with QPCR adhesive plate seals (FroggaBio). The plate was shaken at 600 rpm at 37 °C for 140 hours, in between recording ThT fluorescence.

### 2.2.7 Protein Analysis by Transmission Electron Microscopy

A 210 µL sample was taken from the sample wells of the amyloid beta seeding assay described above. These samples were then partially dried in a vacuum concentrator (Eppendorf Vacufuge plus) to 95 µL, giving a concentration of 17.7 µM aß. The same process was repeated with synthetic AFP6 ice interaction and shaking assay to give a concentration of 720.6 µM AFP6.

A droplet of each sample was added to the surface of Formvar-coated carbon grids (TAAB Laboratories) using a Pasteur pipette. The grid was then dried for 10

minutes before being gently washed with $H_2O$. A drop of 2% uranyl acetate was then added to the grid, incubated at room temperature for 30 seconds, then blotted off with filter paper. The samples were loaded into the transmission electron microscope (JEOL 1230) and imaged at magnifications ranging from 2,500 - 150,000X.

## 2.3 Results

A limiting factor of this project was the amount of pure, soluble AFP6 for experiments. Table 2, below, summaries the several different preparations of synthetic AFP6 that were ordered from three different manufacturers and the issues in the solubility or lack of protein present in each case.

Table 2: Synthetic AFP6 obtained for use in this thesis.

| AFP6 preparation (manufacturer) | Year received | Soluble in aqueous buffer | % Purity (determined by manufacturer) | Mass present / mass ordered |
|---|---|---|---|---|
| BioBasic | 2018 | Yes | 77% | 0.66 |
| Genscript | 2018 | Yes | >95% | 0.13 |
| Biomatik | 2018 | No | >95% | N/A |
| BioBasic | 2019 | Yes | >95% | 0.1 - 0.2 |
| Biomatik | 2019 | Yes | >95% | 0.5 |

### 2.3.1 Evaluation of ThT Fluorescence of AFP6 Ice-Binding Induced Amyloid Formation

While the mass of AFP6 received was much less than ordered, attempts to follow the AFP6 ice-binding induced amyloid formation were made. The method that led to the results below utilized two separate AFP6-ice interaction steps, as described in the Materials and Methods. AFP6 was incubated with an ice surface, then thawed, and incubated with another ice surface before melting again mixing with working ThT solution. The control was instead incubated at 4 °C and had distilled $H_2O$ added to make the volume equal between samples. Using the endpoint assay format, ThT fluorescence was similar in samples of synthetic AFP6 that were allowed to interact with ice and in AFP6 that was incubated at 4 °C without ice (Figure 10).

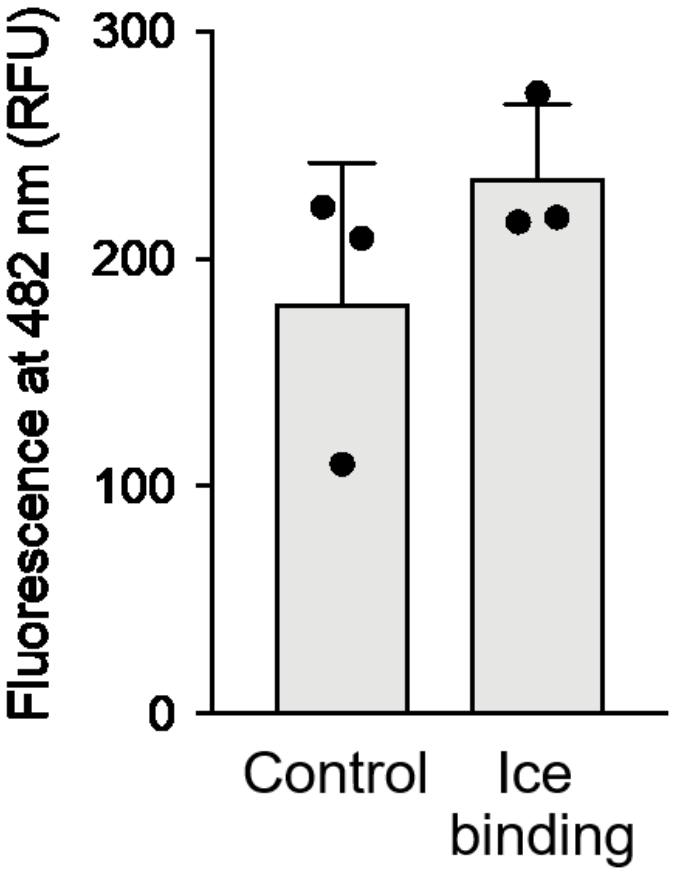


Figure 10: ThT fluorescence of synthetic AFP6 after incubation with and without an ice surface. Synthetic AFP6 (17.5 mM) was pipetted directly onto an ice surface and incubated at -3 °C. The presence of an ice surface increased the ThT fluorescence of synthetic AFP6 compared to a control that was kept at 4 °C. Results are the average of a triplicate and bars represent standard deviation.

As the results from the AFP6 ice-binding induced amyloid formation assay modeled after the assay developed by Dubé et al. (2016) a simpler assay based off the repeated freeze and thaw method proposed by Graether et al. (2003). A shaking step was added afterwards to further attempt to agitate the peptide and ensure amyloid formation. TEM of synthetic AFP6 samples after the repeated freezing and thawing assay described in the Materials and Methods also showed fibril growth (Figure 11). These fibrils were not present in a sample of AFP6 that had been kept at 4 °C instead of freezing.

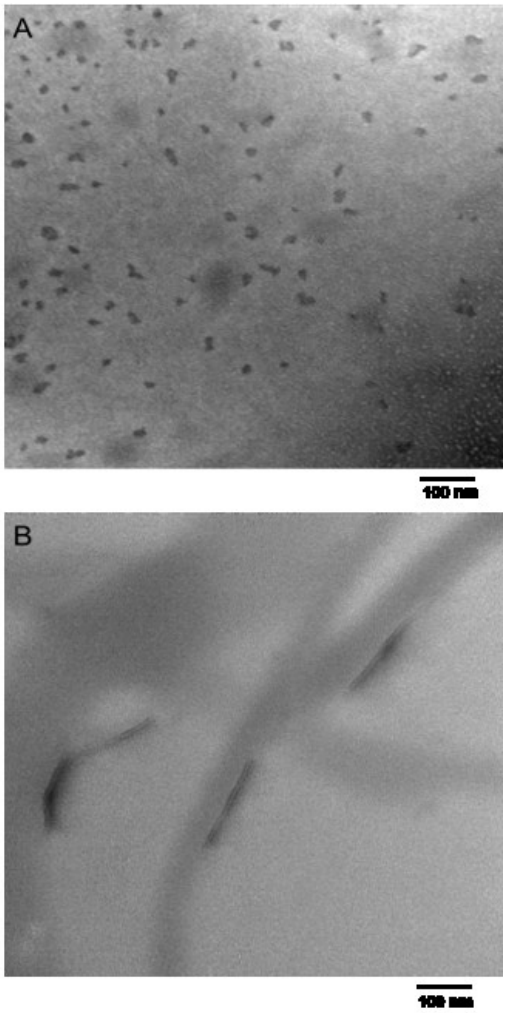


Figure 11: TEM analysis of AFP6 fibrils after repeated freezing and thawing, followed by shaking monomers at 600 rpm at 37 °C. Samples taken from plates were concentrated by vacuum centrifuge from 326 µM to 720.6 µM before staining with uranyl acetate as described in the Materials and Methods. Panels show samples of control AFP6 incubated at 4 °C instead of freezing and thawing (panel A) and AFP6 fibrils formed after repeated freezing and thawing followed by shaking at 37 °C (panel B).

### 2.3.2 Evaluation of ThT fluorescence of AFP6 after AgI induced amyloid assays

As an alternative to ice, silver iodide (AgI) is commonly used in cloud seeding as it exhibits a similar crystalline structure to ice and can induce ice formation in supercooled water (Ćurić & Janc, 2013). If the ice surface necessary for the amyloid formation of AFP6 could be replaced by AgI, it could potentially simplify the assay as the AgI would possibly be able to be reused multiple times for repeated assays, much like a catalyst, and the risk of accidental melting would be eliminated. Preliminary experiments were carried out to test the viability of this theory. ThT fluorescence of AFP6 in the presence of AgI was increased compared to that of AFP6 without it and shaking at 600 rpm increased the fluorescence further (Figure 12).

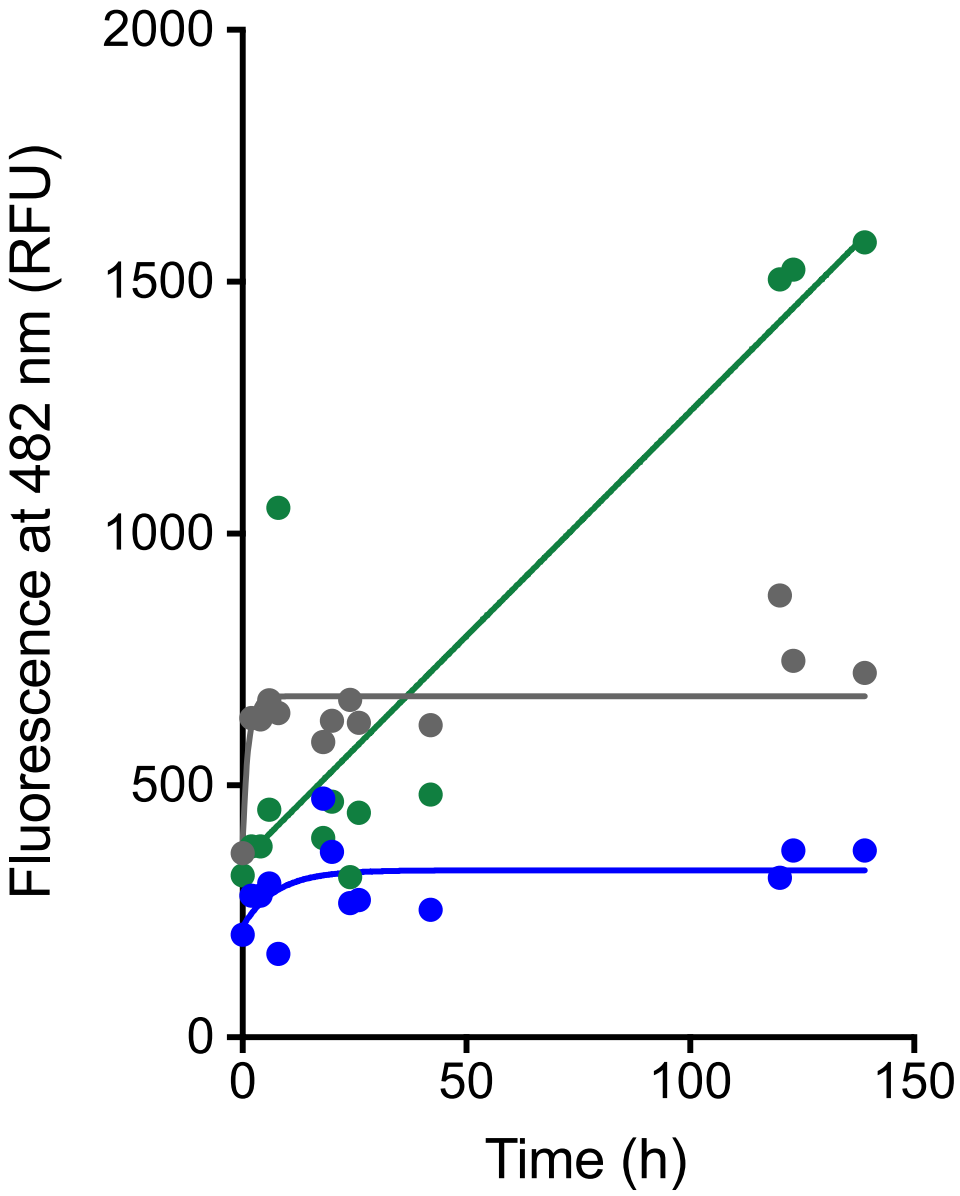


Figure 12: ThT fluorescence of AFP6 (12 mM) in the presence of AgI after shaking at 600 rpm at 37 °C. Triplicate samples of AgI alone (grey), AFP6 with AgI (green), AFP6 alone (blue) were incubated at 4 °C as described in the Materials and Methods was then shaken at 600 rpm, 37 °C, for 149 hours. ThT fluorescence was measured at intervals over this time. Points are the means of duplicate measurements.

### 2.3.3 aβ in-situ amyloid seeding assay

To test cross seeding between AFP6 amyloid and other amyloidogenic compounds, a seeding assay had to be implemented to track fibril formation over time. Before the addition of AFP6 amyloid, a self seeding of aβ amyloid was first implemented. This involved first creating a stock of aβ fibrils by shaking aβ monomer at 600 rpm at 37 °C. The formation of amyloid fibrils was investigated in the aβ monomer samples by TEM following the *in situ* assay (Figure 13). The designed assay revealed that the addition of 60 µL aß fibril shortened the lag phase when shaken at 400 rpm at 37 °C (Figure 14). In comparison, a lower amount of fibril stock (5 µL) had no difference when compared to just aß monomer alone. As shown in Figure 14, the mean initial fluorescence in samples of aß containing no seed, 5 µL seed and 60 µL seed are nearly identical. However, the fluorescence increases far more rapidly in the 60 µL-seeded samples than in the others. The amyloid modulating compound EGCG reduced the ThT fluorescence of aß monomer compared to all other samples. The increasing level of ThT fluorescence throughout the assay had suggested fibril growth and TEM of a prior assay indicated the presence of fibrils consistent with the ThT result (Figure 13).

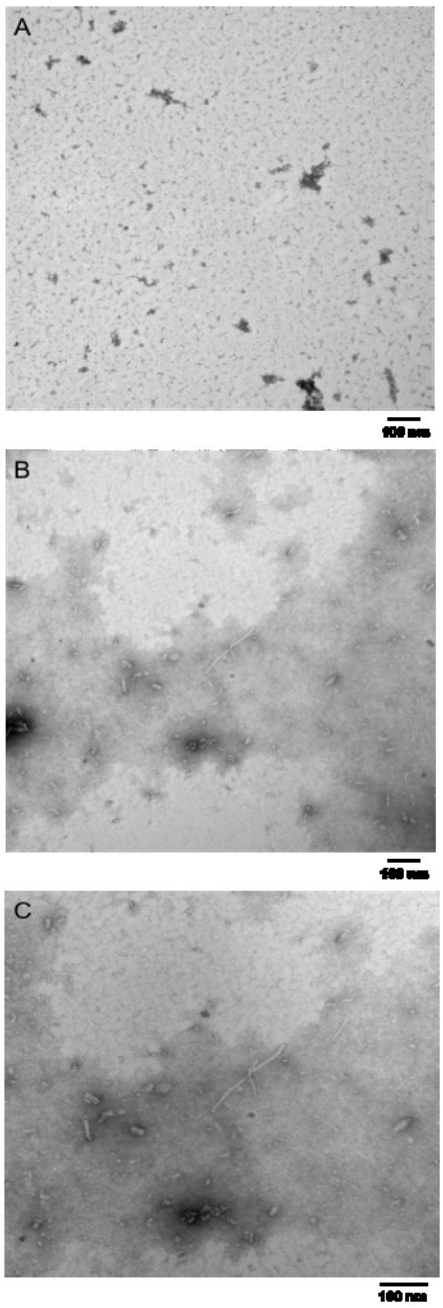


Figure 13: TEM analysis of Aß fibrils after shaking monomers at 600 rpm at 37 °C. Samples taken from plates were concentrated by vacuum centrifuge from 8 µM to 17.68 µM before staining with uranyl acetate as described in the Materials and Methods. Panels show a control sample with no protein (panel A) and a sample of aβ fibrils after shaking at 37 °C for 70 hours (panels B and C)

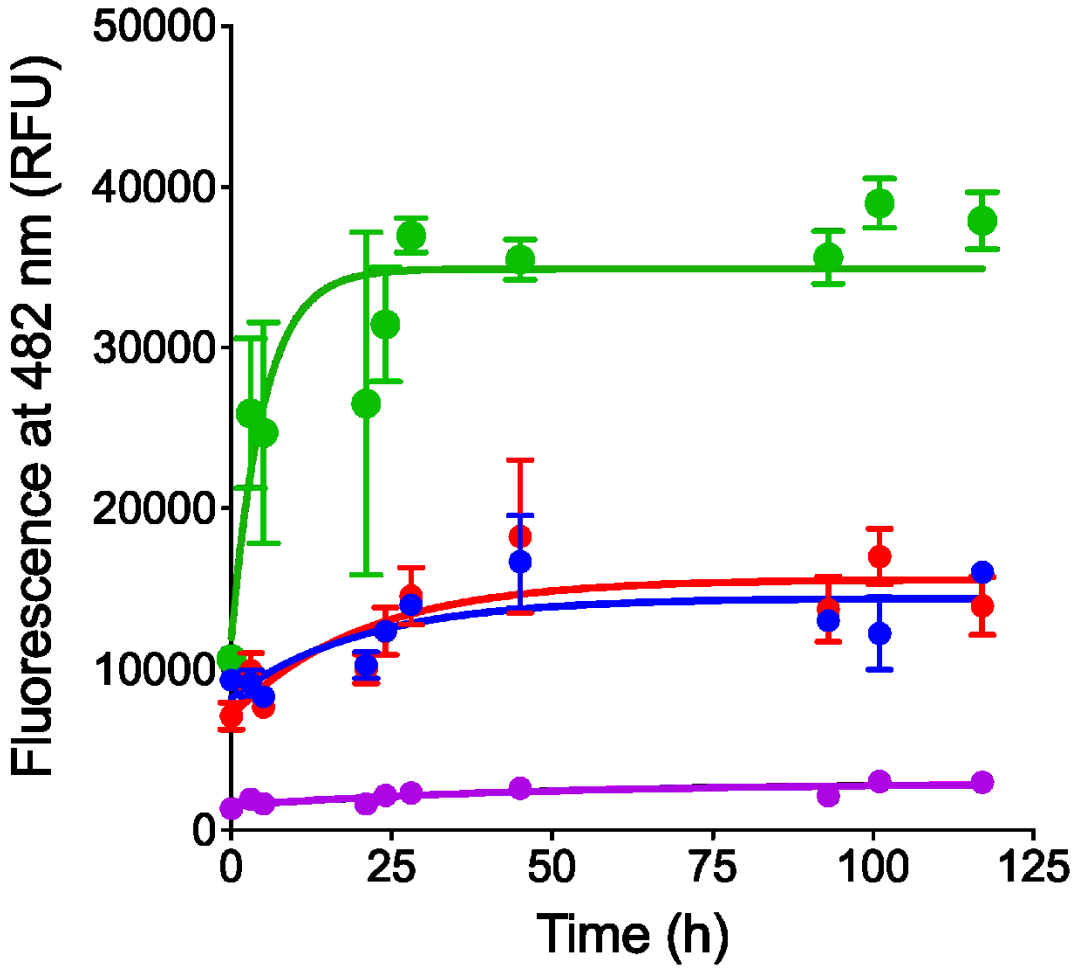


Figure 14: Effect of amyloid seeding and inhibition on the progress of amyloid formation by aß measured using ThT fluorescence. The aß was incubated with and without aß fibril seed after shaking at 37 °C, 400 rpm. The curves above are 8 µM aß monomer with 60 µL of aß fibril stock (green), are 8 µM aß monomer with 5 µL of aß fibril stock (red), 8 µM aß monomer (blue), 8 µM aß monomer, 16 µM EGCG (purple). All samples were prepared in triplicate and shaken at 400 rpm at 37 °C, the bars represent standard deviation.

## 2.4 Discussion

### 2.4.1 Amyloid transition of AFP6 upon interaction with ice

Previous work has shown that AFP6 can transition into amyloid formation upon repeated freezing and thawing (Dubé et al., 2016; Graether et al., 2003; Graether & Sykes, 2009). The work from Dubé et al. (2016) showed that it is binding to the ice surface, rather than the phase change or temperature change, that leads to the formation of amyloid from AFP6. The goal of the current work was to further the understanding of the transition in AFP6 to an amyloid form by exploring aspects of its seeding and templating behaviour, such as the possibility of cross-seeding of the aß transition to an amyloid form. Testing for this required both the replication of the ice interaction assay used by Dubé et al. (2016) as well as the design of a *in-situ* assay that would allow for monitoring of amyloid fibril growth.

Preparation of synthetic AFP6 solutions for this work was a challenge in part because of the poor solubility of some synthetic AFP preparations combined with the high concentrations of AFP required for this transition, as previously reported (Dubé et al., 2016; Graether et al., 2003; Graether & Sykes, 2009). The use of AFP6 in high concentrations is not restricted to those who have worked on its amyloidogenic properties. Prior studies routinely used at concentrations of 7.6 -11 mM (~24.6 -33 mg/ml) of synthetic AFP6, so it is well documented that the synthetic form is soluble at these concentrations (Baardsnes et al., 1999; Haymet et al., 1999; Low, Lin, & Hew, 2003; Wen & Laursen, 1993; W. Zhang & Laursen, 1998).

A problem encountered in the planning and optimization of this assay was the limiting amount of pure synthetic AFP6. This was unprecedented, as noted above. For this project, five orders for pure synthetic AFP6 were placed with two manufacturers. The first of which was a preparation from BioBasic Inc. After some time, the company indicated that they had run into issues and had failed twice in their attempts to synthesize the peptide. On the third attempt the company was able to produce AFP6, but at 77% purity instead of the >95% ordered. This semi-pure preparation was quite soluble and was therefore used in preliminary ice seeding assays as well as in SDS-PAGE experiments. However, it was not at the level of purity that Dubé et al. used in their experiments (Dubé et al., 2016). Table 2 summarizes the challenges faced with ordering synthetic AFP6.

The above synthetic AFP6 from BioBasic Inc. had shown the best solubility thus far, even if the product was less pure, another order was made from the company. While they once again ran into issues preparing the peptide they eventually reported that they were successful in the synthesis of 49 mg AFP6. While this preparation was readily soluble in 10 mM ammonium acetate, SDS-PAGE analysis suggested that the mass of protein received was much lower than 49 mg (Chapter 3, Figures 3.5-3.6). Further quantification revealed the sample to have been roughly 10 mg of AFP6. This was concentrated and used in SDS-PAGE experiments.

A second preparation of 40 mg of AFP6 from Biomatik proved to have a limited mass of AFP6 soluble in 10 mM ammonium acetate. Due to insufficient quantities of the soluble protein, amyloid formation research was not further pursued. Preliminary experiments based on a simpler freezing and thawing method such as that described by Graether et al. (2009) showed increased ThT signal and amyloid fibrils upon examination

with TEM. Attempting to repeat the ice interaction assay from Dubé et al. (2016) on a new circulating chiller however showed inconsistent results. This included preliminary testing with flounder plasma and semi-purified AFP6 as described previously in the Materials and Methods section, as well as limited attempts using synthetic AFP6.

Flounder plasma was used to gain familiarity with the method as well as try out slight modifications to the original method before using synthetic AFP6. This included differences such as changing the incubation time of the samples as – 2 °C or increasing the size of the ice seed. The inconsistencies with the plasma and semi pure AFP6 might be expected, as previous work on the amyloid transition of AFP6 involved pure protein. Although flounder plasma contains AFP6, it is a very different solution than that of synthetic AFP6 in 10 mM ammonium acetate. Fish plasma contains a wide variety of proteins at relatively high concentrations, electrolytes, various metabolites and non-protein nitrogenous compounds (reviewed by McDonald & Milligan, 1992)), and it is at a higher pH than the conditions used by Dubé et al. (2016). All of these may alter amyloid formation or lead to background amyloid formation by other plasma proteins that were not being investigated

A further source of variation in the experimental results from those of Dubé et al. (2016) was the equipment used. While amyloid formation was obtained and visualised by the freezing and thawing method noted above, part of the advantage of studying this amyloid transition is that it is rapidly inducible. Consistent freezing and thawing adds time to the experiment and greatly limits control over the formation of amyloid. It is possible that the differences between the circulating chillers used between this work and

that of Dubé et al. (2016) may have affected the reproducibility. For example, the chiller may have different temperature stability.

An assay was designed to study if AgI could potentially replace ice for inducible amyloid formation of AFP6. The assay showed an increase in ThT fluorescence after incubation and shaking of AFP6 with AgI when compared to AFP6 alone, however the AgI crystals alone are fairly large and may have reflected light, giving a signal at the same wavelength as the ThT.

Experiments were carried out using purified AFP6/8, acetone purified AFP6 (prepared by honours student Melissa Carsky), and synthetic AFP6, with but inconsistent results. Due to the low yield combined with solubility issues of the AFP6 described above, there was not enough pure sample to allow for sufficient optimization to generate a reliable assay. Therefore, this was not pursued further.

### 2.4.2 Implementation of *in-situ* homologous seeding assay of aβ

Self propagating, or homologous seeding is an inherent property of amyloid proteins (Chiti & Dobson, 2006; Dorta-Estremera et al., 2013; Toyama & Weissman, 2011). While specific interaction with ice has been shown to induce amyloid transition in AFP6, it was not yet known if the amyloid formed by this ice interaction could template amyloid formation in other amyloidogenic proteins (Dubé et al., 2016). If the amyloid can seed the natively folded monomer, the amyloid formation would have a shorter lag phase and nucleation would begin sooner. An effective assay was implemented to monitor this, based upon monitoring the amount of fibril growth in samples of monomer versus samples that had monomer along with fibril seeds. This cross seeding of AFP6

fibrils with a known amyloid forming protein lead to the use of aß and the implementation of an *in-situ* amyloid seeding assay.

The *in-situ* seeding assay is based on the binding of ThT to amyloid fibrils. The first implementation was an endpoint assay based on incubation of Aß-42, which has a higher propensity for aggregation that the shorter isoform of Aß-40 (El-Agnaf, Mahil, Patel, & Austen, 2000; Shen, Ji, & Zhang, 2008). Initially, endpoint assays were used based on incubating aß monomer at 37 °C for extended periods of time. This first iteration of the assay did not result in an increase of ThT fluorescence over time, indicating that fibrils were not formed. This led to the addition of a shaking step, also at 37 °C, at 600 rpm the results corresponded to those reported previously the typical sigmoidal amyloid forming plot shown in the literature (Batzli & Love, 2015). TEM analysis showed that with shaking at 600 rpm at 37 °C, fibrils were present in samples collected from the wells of the plate after the end of the assay interval.

After the initial detection of fibrils by TEM, the assay shaking speed was increased, leading to higher maximal ThT fluorescence values. The concentration of fibril seed was varied as well in order to observe whether a higher concentration of fibril seed leads to a quicker nucleation phase than a smaller concentration of fibril seed. If the samples are shaken too fast, or if insufficient early time points measurements are made, the nucleation step can be missed, and the effect of seeding will not be detected. Over several seeding experiments, it was found that shaking at 400 rpm was optimal for observing the transition between lag and nucleation phases of amyloid formation through ThT fluorescence.

Another important aspect in the development of the *in-situ* seeding assay was the inclusion of a known anti-amyloid compound in EGCG. In each experiment it was added in a 1:2 molar ratio with the aß and these samples showed a noted and repeatable lack of increase in ThT fluorescence, suggesting that amyloid did not form. The initial ThT fluorescence measurement was lower for the sample containing ECGG than the aβ monomer alone or aβ monomer with amyloid seed. This may indicate that a portion of the aβ monomer stock has formed some fibrils that the EGCG is modifying. This could be expanded to test multiple other anti amyloid compounds within the same assay, seeing if they affect AFP6 amyloid in the same way they do aß.

This fully implemented assay was then ready for use with AFP6. Homologous seeding would have included first inducing amyloid formation via ice seed, then incubating those amyloid fibrils with native monomer under the same conditions used for the aß to confirm the results found by Graether & Sykes (2009). This would include different concentrations of fibril in comparison with the monomer and incubation with anti amyloid compounds as well. Heterologous seeding, with amyloid of the AFP6 incubated with aß monomer and vice versa would be easily comparable as well.

### 2.4.3 Concluding Remarks

While the capability of AFP6 to cross seed other amyloid -forming compounds was not determined in this research, assays were implemented to ensure this work can be quickly continued in the future. In contrast to earlier studies, a critical limitation in this initiative was the limited availability of soluble synthetic AFP6. Although more work will be required in order to implement the rapid amyloid inducing assay used by Dubé et

al. (2016), amyloid formation from repeated freezing and thawing was detected, in agreement with earlier studies (Graether et al., 2003; Graether & Sykes, 2009).

While the results of ThT assays in this study were equivocal and inconsistent, the TEM studies revealed fibrils typical of amyloid formed by AFP6. Despite this, the implementation of assays for aß seeding and the confirmation of fibril formation by both aβ and antifreeze protein in our assays by TEM set the stage for future work in which possibilities such as cross seeding of aβ fibrillation by AFP6 can be efficiently investigated.

# CHAPTER 3: INTERACTION OF AFP6 WITH CURCUMIN

## 3.1 Introduction

Curcumin is an intensely studied natural product, with studies suggesting a variety of effects relevant to wound healing, antioxidant activity, and neuroprotection. One research application relevant in which it is being investigated is amyloid detection. Curcumin fluoresces at 520 nm when bound to aß, allowing detection in solution, in cells and in tissue sections (Fu & Cui, 2018; Yang et al., 2005). This has raised the additional possibility that curcumin derivatives could eventually find clinical use in the diagnosis of Alzheimer's disease.

Curcumin has low solubility in water. Therefore, studies on curcumin binding to amyloids employ solutions of the compound prepared in organic solvents such as ethanol, some involve the addition of strong acids for further solubilization and eventual dilution into the working aqueous solution ( Liu et al., 2012; Pandey et al., 2008; Yang et al., 2005). These methods of solubilizing curcumin make it difficult to interpret the amyloid-binding results. The involvement of an organic solvent raises the risks of (1) solvent remaining to interfere with the experiment at hand, if not properly controlled for, (2) the precipitation of curcumin from the solution post-dilution, resulting in a lower and unknown concentration (Bahadori & Demiray, 2017).

In addition to its use as a specific stain for aß detection, curcumin has been evaluated as a general fluorescent stain for proteins (Kurien, Dorri, & Scofield, 2012). The preparation of curcumin for this purpose does not involve organic solvents. Protein staining requires the preparation of an aqueous curcumin solution, which must be heated

to boiling in order to achieve a sufficient level of curcumin solubilization (Kurien et al., 2012). This appears to be distinct from the curcumin preparations used in amyloid detection, since the binding of a lysozyme amyloid by curcumin declined with increasing curcumin pre-incubation temperature when evaluated between 10 and 70 °C (Liu et al., 2012).

Following acetone purification of AFP6, SDS-PAGE evaluation was planned. However, the visualization of AFP6 following SDS-PAGE is challenging. Following PAGE, most proteins can be visualized in the gel using Coomassie blue or the more sensitive silver staining procedures (see Chapter 1). However, neither of these stain AFP6. A 0.3 M solution of $CuCl_2$ used as a negative stain, allowed effective detection of AFP6; however, the clear protein bands were faint with gel opacity insufficient for densitometry. Furthermore, with negative staining, band intensity cannot be quantified.

Experiments with curcumin staining following the methods of Kurien et al. (2012) showed that AFP6 subject to SDS-PAGE could be stained fluorescently with curcumin (M. Carsky and E. Donovan, unpublished). For this reason, it was of interest to determine the sensitivity and specificity of the stain and to further examine its binding to AFP6. Therefore, the experiments detailed in this chapter were designed to characterize the binding of curcumin to AFP6.

## 3.2 Materials and Methods:

### 3.2.1 Preparation of AFP6

AFP6 was prepared as described in the Materials and Methods section of Chapter 2, that is solubilized in 10 mM ammonium acetate, pH 6. Three preparations of synthetic AFP6 were used in the experiments described in this chapter. SDS-PAGE experiments used both the 77% and 95% pure BioBasic AFP6 described in table 2 in Chapter 2. All other experiments used the soluble 95% pure Biomatik AFP6 preparation also described in the table 1.

### 3.2.2 Aqueous solubilization of curcumin

The preparation of aqueous curcumin was adapted from the published method by Kurien et al (2012). As curcumin is light-sensitive, this method was carried out with the overhead fluorescent lights turned off, the door closed, and window blinds turned down in order to ensure low-light conditions. A preparation of 100 mg of 95 % curcumin (Alfa Aesar) was weighed. $H_2O$ was heated to 90 ºC and 20 mL were added to the dry curcumin. The preparation was vortexed then placed in a boiling water bath on a hot plate for 10 minutes. The sample was centrifuged in a Sigma 3K15 (Sigma-Aldrich) at 5000 rpm for 10 minutes at room temperature. The supernatant was transferred to a new tube and centrifugation was repeated. The resulting supernatant was transferred to a fresh container and kept at room temperature in the dark for up to 4 hours before used as a protein stain.

### 3.2.3 SDS-PAGE

RunBlue™ TEO-Tricine SDS-PAGE gels with an acrylamide gradient of 4-20% were used along with manufacturer-formulated RunBlue™ SDS running buffer and RunBlue™ LDS sample buffer (Expedeon). The gels were run according to the manufacturer's instructions.

Standard (glycine) SDS-PAGE gels were made and used according to the method of Laemmli (1970) with modifications by Rath, Cunningham and Deber (2013) in order to resolve small peptides. Acrylamide (40%, Bio-Rad) with a 29:1 ratio of acrylamide to bis (38.68 g acrylamide to 1.32 g bis-acrylamide per 100 mL) was used instead of the standard 37.1:1 ratio typically used. The stacking gel was prepared with a total acrylamide concentration of 3% with the resolving gel prepared to18%. The gels were resolved under constant voltage at 140 V until the dye front had reached the end of the gel.

### 3.2.4 Coomassie Blue Staining

Coomassie blue stain was prepared by dissolving 1 g of Coomassie Brilliant Blue R 250 (Bio-Rad) in 250 mL of isopropanol diluted with 400 mL 20% acetic acid, then further diluting with 350 ml distilled $H_2O$ to give a final total volume of 1 L. The final staining solution was 25% isopropanol, 10% acetic acid and 0.1% Coomassie Brilliant Blue R 250.

### 3.2.5 Silver staining

Silver staining was carried out based on an online-published silver staining protocol ("Silver Stain Protocol," Proteomics Resource Center, Rockefeller University). The gel was fixed in 50% methanol, 5% acetic acid for 20 minutes, washed in distilled $H_2O$ for 10 minutes, incubated in in 0.02% sodium thiosulfate twice for 1 minute each and then washed twice in distilled $H_2O$ for 1 minute each. The silver reaction took place in 0.1% silver nitrate, 0.08 % formalin solution in which the gel was incubated for 20 minutes. The gel was washed for 1 minute in distilled $H_2O$ and then developed in 2% sodium carbonate, 0.04% formalin until bands were sufficiently developed. Further development of the bands was stopped by incubation in 5% acetic acid for 10 minutes.

### 3.2.6 Fluorescent staining

VividPro™ fluorescent dye (VWR) was used according to the manufacturer's instructions. The gel was fixed in a solution of 40% ethanol, 10% acetic acid for 20 minutes, washed in distilled water for 15 minutes and then stained in 100 ml of 24% ethanol, 7% acetic acid, and 10 μL of the provided commercial stain.

### 3.2.7 Copper Staining

Staining with copper ions was carried out based on the method published by Lee, Levin & Branton (C. Lee, Levin, & Branton, 1987). The gel was placed in 0.3 M $CuCl_2$ immediately after SDS-PAGE for 15 minutes, then placed in distilled $H_2O$.

### 3.2.8 Aqueous Curcumin Staining

Gels were fixed in 25% ethanol, 10% acetic acid for 10 minutes, then washed with deionized water for 10 minutes before staining with aqueous curcumin by incubating the gel in the heat-solubilized aqueous curcumin described above for 25 minutes in the dark.

### 3.2.9 Imaging

$CuCl_2$ gel images were taken with a S10e mobile phone 12-megapixel camera (Samsung). All other gel images were taken with a Protein Simple FluorChem E system using the ethidium bromide-stained gel detection setting for fluorescent stains and the Coomassie blue and silver stained settings for those respective stains.

### 3.2.10 Acetone Purification of AFP6

Solutions of 100 µL of 1 µg/µL synthetic AFP6 (308 µM) and 100 µL of 1 µg/µL synthetic AFP6, 0.17 µg/µL (308 µM AFP6, 2.56 µM BSA) were prepared in 10 mM ammonium acetate, pH 6. Four hundred µL of 99.5% acetone at -20 °C was added to each sample and the resulting solutions were incubated at -20 °C for 2 hours. Samples were then centrifuged at 13,300 rpm in an IEC Centra-M (International Equipment Company) for 10 mins at 4 °C.

Samples were removed from the centrifuge to wet ice (0 °C) and the supernatant was carefully pipetted into a clean microtube, with the remaining pellet left in the original tube. The pellet and supernatant samples were carefully covered loosely with kimwipes

to protect from dust and placed in the fumehood at room temperature to allow for the acetone to evaporate.

After the samples were completely dry (approximately 2 days), 25 µL of 10 mM ammonium acetate, pH 6, was added to each. Five µL were taken from each reconstituted samples, including pellets and supernatants (AFP6 supernatant, AFP6 pellet, AFP6-BSA supernatant, and AFP6-BSA pellet) were mixed with sample buffer and separated by SDS-PAGE using RunBlue TEO-Tricine gels as noted above. Gels were then stained with Coomassie blue and with aqueous curcumin prepared as noted above.

### 3.2.11 Effect of AFP6 on Curcumin Absorbance and Fluorescence

The solubilization of curcumin for these experiments was a modified version of the curcumin solubilization described above. Fifteen mg of curcumin each was added to 8 separate, 1.5 mL microtubes, then 1.0 mL of 10 mM ammonium acetate, pH 6 was added to each tube. Samples were vortexed, then heated for 10 minutes at 70 °C. The samples were then centrifuged for 5 minutes at 7000 rpm (Scilogex) and the supernatants were transferred to fresh tubes. Centrifugation and the transfer of supernatants was repeated 2 more times.

The AFP6 was quantified by the via the method described in the AFP6 solubilisation section described in the Materials and Methods of Chapter 2. Curcumin samples were quantified by measuring absorbance 425 nm on a spectrophotometer (NanoDrop 1000, ThermoFisher or NanoVue, GE Healthcare) using the Beer-Lambert equation with the molar extinction coefficient of the compound in $H_2O$. (Majhi, Rahman, Panchal, & Das, 2010).

Aqueous curcumin and AFP6 were combined to concentrations of 8 μM curcumin and 102.5 μM AFP6 and then incubated at either room temperature or 70 ºC for 10 minutes before plating. Controls of 8 μM curcumin alone were also incubated alongside the samples described above. Two hundred μL triplicates of 8 μM curcumin controls and curcumin with AFP6 were plated in separate rows of UV-transparent 96-well plate (Corning). Triplicates of 200 μL of 10 mM ammonium acetate, pH were used as a blank. The absorbance spectra from 200 to 700 nm of the plated samples was recorded.

A corresponding experiment was run with the same concentrations, blanks, and volumes described above. These samples were then plated in an opaque 96 well plate (Greiner Bio-One) and the fluorescence spectra from 450 nm to 700 nm were recorded with a fixed excitation of 420 nm. Both absorbance and fluorescence spectra were taken with a Molecular Devices SpectraMax M3.

### 3.2.12 AFP6-Curcumin Binding Assay

Aqueous curcumin and AFP6 were prepared by the methods described earlier in the materials and methods of this chapter, with a few modifications. Curcumin was heat solubilized in 10 mM ammonium acetate, pH 6, through incubation at 70 ºC for 10 minutes. Centrifugation was then used to remove the insoluble curcumin before it was quantified. The AFP6 and curcumin were prepared separately and then combined in an opaque 96 well plate (Greiner Bio-One). Each well contained 200 μL of 5 μM AFP6 and concentrations of curcumin from 0.4 μM to 25 μM, with each combination of AFP6 and curcumin being run in triplicate. Blanks consisting of 200 μL of 10 mM ammonium acetate, pH 6, and 200 μL of each curcumin concentration used (without AFP6) were also

run in triplicate. The plate was incubated at the surface of a 70 ºC water bath for 10 minutes, then cooled to room temperature for 20 minutes before being centrifuged at 2,500 rpm briefly (MPS 1000, Labnet). Fluorescence of these samples from 300-700 nm was measured on a SpectraMax M3 microplate spectrophotometer (Molecular Devices) with a fixed excitation of 420 nm.

### 3.2.13 Circular Dichroism of AFP6 with Curcumin

The secondary structure of AFP6 was examined in the presence and absence of curcumin by circular dichroism (CD). The measurements were carried out using a DSM20 spectropolarimeter (Olis) with a 0.2 cm cuvette.

A stock of 8 mM potassium phosphate buffer consisting of 1.1 mM $K_2HPO_4$ , 6.9 mM $KH_2PO_4$, pH 6, was prepared by dissolving 192 mg of $K_2HPO_4$ and 938 mg of $KH_2PO_4$ in 200 ml of distilled $H_20$ and diluted 1:1 with distilled $H_2O$ to give a solution of 4 mM phosphate buffer (0.55 mM $K_2HPO_4$ , 3.5 mM $KH_2PO_4$). A stock solution of 8 M guanidine was prepared by dissolving 3.52 g of guanidine into in 4.6 ml of the 4 mM potassium phosphate buffer described above. One hundred µM synthetic AFP6 in 10 mM ammonium acetate was buffer exchanged into 4 mM phosphate buffer by filtration through 3-kDa cutoff membranes in microtubes (Vivaspin 3K).

Curcumin was solubilized in the 4 mM phosphate buffer, pH according to the aqueous solubilization protocol described above. Samples were prepared as follows: (1) 4 mM phosphate buffer blank, (2) 20 µM curcumin, (3) 6 M guanidine, (4) 5 µM AFP6, (5) 20 µM curcumin, 5 µM AFP6, (6) 6 M guanidine, 5 µM AFP6. Samples 2, 4, and 5 were all heated to 70 ºC for 10 minutes then cooled to room temperature for 10 minutes before

reading. All samples were read at 5 ºC, with 40 increments between 190-250 nm. Each reading was taken three times and averaged by the system software.

AFP6 is an alpha helical protein, and negative bands at 208 and 222 nm are characteristic CD spectra of alpha helical proteins (Sreerama & Woody, 2004). The molar ellipticity of AFP6 samples at 222 nm was first measured at 5 ºC, then at 5 degree increments up to 70 ºC. This experiment was repeated in full, but with an AFP6 concentration of 3 μM instead of 5 μM.

## 3.3 Results

### 3.3.1 Aqueous curcumin stained AFP6 resolved by SDS-PAGE

Aqueous curcumin, prepared through heat solubilization, binds to AFP6 and fluoresces under UV light. AFP6 does not stain with common laboratory stains such as Coomassie blue, so the staining of AFP6 by aqueous curcumin was evaluated. A series of dilutions of AFP6 were analyzed by tricine SDS-PAGE on 4-20% gradient gels (Figure 15). Aqueous curcumin detected AFP6 at amounts as low as 0.75 μg of AFP6. The relative density of the bands was compared using ImageJ (NIH) and when plotted against AFP6 concentration, resulted in a linear relationship with a regression $R^2$ value of 0.99 (Figure 16).

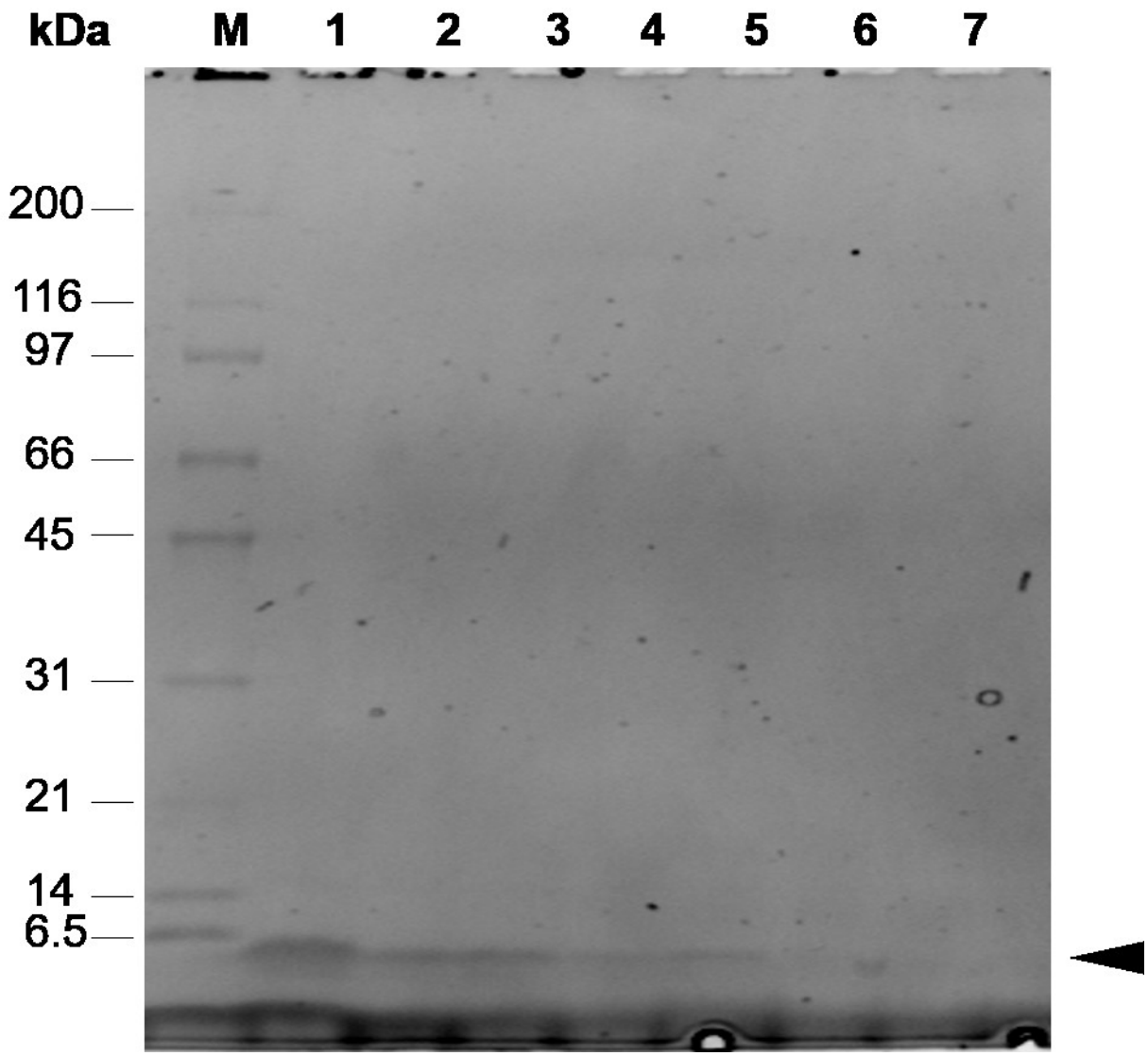


Figure 15: Synthetic AFP6 visualized by aqueous curcumin staining following separation by tricine SDS-PAGE (4-20% acrylamide). Lanes were loaded as follows: Molecular mass markers (lane M), 12 µg AFP6 (lane 1), 6 µg AFP6 (lane 2), 3 µg AFP6 (lane 3), 1.5 µg AFP6 (lane 4), 0.75 µg AFP6 (lane 5), 0.38 µg AFP6 (lane 6), and 0.19 µg of AFP6 (lane 7). Molecular mass markers sizes are indicated in kDa. The position of AFP6 is marked by an arrow.

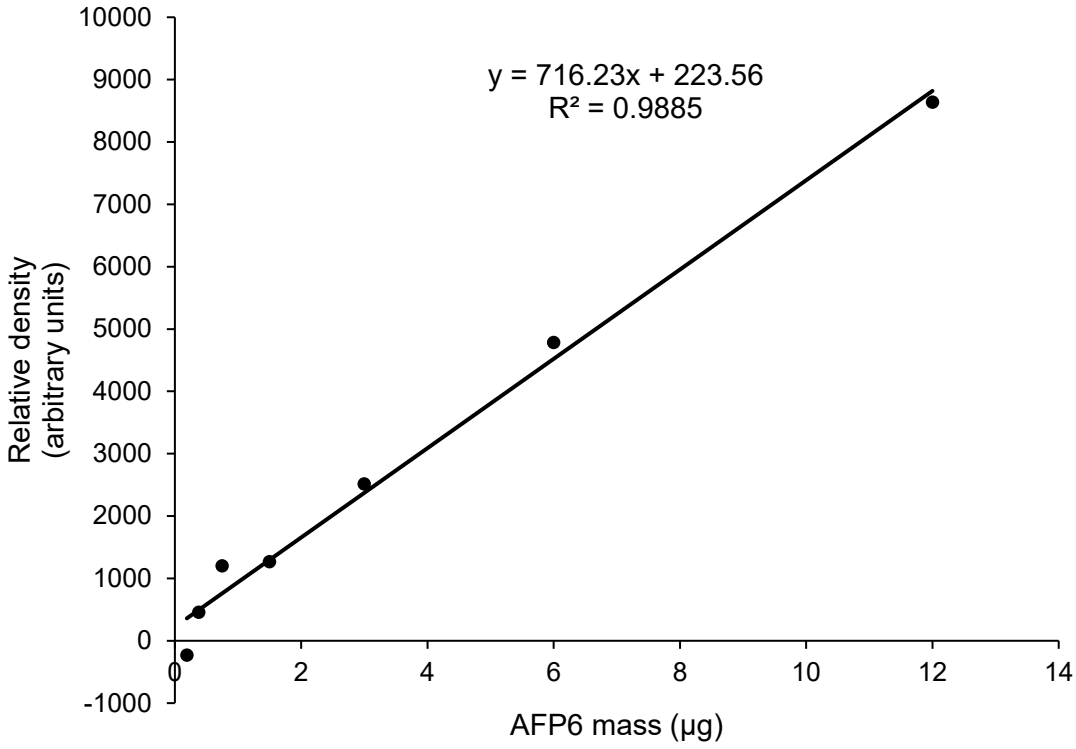


Figure 16: Relative density of AFP6 dilution series visualized by aqueous curcumin following separation by SDS-PAGE. The relative density of the AFP6 bands shown in figure 1 with analysis through ImageJ software.

### 3.3.2 Acetone Purification of AFP6 from a Mixture of Protein

To observe the purification of AFP6 from solutions of AFP6 and AFP6-BSA were separated through tricine SDS-PAGE in 4-20% acrylamide gradient gels and then stained with aqueous curcumin (Figure 17). The AFP6 was only detected in the acetone supernatant; it was absent from the precipitate. Conversely, BSA was not seen in the supernatant taken from the acetone precipitation of the AFP6-BSA mixture, but only in the pellet.

When the same experiment was run, but stained in Coomassie blue prior to curcumin, the AFP6 fluoresced clearly under UV light, while the fluorescence of the BSA and molecular mass markers appeared to be less intensely fluorescent (Figure 18). This suggested that Coomassie blue did not interact with the AFP6.

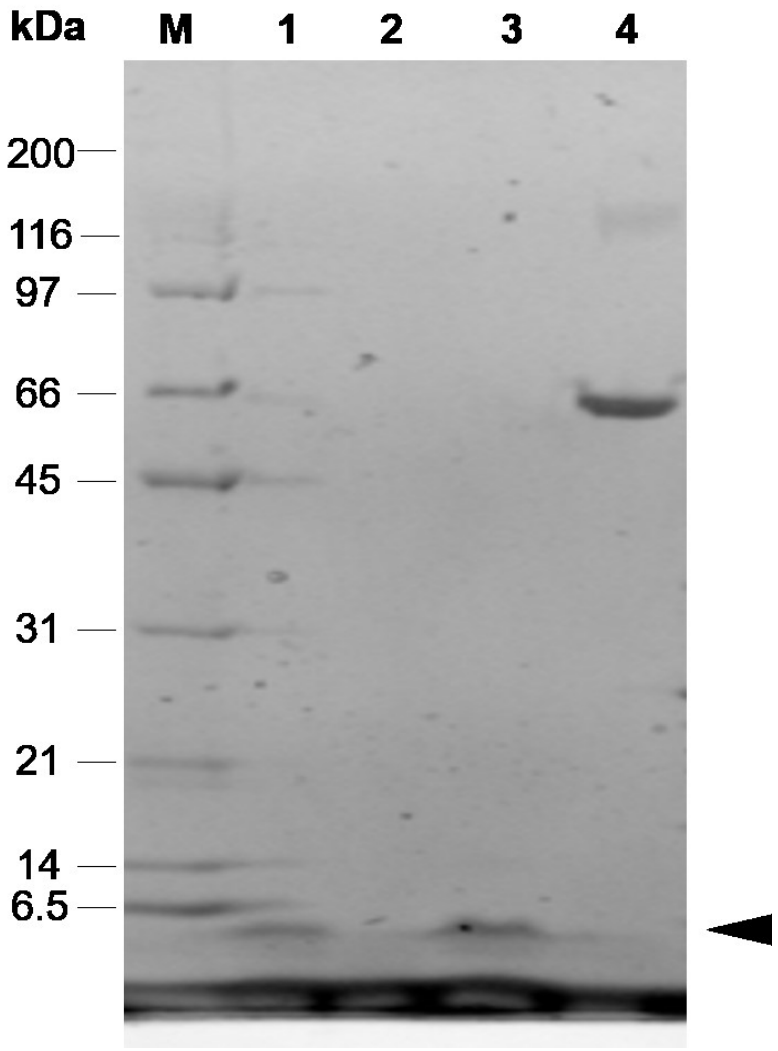


Figure 17: Synthetic AFP6 and BSA visualized by aqueous curcumin staining following separation through acetone precipitation and SDS-PAGE (4-20% acrylamide). Solutions containing 100 µg of synthetic AFP6, alone or 100 µg of AFP6 mixed with 17 µg of BSA were first separated with acetone precipitation as described in the Materials and Methods. Samples were then reconstituted and further separated with SDS-PAGE. Lanes are: molecular mass markers (lane M), supernatant from acetone precipitation of AFP6 (lane 1), pellet from acetone precipitation of AFP6 (lane 2), supernatant from acetone precipitation of AFP6 and BSA (lane 3), pellet from acetone precipitation of AFP6 and BSA (lane 4).

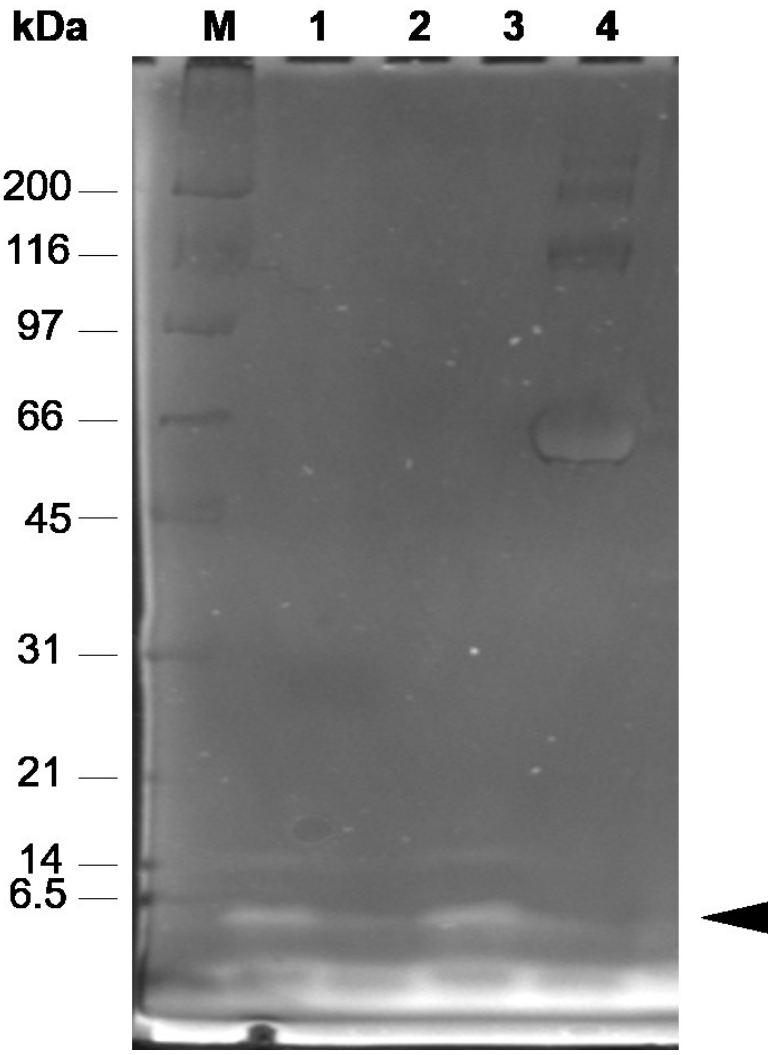


Figure 18: Synthetic AFP6 and BSA visualized by aqueous curcumin staining following separation through acetone precipitation and SDS-PAGE (4-20% acrylamide) and Coomassie blue staining. Solutions containing 100 µL of 1 µg/µL of synthetic AFP6 alone or a mixture of 100 µL of 1 µg/µL of AFP6 and 0.17 µg/µL BSA were separated with acetone precipitation as described in the materials and methods. Samples were reconstituted and separated with SDS-PAGE and consecutively stained with curcumin and Coomassie blue. Lanes are: molecular mass markers (lane M), supernatant from acetone precipitation of AFP6 (lane 1), pellet from acetone precipitation of AFP6 (lane 2), supernatant from acetone precipitation of AFP6 and BSA (lane 3), pellet from acetone precipitation of AFP6 and BSA (lane 4).

### 3.3.3 Glycine-SDS PAGE Separation and Staining of AFP6

Tricine gradient gels were effective in the separation of AFP6 and the aqueous curcumin stained the peptide. The 4-20% acrylamide gradient, however, led to the AFP6 resolving very near the dye front. An 18% acrylamide glycine SDS-PAGE system was set up by experiential learning student Erin Donovan as described in the Materials and Methods of this chapter that resolved the AFP6 closer to the middle of the gel. The 18% acrylamide gel separated out purified AFP6/8 as well as synthetic AFP6 and was compatible with aqueous curcumin stain (Figure 19). Resolution and curcumin staining of the semi-pure AFP and the synthetic AFP6 was evident (Figure 20).

Multiple different stains were used in conjunction with SDS-PAGE (18% acrylamide) to investigate whether they allowed detection of AFP6. Aqueous curcumin, silver, Coomassie blue, and a general fluorescent stain (VividPro) were all used to stain the same set of proteins (Figure 21). Only aqueous curcumin revealed a band at the expected position for the AFP6, while silver staining resulted in a minor band smaller than expected. Coomassie and VividPro did not stain anything in the lane containing AFP6. The stains also differed in their effectiveness of staining for the protein markers. For example, curcumin did not allow clear detection of the 10 and 15 kDa markers, whereas silver stain provided a very weak signal for the 25 kDa marker.

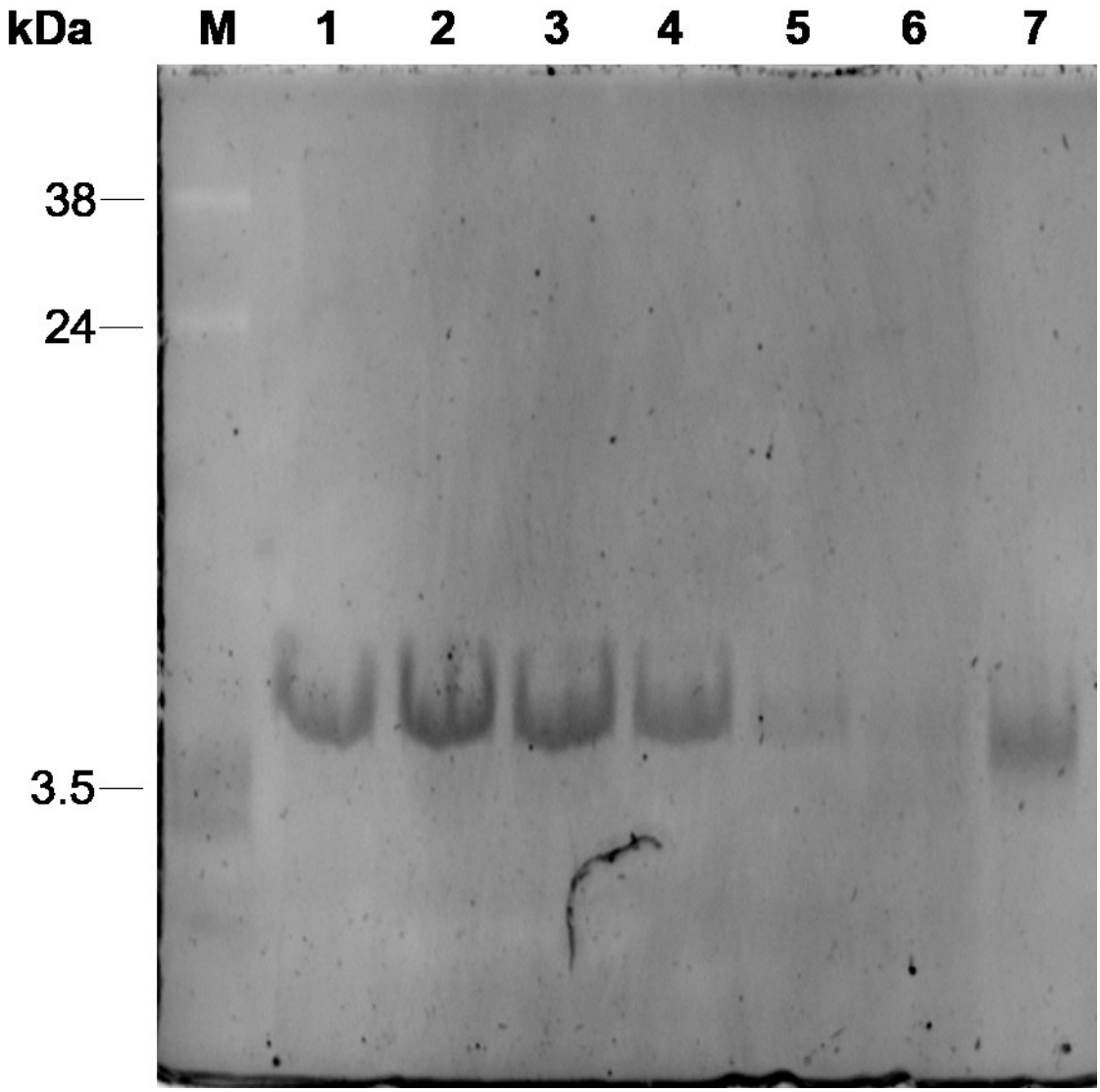


Figure 19: Purified AFP6/8 and 95% pure synthetic AFP6 visualized by aqueous curcumin staining after separation via SDS-PAGE (18% acrylamide). Experiment performed and image prepared by Erin Donovan, prior experiential learning student. Lanes were loaded as follows: Molecular mass markers (lane M), 13.2 µg AFP6/8 (lane 1), 11 µg AFP6/8 (lane 2), 8.8 µg AFP6/8 (lane 3), 6.6 µg AFP6/8 (lane 4), 4.4 µg AFP6/8 (lane 5), 2.2 µg AFP6/8 (lane 6), and 6.6 µg of synthetic AFP6. Molecular mass markers sizes are indicated in kDa.

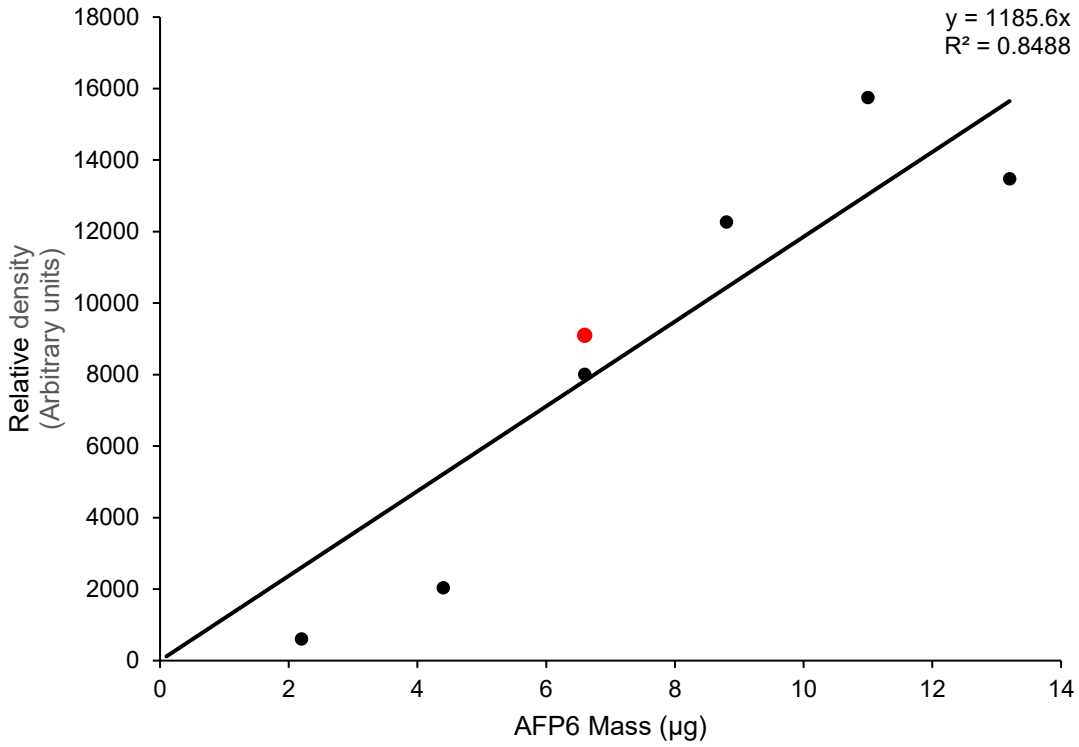


Figure 20: Relative density of a semi pure AFP6/8 series (black dots) along with a sample of synthetic AFP6 (red dot) visualized by aqueous curcumin following separation from SDS-PAGE. The synthetic AFP6 was not included in the regression analysis. The relative density of the AFP6 bands shown in figure 5 with analysis through ImageJ software.

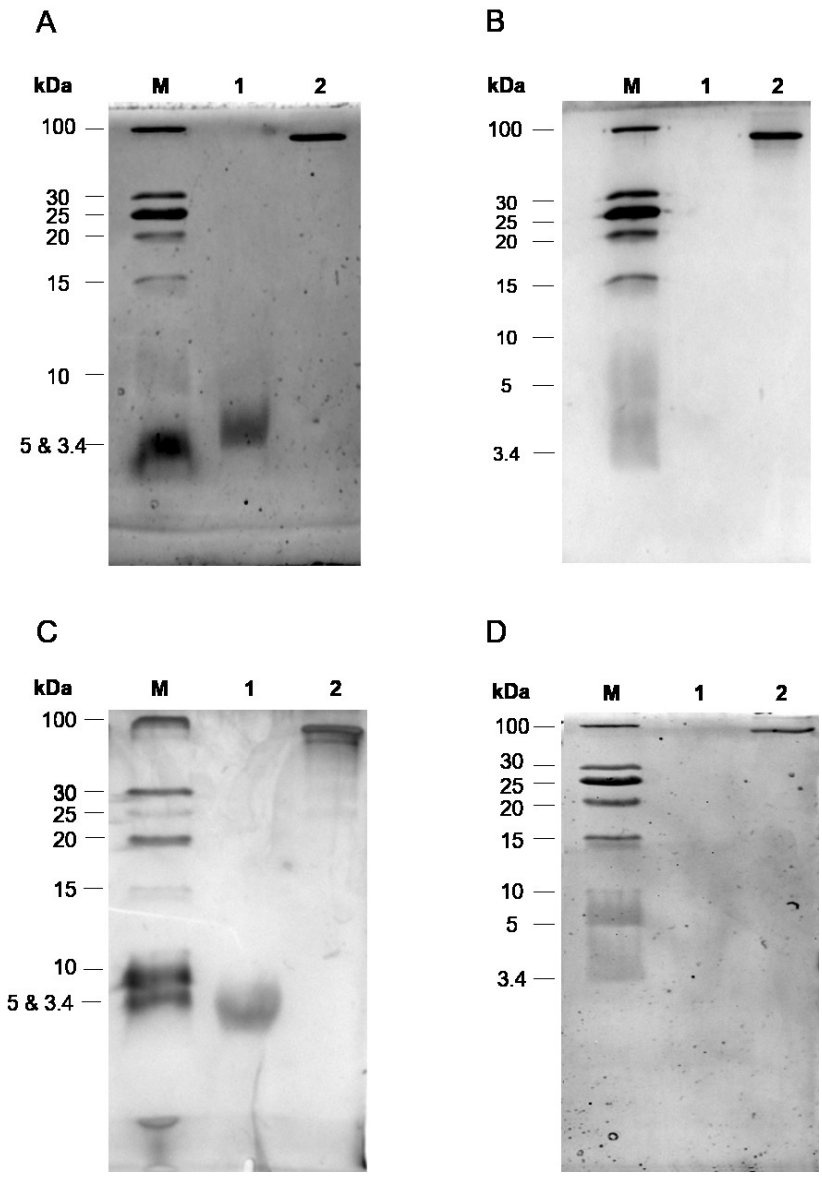


Figure 21: SDS-PAGE analysis of AFP6 with four protein stains. Lanes were loaded as follows: Molecular mass markers (lane M), 12 µg of 77% pure synthetic AFP6 (lane 1), and 1 µg of BSA (lane 2). Samples were separated by SDS-PAGE (18% acrylamide) and stained using four methods; aqueous curcumin (panel A), Coomassie Blue (panel B), silver (panel C), and VividPro fluorescent stain (panel C). Molecular mass markers are indicated in kDa.

$CuCl_2$ only weakly stained the gel when using the 18% acrylamide gels (Figure 22). The $CuCl_2$ produces a negative stain, where the gel itself is stained while the protein bands in the gel are not. The $CuCl_2$ stain also allows for the visualization of AFP6 as well, but it is more difficult to quantify the image. The stains pictured in Figures 21 and 22 show that AFP6 is clearly visible by curcumin, but is not with Coomassie, or VividPro. A band with a lower molecular weight than AFP6 is visible with silver staining.

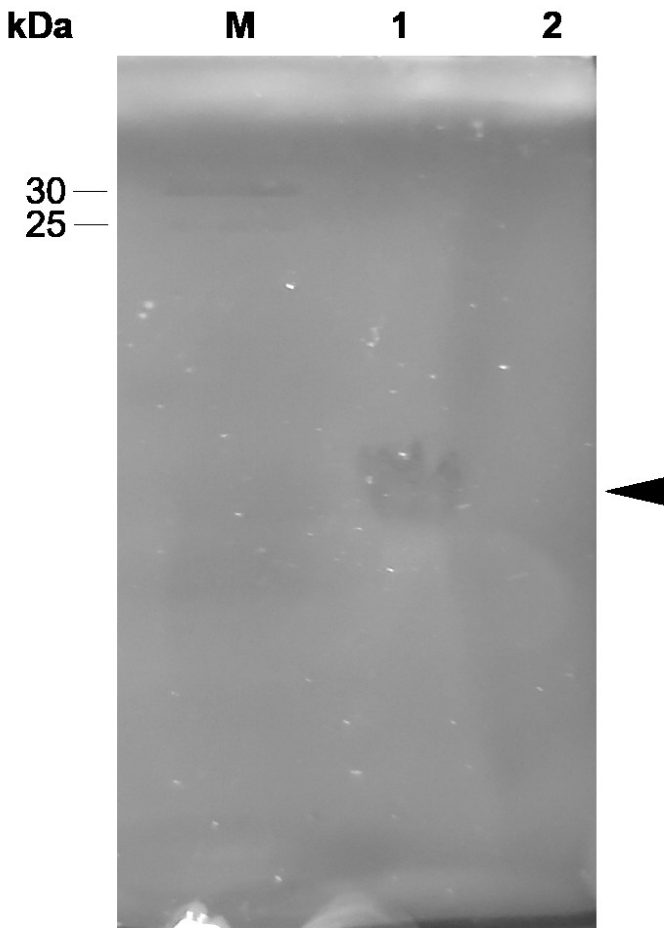


Figure 22: SDS-PAGE analysis of AFP6 with $CuCl_2$ staining. Lanes were loaded as follows: Molecular mass marker (lane M), 12 µg of 77% pure synthetic AFP6 (lane 1) and 1 µg of BSA (lane 2). Samples were separated by SDS-PAGE (18% acrylamide) before staining with 0.3 M $CuCl_2$. Sizes of detectable molecular mass markers are indicated.

### 3.3.4 Absorbance and Fluorescence of Curcumin in the Presence of AFP6

After observing the binding of curcumin by AFP6 after SDS-PAGE, the interaction between the two molecules was further investigated. First, the absorbance and fluorescence properties of curcumin in the presence of AFP6 was measured. By using aqueous curcumin at its solubility limit (~20 μM) with an excess of AFP6 (103 μM), the probability of all the curcumin molecules being bound to AFP6 upon measurement is maximized. The 70 ºC incubation step was added to ensure the AFP6 was denatured as it is during SDS-PAGE. This heating step increased both the absorbance and fluorescence of curcumin in the presence of AFP6 (Figure 23).

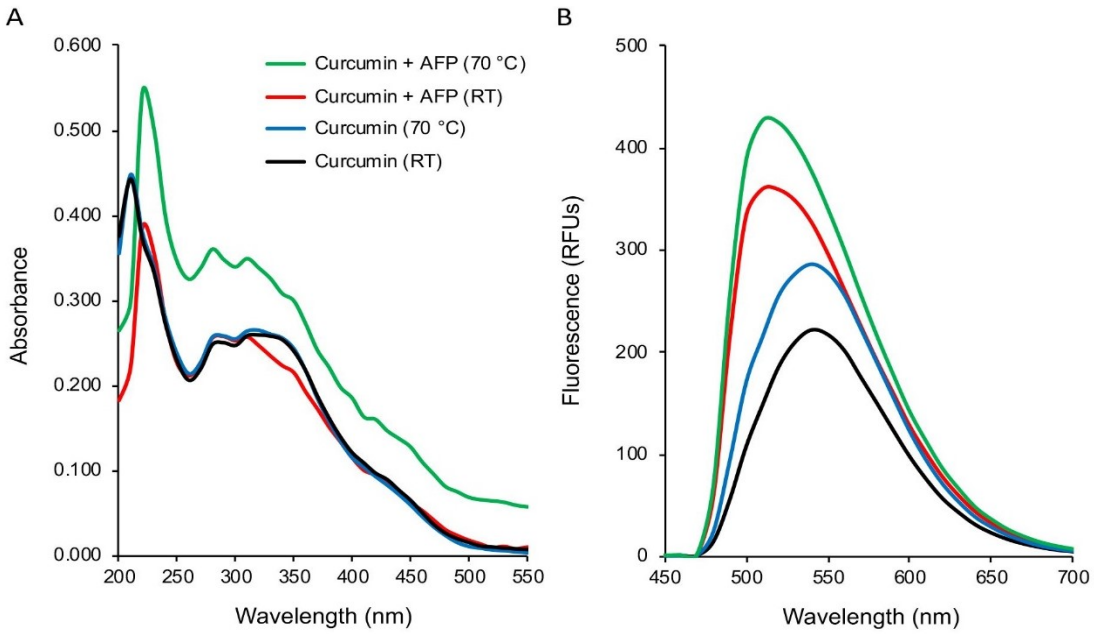


Figure 23: Effect of AFP6 on the absorbance and fluorescence of curcumin. Panel A: The incubation of 8 µM curcumin with 103 µM AFP6 at 70 ºC results in a change in curcumin absorbance. Panel B: Incubation of curcumin with 103 µM AFP6 Each spectrum was the mean of three technical replicates.

The absorbance and fluorescence spectra of curcumin underwent changes in the presence of AFP6 and these were greater when the solution was heated. The absorbance maxima of the curcumin in the absence of protein were to be in the vicinity of 350 nm while the samples with AFP6 did not show this peak. The fluorescence emission of curcumin increased when incubated with AFP6 at either room temperature or 70 ºC. The fluorescence was also blue shifted when compared to the spectra of samples with curcumin alone, which results from emission at a shorter wavelength, and thus higher energy. In the presence of AFP6, curcumin had a fluorescence maximum of 520 nm while in the absence of AFP6, curcumin had a maximum of 540 nm.

The next experiment aimed to investigate the binding of curcumin to AFP6. Fluorescence over a range of curcumin concentrations was recorded after excitation at 420 nm and emission at 500 nm. After subtraction of curcumin fluorescence at each concentration, the fluorescence of the curcumin with AFP6 at 500 nm was plotted (Figure 24). The increase in curcumin fluorescence in the presence of AFP6 was linear over the range of concentrations tested up to the maximum solubility of aqueous curcumin. As the increase in fluorescence at 500 nm was still linear at this curcumin concentration, a dissociation constant ($K_d$) could not be determined.

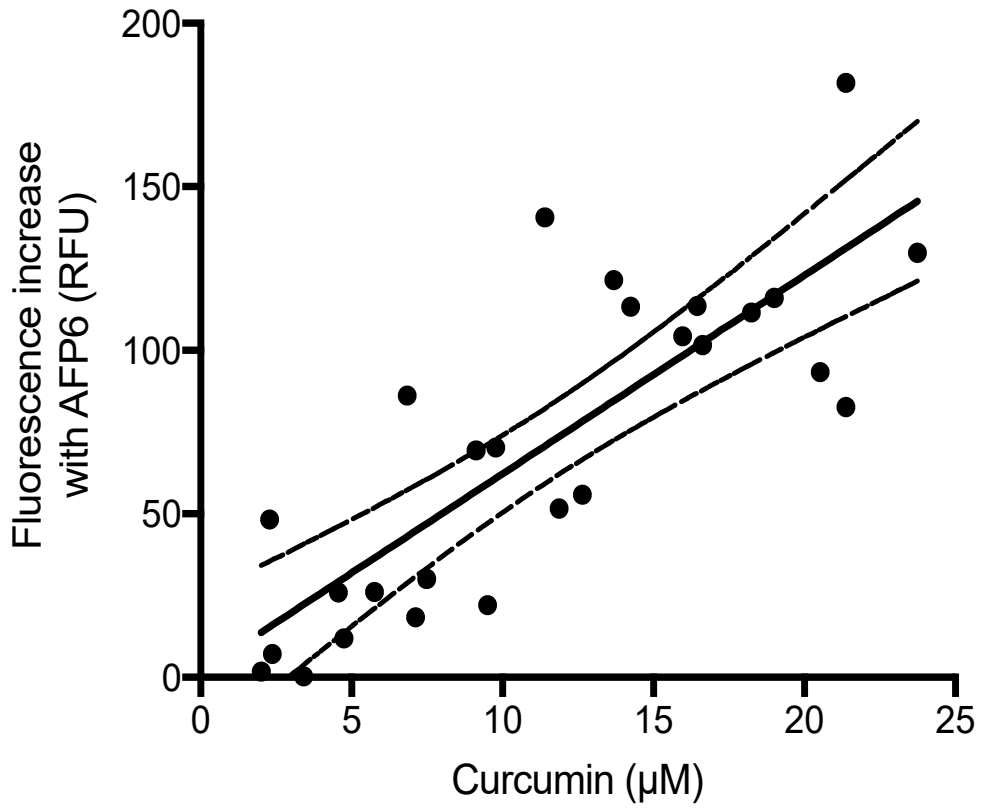


Figure 24: Binding curve of AFP6 and curcumin. The fluorescence of curcumin was determined over a range of concentrations in the presence of 5 µM AFP6, which was kept constant in 10 mM ammonium acetate, pH 6. Fluorescence at 500 nm was recorded after excitation at 420 nm. The solid line is a linear regression and the dotted lines represent the 95% confidence intervals. Each point is the mean value of three measurements.

### 3.3.5 Structure of AFP6 in the presence of curcumin

After exploring how AFP6 effected the absorbance and fluorescence of curcumin, the effects of curcumin on the structure of AFP6 were explored as well. Following pre-heating to 70 ºC and cooling, the AFP6 in the absence of curcumin showed a typical alpha-helical CD spectrum at 5 ºC, with two strong minima at 208 and 222 nm (Figure 25) and a spectrum consistent with unfolded protein in the presence of guanidine. This confirms that the protein readily refolds after the heating step. AFP preheated in the presence of curcumin showed a nearly identical spectrum, suggesting that curcumin binding does not affect the refolding of AFP after heating. Furthermore, in temperature-induced denaturation experiments, the Tm of AFP was virtually identical in the presence and absence of curcumin. Melting curves of AFP6 with and without curcumin were also investigated (Figure 26). In this experiment, the calculated Tm was shifted very slightly from 34 ºC to 36 ºC with curcumin. A prior experiment showed the Tm was shifted from 35.6 ºC without curcumin to 35.7 ºC with curcumin.

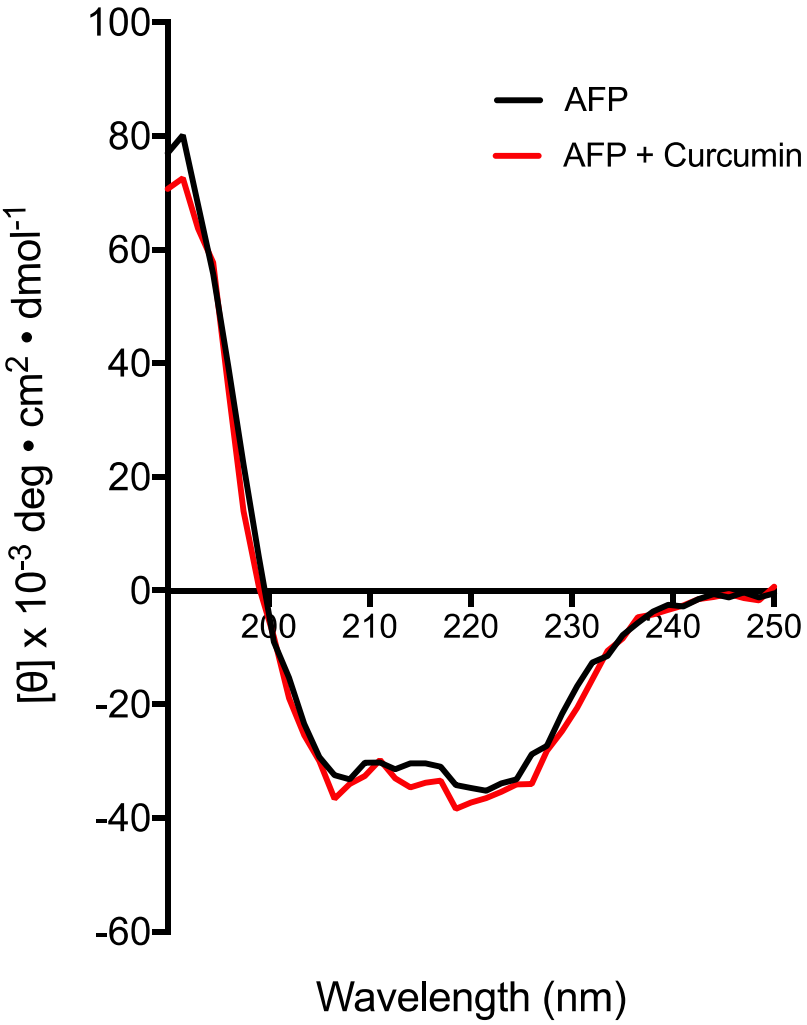


Figure 25: Secondary structure of AFP6 in the presence and absence of curcumin. AFP6 at a concentration 3 µM remained alpha helical after a 10 minute incubation with 20 µM curcumin at 70 ºC.

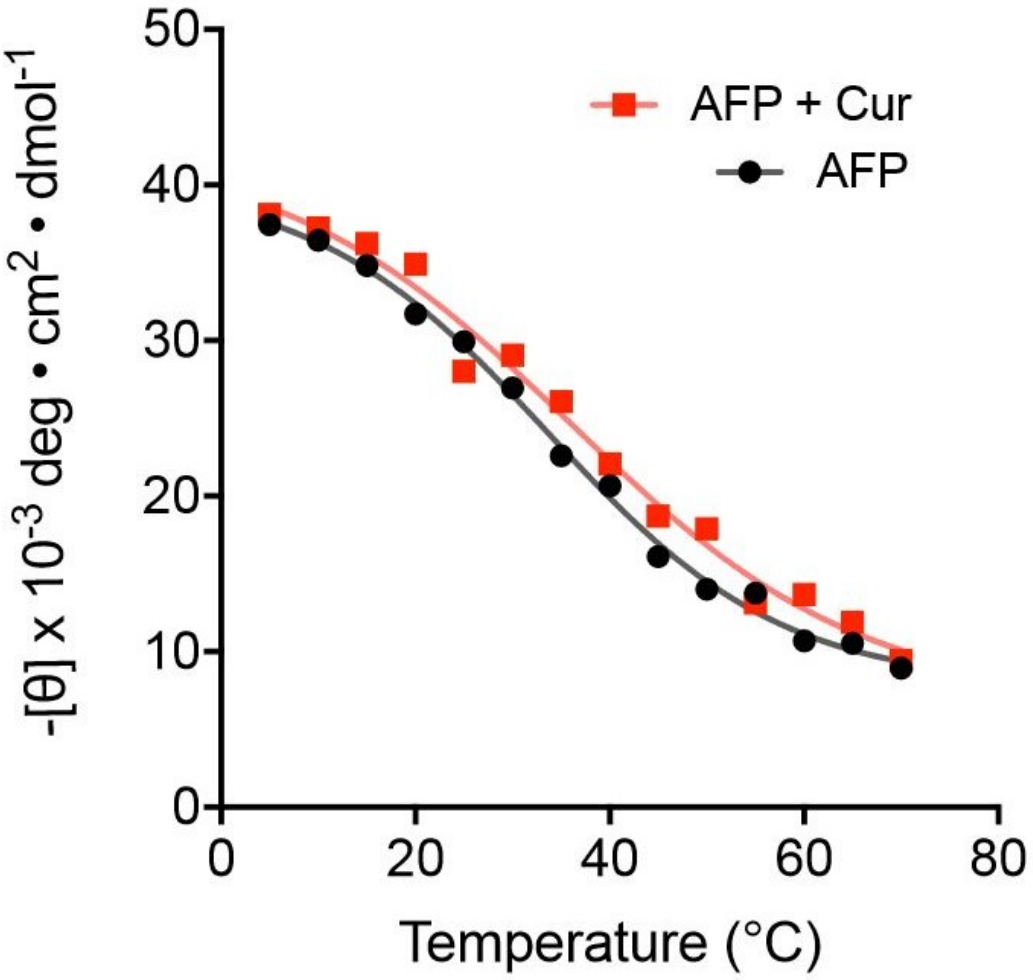


Figure 26: Melting curve of AFP6 in the presence and absence of curcumin. AFP6 at a concentration of 3 μM had approximately the same melting point in 20 μM aqueous curcumin as it did alone.

## 3.4 Discussion:

### 3.4.1 Acetone Purification of AFP6 from a Mixture of Protein

Acetone is a commonly used organic solvent to precipitate proteins from a sample, sometimes as part of purification before further downstream experiments like mass spectroscopy (Crowell, Wall, & Doucette, 2013). Acetone has also been used to solubilize AFP6 at high concentrations in order to allow protein crystal formation for use in protein structure determination (Sicheri & Yang, 1995; Yang, Chung, Chen, Rose, & Hew, 1986). In this work, AFP6 is shown to be soluble in acetone and, since the majority of proteins precipitate in acetone solutions, the AFP can be purified from a mixture of different proteins by way of acetone precipitation. Since AFP6 is abundant in flounder plasma and yet soluble in acetone, this raises the possibility that some peptides in plasma and other tissues might be lost in routine acetone precipitations because of unusual acetone solubility.

### 3.4.2 AFP6 Staining with Curcumin Compared to Other Protein Stains

In order to detect AFP6 following electrophoretic analysis, staining options were evaluated. The systematic comparison of staining by 5 methods revealed that AFP6 bands could be detected using $CuCl_2$ or curcumin, whereas it produced no signal at the appropriate position with more typical staining methods including silver, Coomassie blue and a commercial fluorescent product. Although the aqueous curcumin stain was effective for AFP6, it did not appear to stain marker proteins with even intensity. Therefore, contrary to the proposal that curcumin is a general protein stain (Kurien et al.,

2012), it may not be a widely effective stain . For this reason and because aqueous curcumin did stain AFP6, the interaction between these molecules was further examined here.

Kurien et al. showed that curcumin failed to bind bovine serum albumin (BSA) after BSAhad been stained by silver (Kurien, Dorri, & Scofield, 2012). This led to a hypothesis that silver may share the same binding site as curcumin (Kurien et al., 2012). Silver staining is hypothesized to work by reduction of silver ions that are bound to negatively charged residues (Hempelmann & Krafts, 2017). AFP6 has two aspartic acid residues, one at the N terminus and one at residue 5, which might indicate the possibility of staining by silver. AFP6 also has a Glu22 residue, but it forms a salt bridge with Lys18.

Here we observed that AFP6 was not visible with silver staining on protein gels but is visible with aqueous curcumin staining. While a low molecular weight product did appear after staining 77% pure AFP6, it was smaller than the molecular mass markers at 3.4 kDa. This differed from the AFP6 band visible with aqueous curcumin stain, which stains closer to 5 kDa. Coomassie blue is believed to interact with basic residues on a protein primarily and aromatic residues secondarily (Georgiou et al., 2008). AFP6 has two positively charged residues, a lysine at residue 18 and an arginine at the N terminus. Lys18 forms a salt bridge with Glu22 as noted above. The peptide has no aromatic residues.

A tricine gel with samples separated by SDS-PAGE that was first stained in Coomassie blue, then immediately followed by aqueous curcumin showed poor Coomassie blue staining of the mass markers and BSA, resulting in bands difficult to

distinguish from the background, such as Coomassie blue binding occluded curcumin-binding surfaces. Since the AFP6 bands stained normally with curcumin following Coomassie blue, it suggested that they had not interacted with Coomassie blue as the other separated proteins had. Figure 21, panel B further shows this, where the AFP6 is not visible on an 18% gel arylamide gel after SDS-PAGE and Coomassie blue staining, but it is visible after staining by aqueous curcumin under the same conditions.

The VividPro stain used is marketed as a general protein stain, but it did not stain AFP6 either. Of the stains tested in this work, only aqueous curcumin and aqueous $CuCl_2$ allowed for visualization of AFP6. Thus, although aqueous curcumin does not appear to stain all proteins, it shows promise as a cheap, biosafe method of AFP6 visualization.

### 3.4.3 Effect of AFP6 on Curcumin Absorbance

The changes in absorbance and fluorescence spectra of aqueous curcumin in the presence of AFP6 are consistent with binding to the protein. Although the affinity of AFP6 for aqueous curcumin is unknown, full binding of curcumin was favoured by incubating in a greater than 10-fold molar excess of AFP6. The changes observed in absorbance and fluorescence spectra of curcumin upon AFP binding were similar to those occurring with binding of curcumin to other proteins (Barakat & Patra, 2013; Tapal & Tiku, 2012). Specifically, fluorescence magnitude was generally increased and blue shifted when curcumin is bound to protein compared to free curcumin (Barakat & Patra, 2013; Tapal & Tiku, 2012). Some other studies instead measured the quenching of protein intrinsic fluorescence in their observations of curcumin binding (Yujia Liu et al., 2018).

Studies observing UV-absorbance of curcumin-protein sometimes focus more on the absorbance at lower wavelengths than the 350-450 absorbance range expected for curcumin. In examples with curcumin and BSA and soy protein isolate, absorbance spectra showed a shoulder at approximately 425 nm (Barik, Priyadarsini, & Mohan, 2003; Tapal & Tiku, 2012). This point corresponds to the absorbance of the enol tautomer of curcumin, which is the favored structure of curcumin in organic solvents (Manolova et al., 2014). In both cases cited above the curcumin was solubilized in methanol before diluting into buffer with protein (Barik et al., 2003; Tapal & Tiku, 2012). It may be possible that a small amount of methanol is still interacting in curcumin in those studies, favouring the enol tautomer that appears as a shoulder at 425 nm. In comparison, the aqueous curcumin used in this study shows a shoulder at 350 nm, corresponding to the diketo form of curcumin, which is more prevalent in aqueous solution (Manolova et al., 2014).

Incubation of curcumin with AFP6 at 70 °C increased the magnitude of both the absorbance and fluorescence spectra when compared to incubation at room temperature. The effect of temperature pre-incubation was an additional aspect of this study that was not seen in previous literature. Curcumin itself shows a low fluorescence in solution, but upon binding to AFP6 the fluorescence is increased, and a blue shift is seen. This means the fluorescence emitted when curcumin is bound to AFP6 was of a lower (high energy) wavelength compared to curcumin alone. The addition of an incubation step at 70 °C further increased the fluorescence from curcumin.

The absorbance of curcumin in the presence of AFP6 only changed maximally when both were heated to 70 °C. Pre-incubation of curcumin or of the curcumin and

AFP6 together at room temperature resulted in far less change upon binding. The absorbance maximum of curcumin is reported as 425 nm in water (Majhi et al., 2010), yet the spectra of this graph shows that the absorbance is not highest there, but instead shows a shoulder peak at approximately 350 nm. This shoulder peak was not present when the curcumin was incubated with AFP6, suggesting that it undergoes a change due to protein binding.

Studies have reported that the absorbance of curcumin in the 350-355 nm range is a result of the diferuloyl structure of the diketo tautomeric form of curcumin (Ke et al., 2011; Moussa, Chebl, & Patra, 2017). This may indicate that the curcumin in aqueous solution is in diketo form as opposed to the enol form (Manolova et al., 2014). Curcumin is predominantly in the enol form when solid or in organic solvents (Kawano, Inohana, Hashi, & Lin, 2013) but there is the possibility that the percentage of diketo form increases as the percentage of aqueous solvent does (Kawano et al., 2013; Manolova et al., 2014). These results seemingly support the latter.

### 3.4.4 Effect of AFP6 on Curcumin Fluorescence

While free curcumin fluoresces lightly at about 540 nm after excitation at 420 nm, its fluorescence increases and the maxima undergoes a blue shift to 520 nm after binding to AFP6. This appears consistent across most proteins, with the increase and blue shift seen after curcumin binds bovine serum albumin, bovine casein micelles, and soy protein isolate (Barik et al., 2003; Sahu, Kasoju, & Bora, 2008; Tapal & Tiku, 2012). The authors suggest that this may be due to the curcumin moving from a more polar to a less polar micro environment (Barik et al., 2003; Sahu et al., 2008; Tapal & Tiku, 2012). This

would seem in agreement with the possibility that curcumin may interact with the hydrophobic face of AFP6. It is not clear from these results what the role of heating is in enhanced binding. At 70 ºC, the AFP is unfolded (Chakrabartty, Ananthanarayanan, & Hew, 1989), and the unfolded protein may have more binding surfaces for curcumin. However, this deserves further study.

### 3.4.5 Structural Effect of Curcumin Binding to AFP6

The prior experiments examined the effect of AFP6 binding on the absorbance and fluorescence of curcumin. Therefore, subsequent binding studies were designed in which a very low concentration of AFP6 was incubated with a series of concentrations of curcumin and monitored by curcumin fluorescence, The linearity of the curve obtained indicated that the maximal solubility of aqueous curcumin did not reach the saturation point for AFP6 binding, precluding $K_d$ determination. However, a clear dose-response relationship was evident, consistent with a measurable difference in curcumin fluorescence with AFP binding. The effect of curcumin on proteins seems to differ. Like AFP6, collagen and gelatin have been shown to retain their secondary structures in the presence of curcumin (Fathima, Devi, Rekha, & Dhathathreyan, 2009; T. Yang, Yang, Fan, Li, & Hou, 2018), whereas human serum albumin and ovalbumin both showed slight changes in secondary structure (Bourassa, Kanakis, Tarantilis, Pollissiou, & Tajmir-Riahi, 2010; Liu et al., 2018). This slight change may not occur if the binding site is not a hydrophobic pocket within the structure, perhaps explaining why collagen's triple helix structure and AFP6's alpha helical structure do not change in the presence of AFP6. This same train of thought may explain why AFP6 alone and AFP6 in the presence of

curcumin did not show any change in melting temperature while the presence of curcumin lowers the melting point of ovalbumin (Yujia Liu et al., 2018). Curcumin may change the local environment of the hydrophobic pocket of more globular proteins and this slight shift in secondary structure may make them more susceptible to denaturation (Liu et al., 2018).

Thus, although the AFP6 has only 37 residues and no tertiary structure, it is able to interact with the curcumin. The AFP may therefore be a good model for the investigation of curcumin interaction with proteins. With experiments showing an increase of curcumin fluorescence when incubated with AFP6 at 70 ºC compared to room temperature, the question of if the heating step might cause melting of the AFP6 which would allow more curcumin to interact with the peptide. Circular dichroism was used to observe the secondary structure of AFP6 after pre-heating alone or in the presence of curcumin or guanidine. As expected, the AFP showed a typical alpha helical CD spectrum, with two strong minima at 208 and 222 nm and a spectrum consistent with unfolded protein in the presence of guanidine.

With curcumin showing no detectable effect on protein refolding to a helical form at 5 ºC. the melting point was determined by monitoring the molar ellipticity at 222 nm over a range of temperatures.

### 3.4.8 Concluding Remarks

The viability of curcumin as a stain for visualization of AFP6 was confirmed. Furthermore, the interaction of AFP6 and curcumin was shown to alter curcumin absorbance and fluorescence while having little if any effect on folding of the AFP.

Although the solubility of aqueous curcumin was still too low to observe the dissociation constant, it was sufficient to show a dose-response to AFP binding. Taken together, these results suggest that curcumin can be employed as an effective stain for AFP after gel electrophoresis and that it may hold promise for use in solution-based assays involving the AFP if absorbance or fluorescence changes are quantified.

# CHAPTER 4: DISCUSSION

This study was initially undertaken in order to gain insight into the mechanism of amyloid formation by AFP6 and to assess its similarity to more typical amyloids, such as aß. The dual goals were to better understand the amyloid behaviour of this antifreeze protein and to assess its potential as an inducible model for the study of amyloid formation more generally. As a number of technical problems made this work difficult to complete, our solution to one problem led to another line of investigation. As AFP6 cannot be detected with typical protein stains, we implemented a curcumin staining procedure. The interaction of AFP6 and curcumin were therefore further examined.

AFP6 has previously been shown to form amyloid upon specific interaction with ice (Dubé et al., 2016). Prior work had also established that these amyloid fibrils could self-propagate by seeding (Graether & Sykes, 2009) in which incubation of natively folded AFP6 with pre-formed AFP6 amyloid led to the conversion of the former to amyloid. Self-seeding of fibril formation is a known property of pathogenic amyloid-forming proteins (Chiti & Dobson, 2006; Dorta-Estremera et al., 2013). This prion-like templating of amyloid formation may be a feature of most or all amyloids (Chiti & Dobson, 2017). More recently, it has been shown that pathogenic amyloids not only induce fibril formation in the same protein, but may be able to induce fibril transition in a subset of related or structurally similar amyloids (Bassil et al., 2020; Mukherjee & Soto, 2017; Ono, Takahashi, Ikeda, & Yamada, 2012; Yam et al., 2011). For these reasons, the cross-seeding potential of AFP6 for aß fibrillation was of interest because this would allow an assessment of its templating similarity to the best-studied human amyloid. In a first approach, AFP6 was prepared and an aß fibrillation assay was tested.

AFP6 was obtained in synthetic form from commercial suppliers. In contrast to the synthetic AFP preparations obtained and used in earlier studies (Baardsnes et al., 1999; Dubé et al., 2016; Graether et al., 2003; Graether & Sykes, 2009; Haymet et al., 1999; Low et al., 2003; Wen & Laursen, 1993; Zhang & Laursen, 1998), the synthetic AFP obtained for this study was supplied at yields far lower than reported, in insoluble form or at low purity. Therefore, the material required for study was severely limited and precluded a full study of amyloid formation and amyloid cross-seeding by AFP6. Material purified from fish blood plasma was used in place of AFP6 in some of the experiments reported here. However, this preparation is a mixture of two closely related isoforms, AFP6 and AFP8, which would make the interpretation of any observed amyloid-seeding effect less clear.

Evaluation of AFP6 cross-seeding required preparation of the amyloid form of this protein. The repeated freeze-thaw method (Graether et al., 2003; Graether & Sykes, 2009) and the equilibrium ice method (Dubé et al., 2016) did not result in decisive increases in ThT fluorescence that are typically considered as indicative of amyloid formation. However, TEM revealed the presence of fibrils in the repeatedly freeze-thawed samples, suggesting that amyloid was indeed formed. A lack of repeatability in the ice method indicated that aspects of the peptide preparation, chiller conditions or other parameters remain to be optimized. This can include changes to the concentration of AFP6 used, the temperature of the chiller, and the adjustment to the size of ice surface used.

A real-time *in-situ* aß seeding assay was implemented according to published methods (Salvadores, Shahnawaz, Scarpini, Tagliavini, & Soto, 2014). It was tested

using homologous seeding with pre-formed aß fibrils to evaluate accelerated or enhanced fibrillation and it was also tested using EGCG for inhibition of fibrillation. The data showed that both effects could be clearly discerned, tracked and quantified, if needed, from the results obtained. Furthermore, TEM analysis revealed fibrils in the post-incubation material, confirming the formation of amyloid. The assay can be used in precisely the same way to examine heterologous seeding; therefore, it is ready for use for that purpose. When AFP6 is readily available for study or when other amyloid seeds or inhibitors are to be tested, this assay can be used in its current form.

The potential cross-seeding capabilities of AFP6 were not investigated since the repeatable formation of amyloid by AFP6 was not achieved. Nonetheless, the question of amyloid cross-seeding by AFP6 is still very intriguing. Current *in vitro* amyloid conversion assays all rely on agitation and incubations that can take hours to days, much like the seeding assay implemented in this work (Becker et al., 2018; Salvadores et al., 2014; Singh & DeMarco, 2020). AFP6, however, instead forms amyloid after inducible ice interaction and this occurs within 2 hours, and may even begin after 15 minutes (Dubé et al., 2016; Graether & Sykes, 2009). Thus, if an abundant source of AFP6 were obtained, the optimization of amyloid formation and the cross-seeding experiment could be rapidly completed. Expression of AFP6 in *E. coli* is now underway in the lab (unpublished). If successful, this project will hopefully be resumed.

Over the course of preparing and studying AFP6 for the above project, methods were sought to efficiently purify AFP6. Purification based on the unusual acetone solubility of AFP6 was very efficient, as all other proteins tested appeared to be precipitated, while AFP6 was soluble in acetone. Therefore, the dogma that acetone

efficiently precipitates all proteins must be questioned when undertaking proteomics or similar scans of protein abundance. The AFP6 may not be unique and therefore the possibility of one or more acetone-soluble proteins in a proteome sample, for example, cannot be discounted.

In this project, methods were also required to detect the AFP after SDS-PAGE since common protein stains such as Coomassie blue and silver are unsuitable for this protein. This could possibly be due to its small size along with the preponderance of alanine residues and lack of aromatic residues. Aqueous solubilised curcumin had been reported as a general protein stain (Kurien et al., 2012) and was therefore evaluated for staining of AFP6. The AFP6 was stained using aqueous curcumin stain, which adds a new visualization tool for the study of AFP6, allowing for the detection of AFP6 by SDS-PAGE and possibly its detection in solution assays as well. However, in the current studies, several proteins were not stained, which suggested that curcumin is a somewhat specific stain rather than a general one.

As noted in Chapter 3, the basis for binding of AFP6 to curcumin is unknown. However, it is an interesting question that could be addressed by studying the binding of natural AFP variants or expressed mutants to curcumin. Given the specificity of the curcumin stain, its interaction with AFP6 was further investigated. The absorbance of curcumin at lower wavelengths was increased when incubated at 70 ºC for 10 minutes before incubation and when incubated with AFP under the same conditions. It was interesting that unbound aqueous curcumin showed a maximal absorbance at 355 nm, consistent with the diketo tautomeric form (Majhi et al., 2010; Manolova et al., 2014). In contrast, the enol form absorbs more strongly at 425 nm due to the diferuloyl structure

(Ke et al., 2011; Moussa et al., 2017) and it is the expected form in organic solutions. Since the 355 nm peak diminishes upon binding AFP6, it appears that this form is binding to the protein.

Incubation of curcumin with AFP6 at 70 ºC for 10 minutes showed a substantial increase in fluorescence intensity compared with a room temperature incubation with AFP6 of pre-heated curcumin. This suggests that denaturation of AFP6 favours its binding with curcumin. Further insight into this interaction was sought from binding studies; however, concentrations of curcumin required for a complete dataset exceeded the solubility of aqueous curcumin.

Since the curcumin appeared to bind the AFP, the effects of curcumin binding on the structure and function of AFP6 were examined. After a 70 ºC incubation in the presence of curcumin, AFP6 regained its native alpha-helical structure. Furthermore, the melting point of the AFP did not change appreciably with curcumin presence, suggesting that binding does not interfere with folding or fold stability. As noted in Chapter 3, this appears to be consistent with surface binding, which would also appear to be the only means of interaction with AFP6, as no tertiary fold or hydrophobic pocket are present (Liu et al., 2018).

Several questions and new directions of investigation have stemmed from this study.

(1) The interaction of curcumin with AFP6 is interesting and can be tied into many different avenues for research and development. The most immediate product of this work is the easy and effective staining of AFP6 with curcumin. It is sensitive,

effective and has the added advantage of being environmentally responsible, producing no solvent (when choosing ethanol) or stain waste requiring chemical disposal. Since the signal is fluorescent, the stain may also find use in various AFP6 assays, as a substitute for the Bradford assay (Bradford, 1976), for example. The recognition of AFP6 using this stain also suggests a means to detect other small peptides that could be difficult to stain by typical means as is the AFP6.

(2) The form of curcumin that is bound by the AFP could be determined. As noted in Chapter 3, the spectral change suggests binding in the keto form. However, structural investigation of AFP6 and curcumin using NMR might provide insight into the form of curcumin bound and the precise interactions that mediate binding.

(3) AFP6 or a crude (food-grade) mixture of flounder AFPs could perhaps find use in curcumin delivery. Despite the potential effects of curcumin on aspects of human health, its use as a nutraceutical or pharmaceutical has been limited by its poor solubility and bioavailability. Therefore, AFP6 either as a crude mixture, as a pure peptide or as the starting point for engineering of a pared-down binding agent might offer a solution by acting as a potential carrier protein for curcumin.

Thus, although this project did not achieve the initial goals, an assay was successfully set up for that purpose. Furthermore, the investigation of AFP6-curcumin interaction may lead to new discoveries and applications in a variety of areas.

# REFERENCES


Aggarwal, B. B., & Sung, B. (2009). Pharmacological basis for the role of curcumin in chronic diseases: an age-old spice with modern targets. *Trends in Pharmacological Sciences*, *30*(2), 85–94. https://doi.org/10.1016/j.tips.2008.11.002

Agrawal, N., & Skelton, A. A. (2019, August 15). Structure and Function of Alzheimer's Amyloid βeta Proteins from Monomer to Fibrils: A Mini Review. *Protein Journal*. Springer New York LLC. https://doi.org/10.1007/s10930-019-09854-3

Amir, G., Rubinsky, B., Kassif, Y., Horowitz, L., Smolinsky, A. K., & Lavee, J. (2003). Preservation of myocyte structure and mitochondrial integrity in subzero cryopreservation of mammalian hearts for transplantation using antifreeze proteins--an electron microscopy study. *European Journal of Cardio-Thoracic Surgery : Official Journal of the European Association for Cardio-Thoracic Surgery*, *24*(2), 292–296; discussion 296-7. https://doi.org/10.1016/s1010-7940(03)00306-3

Ammon, H., & Wahl, M. (1991). Pharmacology of *Curcuma longa*. *Planta Medica*, *57*(01), 1–7. https://doi.org/10.1055/s-2006-960004

Anand, P., Sundaram, C., Jhurani, S., Kunnumakkara, A. B., & Aggarwal, B. B. (2008). Curcumin and cancer: An "old-age" disease with an "age-old" solution. *Cancer Letters*, *267*(1), 133–164. https://doi.org/10.1016/j.canlet.2008.03.025

Antson, A. A., Smith, D. J., Roper, D. I., Lewis, S., Caves, L. S. D., Verma, C. S., … Hubbard, R. E. (2001). Understanding the mechanism of ice binding by type III antifreeze proteins. *Journal of Molecular Biology*, *305*(4), 875–889. https://doi.org/10.1006/JMBI.2000.4336

Arslan, P. E., & Chakrabartty, A. (2009). Probing Alzheimer amyloid peptide aggregation using a cell-free fluorescent protein refolding method. *Biochemistry and Cell Biology*, *87*(4), 631–639. https://doi.org/10.1139/O09-038

Atarashi, R., Moore, R. A., Sim, V. L., Hughson, A. G., Dorward, D. W., Onwubiko, H. A., … Caughey, B. (2007). Ultrasensitive detection of scrapie prion protein using seeded conversion of recombinant prion protein. *Nature Methods*, *4*(8), 645–650. https://doi.org/10.1038/nmeth1066

Baardsnes, J., & Davies, P. L. (2001, August 1). Sialic acid synthase: The origin of fish type III antifreeze protein? *Trends in Biochemical Sciences*. Elsevier Ltd. https://doi.org/10.1016/S0968-0004(01)01879-5

Baardsnes, J., Kondejewski, L. H., Hodges, R. S., Chao, H., Kay, C., & Davies, P. L. (1999). New ice-binding face for type I antifreeze protein. *FEBS Letters*, *463*(1–2), 87–91. https://doi.org/10.1016/S0014-5793(99)01588-4

Bahadori, F., & Demiray, M. (2017). A Realistic View on The Essential Medicinal Chemistry of Curcumin. *ACS Medicinal Chemistry Letters*, *8*(9), 893–896. https://doi.org/10.1021/acsmedchemlett.7b00284

Bar-Dolev, M., Celik, Y., Wettlaufer, J. S., Davies, P. L., & Braslavsky, I. (2012). New insights into ice growth and melting modifications by antifreeze proteins. *Journal of the Royal Society, Interface*, *9*(77), 3249–3259. https://doi.org/10.1098/rsif.2012.0388

Bar Dolev, M., Braslavsky, I., & Davies, P. L. (2016). Ice-Binding Proteins and Their Function. *Annual Review of Biochemistry*, *85*(1), 515–542. https://doi.org/10.1146/annurev-biochem-060815-014546

Barakat, C., & Patra, D. (2013). Combining time-resolved fluorescence with synchronous fluorescence spectroscopy to study bovine serum albumin-curcumin complex during unfolding and refolding processes. *Luminescence*, *28*(2), 149–155. https://doi.org/10.1002/bio.2354

Barik, A., Priyadarsini, K. I., & Mohan, H. (2003). Photophysical Studies on Binding of Curcumin to Bovine Serum Albumin. *Photochemistry and Photobiology*, *77*(6), 597. https://doi.org/10.1562/0031-8655(2003)077<0597:psoboc>2.0.co;2

Barnhart, M. M., & Chapman, M. R. (2006). Curli Biogenesis and Function. *Annual Review of Microbiology*, *60*(1), 131–147. https://doi.org/10.1146/annurev.micro.60.080805.142106

Bartels, T., Choi, J. G., & Selkoe, D. J. (2011). α-Synuclein occurs physiologically as a helically folded tetramer that resists aggregation. *Nature*, *477*(7362), 107–111. https://doi.org/10.1038/nature10324

Bassil, F., Brown, H. J., Pattabhiraman, S., Iwasyk, J. E., Maghames, C. M., Meymand, E. S., … Lee, V. M. Y. (2020). Amyloid-Beta (Aβ) Plaques Promote Seeding and Spreading of Alpha-Synuclein and Tau in a Mouse Model of Lewy Body Disorders with Aβ Pathology. *Neuron*, *105*(2), 260-275.e6. https://doi.org/10.1016/j.neuron.2019.10.010

Batzli, K. M., & Love, B. J. (2015, March 1). Agitation of amyloid proteins to speed aggregation measured by ThT fluorescence: A call for standardization. *Materials Science and Engineering C*. Elsevier Ltd. https://doi.org/10.1016/j.msec.2014.09.015

Becker, K., Wang, X., Vander Stel, K., Chu, Y., Kordower, J., & Ma, J. (2018). Detecting Alpha Synuclein Seeding Activity in Formaldehyde-Fixed MSA Patient Tissue by PMCA. *Molecular Neurobiology*, *55*(11), 8728–8737. https://doi.org/10.1007/s12035-018-1007-y

Bhowmick, D. C., Singh, S., Trikha, S., & Jeremic, A. M. (2018). The Molecular Physiopathogenesis of Islet Amyloidosis. *Handbook of Experimental Pharmacology*, *245*, 271–312. https://doi.org/10.1007/164_2017_62

Biancalana, M., & Koide, S. (2010). Molecular mechanism of Thioflavin-T binding to amyloid fibrils. *Biochimica et Biophysica Acta*, *1804*(7), 1405–1412. https://doi.org/10.1016/j.bbapap.2010.04.001

Bieschke, J., Russ, J., Friedrich, R. P., Ehrnhoefer, D. E., Wobst, H., Neugebauer, K., & Wanker, E. E. (2010). EGCG remodels mature alpha-synuclein and amyloid-beta fibrils and reduces cellular toxicity. *Proceedings of the National Academy of Sciences of the United States of America*, *107*(17), 7710–7715. https://doi.org/10.1073/pnas.0910723107

Bigelow, H., & Schroeder, W. (1953). *Fishes of the Gulf of Maine*. Retrieved from http://spo.nmfs.noaa.gov/sites/default/files/pdf-content/fish-bull/fb53.1.pdf

Blanco, L. P., Evans, M. L., Smith, D. R., Badtke, M. P., & Chapman, M. R. (2012). Diversity, biogenesis and function of microbial amyloids. *Trends in Microbiology*, *20*(2), 66–73. https://doi.org/10.1016/j.tim.2011.11.005

Bloom, G. S. (2014). Amyloid-β and tau: The trigger and bullet in Alzheimer disease pathogenesis. *JAMA Neurology*, *71*(4), 505–508. https://doi.org/10.1001/jamaneurol.2013.5847

Bourassa, P., Kanakis, C. D., Tarantilis, P., Pollissiou, M. G., & Tajmir-Riahi, H. A. (2010). Resveratrol, genistein, and curcumin bind bovine serum albumin. *Journal of Physical Chemistry B*, *114*(9), 3348–3354. https://doi.org/10.1021/jp9115996

Bradford, M. (1976). A Rapid and Sensitive Method for the Quantitation of Microgram Quantities of Protein Utilizing the Principle of Protein-Dye Binding. *Analytical Biochemistry*, *72*(1–2), 248–254. https://doi.org/10.1006/abio.1976.9999

Brand, G. D., Ramada, M. H. S., Manickchand, J. R., Correa, R., Ribeiro, D. J. S., Santos, M. A., … Bloch, C. (2019). Intragenic antimicrobial peptides (IAPs) from human proteins with potent antimicrobial and anti-inflammatory activity. *PLoS ONE*, *14*(8). https://doi.org/10.1371/journal.pone.0220656

Bredow, M., Vanderbeld, B., & Walker, V. K. (2016). Knockdown of Ice-Binding Proteins in Brachypodium distachyon Demonstrates Their Role in Freeze Protection. *PloS One*, *11*(12), e0167941. https://doi.org/10.1371/journal.pone.0167941

Brooke-Taylor, C. A., Grant, G. H., Elcock, A. H., & Graham Richards, W. (1996). Mechanism of action of antifreeze polypeptide HPLC6 in solution: analysis of solvent behaviour by molecular dynamics. *Chemical Physics*, *204*(2–3), 251–261. https://doi.org/10.1016/0301-0104(95)00337-1

Bu, X.-L., Rao, P. P. N., & Wang, Y.-J. (2016). Anti-amyloid Aggregation Activity of Natural Compounds: Implications for Alzheimer's Drug Discovery. *Molecular Neurobiology*, *53*(6), 3565–3575. https://doi.org/10.1007/s12035-015-9301-4

Bucciantini, M., Giannoni, E., Chiti, F., Baroni, F., Formigli, L., Zurdo, J., … Stefani, M. (2002). Inherent toxicity of aggregates implies a common mechanism for protein misfolding diseases. *Nature*, *416*(6880), 507–511. https://doi.org/10.1038/416507a

Celik, Y., Graham, L. A., Mok, Y. F., Bar, M., Davies, P. L., & Braslavsky, I. (2010). Superheating of ice crystals in antifreeze protein solutions. *Proceedings of the National Academy of Sciences of the United States of America*, *107*(12), 5423–5428. https://doi.org/10.1073/pnas.0909456107

Chakrabartty, A., Ananthanarayanan, V. S., & Hew, C. L. (1989). Structure-function relationships in a winter flounder antifreeze polypeptide. I. Stabilization of an alpha-helical antifreeze polypeptide by charged-group and hydrophobic interactions. *The Journal of Biological Chemistry*, *264*(19), 11307–11312. Retrieved from http://www.ncbi.nlm.nih.gov/pubmed/2738067

Chakraborty, S., & Jana, B. (2017). Conformational and hydration properties modulate ice recognition by type I antifreeze protein and its mutants. *Physical Chemistry Chemical Physics*, *19*(18), 11678–11689. https://doi.org/10.1039/C7CP00221A

Chakraborty, S., & Jana, B. (2018). Optimum Number of Anchored Clathrate Water and Its Instantaneous Fluctuations Dictate Ice Plane Recognition Specificities of Insect Antifreeze Protein. *The Journal of Physical Chemistry. B*, *122*(12), 3056–3067. https://doi.org/10.1021/acs.jpcb.8b00548

Chao, H., Hodges, R. S., Kay, C. M., Gauthier, S. Y., & Davies, P. L. (1996). A natural variant of type I antifreeze protein with four ice-binding repeats is a particularly potent antifreeze. *Protein Science : A Publication of the Protein Society*, *5*(6), 1150–1156. https://doi.org/10.1002/pro.5560050617

Chao, H., Houston, M. E., Hodges, R. S., Kay, C. M., Sykes, B. D., Loewen, M. C., … Sönnichsen, F. D. (1997). A diminished role for hydrogen bonds in antifreeze protein binding to ice. *Biochemistry*, *36*(48), 14652–14660. https://doi.org/10.1021/bi970817d

Chaudhary, N., Singh, S., & Nagaraj, R. (2011). Aggregation properties of a short peptide that mediates amyloid fibril formation in model proteins unrelated to disease. *Journal of Biosciences*, *36*(4), 679–689. https://doi.org/10.1007/s12038-011-9104-3

Cheng, B., Gong, H., Xiao, H., Petersen, R. B., Zheng, L., & Huang, K. (2013). Inhibiting toxic aggregation of amyloidogenic proteins: a therapeutic strategy for protein misfolding diseases. *Biochimica et Biophysica Acta*, *1830*(10), 4860–4871. https://doi.org/10.1016/j.bbagen.2013.06.029

Chiti, F., & Dobson, C. M. (2006). Protein Misfolding, Functional Amyloid, and Human Disease. *Annual Review of Biochemistry*, *75*(1), 333–366. https://doi.org/10.1146/annurev.biochem.75.101304.123901

Chiti, F., & Dobson, C. M. (2017). Protein Misfolding, Amyloid Formation, and Human Disease: A Summary of Progress Over the Last Decade. *Annual Review of Biochemistry*, *86*(1), 27–68. https://doi.org/10.1146/annurev-biochem-061516-045115

Chuang, E., Hori, A. M., Hesketh, C. D., & Shorter, J. (2018, April 15). Amyloid assembly and disassembly. *Journal of Cell Science*. Company of Biologists Ltd. https://doi.org/10.1242/jcs.189928

Crowell, A. M. J., Wall, M. J., & Doucette, A. A. (2013). Maximizing recovery of water-soluble proteins through acetone precipitation. *Analytica Chimica Acta*, *796*, 48–54. https://doi.org/10.1016/j.aca.2013.08.005

Ćurić, M., & Janc, D. (2013). Wet deposition of the seeding agent after weather modification activities. *Environmental Science and Pollution Research*, *20*(9), 6344–6350. https://doi.org/10.1007/s11356-013-1705-y

Darvesh, A. S., Carroll, R. T., Bishayee, A., Novotny, N. A., Geldenhuys, W. J., & Van der Schyf, C. J. (2012). Curcumin and neurodegenerative diseases: a perspective. *Expert Opinion on Investigational Drugs*, *21*(8), 1123–1140. https://doi.org/10.1517/13543784.2012.693479

Davies, P. L. (2014). Ice-binding proteins: a remarkable diversity of structures for stopping and starting ice growth. *Trends in Biochemical Sciences*, *39*(11), 548–555. https://doi.org/10.1016/j.tibs.2014.09.005

De Maayer, P., Anderson, D., Cary, C., & Cowan, D. A. (2014). Some like it cold: understanding the survival strategies of psychrophiles. *EMBO Reports*, *15*(5), 508–517. https://doi.org/10.1002/embr.201338170

Deng, G., Andrews, D. W., & Laursen, R. A. (1997). Amino acid sequence of a new type of antifreeze protein, from the longhorn sculpin, *Myoxocephalus octodecimspinosis*. *FEBS Letters*, *402*(1), 17–20. https://doi.org/10.1016/S0014-5793(96)01466-4

Dettmer, U., Ramalingam, N., von Saucken, V. E., Kim, T. E., Newman, A. J., Terry-Kantor, E., … Selkoe, D. (2017). Loss of native α-synuclein multimerization by strategically mutating its amphipathic helix causes abnormal vesicle interactions in neuronal cells. *Human Molecular Genetics*, *26*(18), 3466–3481. https://doi.org/10.1093/HMG/DDX227

Devries, A. L. (1971). Glycoproteins as Biological Antifreeze Agents in Antarctic Fishes. *Science*, *172*(3988), 1152–1155. https://doi.org/10.1126/science.172.3988.1152

DeVries, A. L., Vandenheede, J., & Feeney, R. E. (1971). Primary structure of freezing point-depressing glycoproteins. *The Journal of Biological Chemistry*, *246*(2), 305–308. Retrieved from http://www.ncbi.nlm.nih.gov/pubmed/5542001

DeVries, A. L., & Wohlschlag, D. E. (1969). Freezing Resistance in Some Antarctic Fishes. *Science*, *163*(3871), 1073–1075. https://doi.org/10.1126/science.163.3871.1073

Dorta-Estremera, S. M., Li, J., & Cao, W. (2013). Rapid generation of amyloid from native proteins in vitro. *Journal of Visualized Experiments : JoVE*, (82), 50869. https://doi.org/10.3791/50869

Drombosky, K. W., Rode, S., Kodali, R., Jacob, T. C., Palladino, M. J., & Wetzel, R. (2018). Mutational analysis implicates the amyloid fibril as the toxic entity in Huntington's disease. *Neurobiology of Disease*, *120*, 126–138. https://doi.org/10.1016/j.nbd.2018.08.019

Dubé, A., Leggiadro, C., & Ewart, K. V. (2016). Rapid amyloid fibril formation by a winter flounder antifreeze protein requires specific interaction with ice. *FEBS Letters*, *590*(9), 1335–1344. https://doi.org/10.1002/1873-3468.12175

Duman, J. G., & Devries, A. L. (1974). Freezing resistance in winter flounder *Pseudopleuronectes americanus*. *Nature*, *247*(5438), 237–238. https://doi.org/10.1038/247237a0

Ehrnhoefer, D. E., Bieschke, J., Boeddrich, A., Herbst, M., Masino, L., Lurz, R., … Wanker, E. E. (2008). EGCG redirects amyloidogenic polypeptides into unstructured, off-pathway oligomers. *Nature Structural & Molecular Biology*, *15*(6), 558–566. https://doi.org/10.1038/nsmb.1437

Ehrnhoefer, D. E., Duennwald, M., Markovic, P., Wacker, J. L., Engemann, S., Roark, M., … Wanker, E. E. (2006). Green tea (-)-epigallocatechin-gallate modulates early events in huntingtin misfolding and reduces toxicity in Huntington's disease models. *Human Molecular Genetics*, *15*(18), 2743–2751. https://doi.org/10.1093/hmg/ddl210

El-Agnaf, O., Mahil, D., Patel, B., & Austen, B. (2000). Oligomerization and Toxicity of beta-amyloid-42 Implicated in Alzheimer's Disease. *Biochemical and Biophysical Research Communications*, *273*(3). https://doi.org/10.1006/BBRC.2000.3051

Englander, S. W., & Mayne, L. (2014). The nature of protein folding pathways. *Proceedings of the National Academy of Sciences*, *111*(45), 15873–15880. https://doi.org/10.1073/pnas.1411798111

Evans, M. L., & Chapman, M. R. (2014). Curli biogenesis: order out of disorder. *Biochimica et Biophysica Acta*, *1843*(8), 1551–1558. https://doi.org/10.1016/j.bbamcr.2013.09.010

Fathima, N. N., Devi, R. S., Rekha, K. B., & Dhathathreyan, A. (2009). Collagen-curcumin interaction - A physico-chemical study. *Journal of Chemical Sciences*, *121*(4), 509–514. https://doi.org/10.1007/s12039-009-0061-4

Fazekas de St Groth, S., Webster, R. G., & Datyner, A. (1963). Two new staining procedures for quantitative estimation of proteins on electrophoretic strips. *Biochimica et Biophysica Acta*, *71*, 377–391. https://doi.org/10.1016/0006-3002(63)91092-8

Feeney, R E. (1974). A biological antifreeze. *American Scientist*, *62*(6), 712–719. Retrieved from http://www.ncbi.nlm.nih.gov/pubmed/4440942

Feeney, Robert E, & Yeh, Y. (1998). Antifreeze proteins: Current status and possible food uses. *Trends in Food Science & Technology*, *9*(3), 102–106. https://doi.org/10.1016/S0924-2244(98)00025-9

Fernandez-Flores, A. (2011). A review of amyloid staining: methods and artifacts. *Biotechnic & Histochemistry : Official Publication of the Biological Stain Commission*, *86*(5), 293–301. https://doi.org/10.3109/10520291003784493

Fletcher, G. L., Hew, C. L., & Davies, P. L. (2001). Antifreeze Proteins of Teleost Fishes. *Annual Review of Physiology*, *63*(1), 359–390. https://doi.org/10.1146/annurev.physiol.63.1.359

Fletcher, G. L., Idler, D. R., Vaisius, A., & Hew, C. L. (1989). Hormonal regulation of antifreeze protein gene expression in winter flounder. *Fish Physiology and Biochemistry*, *7*(1–6), 387–393. https://doi.org/10.1007/BF00004733

Fourney, R. M., Joshi, S. B., Kao, M. H., & Hew, C. L. (1984). Heterogeneity of antifreeze polypeptides from the Newfoundland winter flounder, *Pseudopleuronectes americanus*. *Canadian Journal of Zoology*, *62*(1), 28–33. https://doi.org/10.1139/z84-006

Franko, A., Rodriguez Camargo, D. C., Böddrich, A., Garg, D., Rodriguez Camargo, A., Rathkolb, B., … Hrabě de Angelis, M. (2018). Epigallocatechin gallate (EGCG) reduces the intensity of pancreatic amyloid fibrils in human islet amyloid polypeptide (hIAPP) transgenic mice. *Scientific Reports*, *8*(1), 1116. https://doi.org/10.1038/s41598-017-18807-8

Frisk, M. G., Dolan, T. E., McElroy, A. E., Zacharias, J. P., Xu, H., & Hice, L. A. (2018). Assessing the drivers of the collapse of Winter Flounder: Implications for management and recovery. *Journal of Sea Research*, *141*, 1–13. https://doi.org/10.1016/j.seares.2018.07.009

Fu, H., & Cui, M. (2018). Fluorescent Imaging of Amyloid-β Deposits in Brain: An Overview of Probe Development and a Highlight of the Applications for In Vivo Imaging. *Current Medicinal Chemistry*, *25*(23), 2736–2759. https://doi.org/10.2174/0929867325666180214110024

Gade Malmos, K., Blancas-Mejia, L., Weber, B., Buchner, J., Ramirez-Alvarado, M., Naiki, H., & Otzen, D. (2017). ThT 101: A Primer on the Use of Thioflavin T to Investigate Amyloid Formation. *Amyloid : The International Journal of Experimental and Clinical Investigation : The Official Journal of the International Society of Amyloidosis*, *24*(1). https://doi.org/10.1080/13506129.2017.1304905

Garcia-Alloza, M., Borrelli, L. A., Rozkalne, A., Hyman, B. T., & Bacskai, B. J. (2007). Curcumin labels amyloid pathology in vivo, disrupts existing plaques, and partially restores distorted neurites in an Alzheimer mouse model. *Journal of Neurochemistry*, *102*(4), 1095–1104. https://doi.org/10.1111/j.1471-4159.2007.04613.x

Garnham, C. P., Campbell, R. L., & Davies, P. L. (2011). Anchored clathrate waters bind antifreeze proteins to ice. *Proceedings of the National Academy of Sciences*, *108*(18), 7363–7367. https://doi.org/10.1073/pnas.1100429108

Gauthier, S. Y., Scotter, A. J., Lin, F.-H., Baardsnes, J., Fletcher, G. L., & Davies, P. L. (2008). A re-evaluation of the role of type IV antifreeze protein. *Cryobiology*, *57*(3), 292–296. https://doi.org/10.1016/J.CRYOBIOL.2008.10.122

Ge, J.-F., Qiao, J.-P., Qi, C.-C., Wang, C.-W., & Zhou, J.-N. (2012). The binding of resveratrol to monomer and fibril amyloid beta. *Neurochemistry International*, *61*(7), 1192–1201. https://doi.org/10.1016/J.NEUINT.2012.08.012

Geoghegan, K. F., Osuga, D. T., Ahmed, A. I., Yeh, Y., & Feeney, R. E. (1980). Antifreeze glycoproteins from Polar fish. Structural requirements for function of glycopeptide 8. *The Journal of Biological Chemistry*, *255*(2), 663–667. Retrieved from http://www.ncbi.nlm.nih.gov/pubmed/7356637

Georgiou, C. D., Grintzalis, K., Zervoudakis, G., & Papapostolou, I. (2008). Mechanism of Coomassie brilliant blue G-250 binding to proteins: a hydrophobic assay for nanogram quantities of proteins. *Analytical and Bioanalytical Chemistry*, *391*(1), 391–403. https://doi.org/10.1007/s00216-008-1996-x

Ghosh, S., Banerjee, S., & Sil, P. C. (2015). The beneficial role of curcumin on inflammation, diabetes and neurodegenerative disease: A recent update. *Food and Chemical Toxicology : An International Journal Published for the British Industrial Biological Research Association*, *83*, 111–124. https://doi.org/10.1016/j.fct.2015.05.022

Giorgetti, S., Greco, C., Tortora, P., & Aprile, F. A. (2018). Targeting Amyloid Aggregation: An Overview of Strategies and Mechanisms. *International Journal of Molecular Sciences*, *19*(9). https://doi.org/10.3390/ijms19092677

Goedert, M., Jakes, R., & Spillantini, M. G. (2017). The Synucleinopathies: Twenty Years on. *Journal of Parkinson's Disease*. IOS Press. https://doi.org/10.3233/JPD-179005

Gong, Z., Ewart, K. V, Hu, Z., Fletcher, G. L., & Hew, C. L. (1996). Skin antifreeze protein genes of the winter flounder, *Pleuronectes americanus*, encode distinct and active polypeptides without the secretory signal and prosequences. *The Journal of Biological Chemistry*, *271*(8), 4106–4112. https://doi.org/10.1074/jbc.271.8.4106

Gong, Z. Y., King, M. J., Fletcher, G. L., & Hew, C. L. (1995). The Antifreeze Protein Genes of the Winter Flounder, *Pleuronectus americanus*, Are Differentially Regulated in Liver and Nonliver Tissues. *Biochemical and Biophysical Research Communications*, *206*(1), 387–392. https://doi.org/10.1006/BBRC.1995.1053

Graether, S. P., Kuiper, M. J., Walker, V. K., Jia, Z., Sykes, B. D., & Davies, P. L. (2000). Beta-Helix structure and ice-binding properties of a hyperactive antifreeze protein from an insect. *Nature, 406*(6793), 325–328. https://doi.org/10.1038/35018610

Graether, S. P., Slupsky, C. M., & Sykes, B. D. (2003). Freezing of a fish antifreeze protein results in amyloid fibril formation. *Biophysical Journal*, *84*(1), 552–557. https://doi.org/10.1016/S0006-3495(03)74874-7

Graether, S. P., & Sykes, B. D. (2009). Structural Characterization of Amyloidotic Antifreeze Protein Fibrils and Intermediates. *Journal of Toxicology and Environmental Health, Part A*, *72*(17–18), 1030–1033. https://doi.org/10.1080/15287390903084272

Griffith, M., & Yaish, M. W. F. (2004). Antifreeze proteins in overwintering plants: a tale of two activities. *Trends in Plant Science*, *9*(8), 399–405. https://doi.org/10.1016/j.tplants.2004.06.007

Gronwald, W, Chao, H., Reddy, D. V, Davies, P. L., Sykes, B. D., & Sönnichsen, F. D. (1996). NMR characterization of side chain flexibility and backbone structure in the type I antifreeze protein at near freezing temperatures. *Biochemistry*, *35*(51), 16698–16704. https://doi.org/10.1021/bi961934w

Gronwald, Wolfram, Loewen, M. C., Lix, B., Daugulis, A. J., Sönnichsen, F. D., Davies, P. L., & Sykes, B. D. (1998). The Solution Structure of Type II Antifreeze Protein Reveals a New Member of the Lectin Family. *Biochemistry*, *37*(14), 4712–4721. https://doi.org/10.1021/bi972788c

Guo, Q., Bin Huang, Cheng, J., Seefelder, M., Engler, T., Pfeifer, G., … Kochanek, S. (2018). The cryo-electron microscopy structure of huntingtin. *Nature*, *555*(7694), 117–120. https://doi.org/10.1038/nature25502

Guo, S., Garnham, C. P., Whitney, J. C., Graham, L. A., & Davies, P. L. (2012). Re-evaluation of a bacterial antifreeze protein as an adhesin with ice-binding activity. *PloS One*, *7*(11), e48805. https://doi.org/10.1371/journal.pone.0048805

Gupta, R., & Deswal, R. (2014). Antifreeze proteins enable plants to survive in freezing conditions. *Journal of Biosciences*, *39*(5), 931–944. Retrieved from http://www.ncbi.nlm.nih.gov/pubmed/25431421

Gupta, S. C., Patchva, S., Koh, W., & Aggarwal, B. B. (2012). Discovery of curcumin, a component of golden spice, and its miraculous biological activities. *Clinical and Experimental Pharmacology & Physiology*, *39*(3), 283–299. https://doi.org/10.1111/j.1440-1681.2011.05648.x

Gupta, S. C., Prasad, S., Kim, J. H., Patchva, S., Webb, L. J., Priyadarsini, I. K., & Aggarwal, B. B. (2011). Multitargeting by curcumin as revealed by molecular interaction studies. *Natural Product Reports*, *28*(12), 1937. https://doi.org/10.1039/c1np00051a

Hakim, A., Nguyen, J. B., Basu, K., Zhu, D. F., Thakral, D., Davies, P. L., … Meng, W. (2013). Crystal structure of an insect antifreeze protein and its implications for ice binding. *The Journal of Biological Chemistry*, *288*(17), 12295–12304. https://doi.org/10.1074/jbc.M113.450973

Hanada, Y., Nishimiya, Y., Miura, A., Tsuda, S., & Kondo, H. (2014). Hyperactive antifreeze protein from an Antarctic sea ice bacterium Colwellia sp. has a compound ice-binding site without repetitive sequences. *The FEBS Journal*, *281*(16), 3576–3590. https://doi.org/10.1111/febs.12878

Harding, M. M., Anderberg, P. I., & Haymet, A. D. J. (2003). "Antifreeze" glycoproteins from polar fish. *European Journal of Biochemistry*, *270*(7), 1381–1392. https://doi.org/10.1046/j.1432-1033.2003.03488.x

Harel, M., Sonoda, L. K., Silman, I., Sussman, J. L., & Rosenberry, T. L. (2008). Crystal structure of thioflavin T bound to the peripheral site of *Torpedo californica* acetylcholinesterase reveals how thioflavin T acts as a sensitive fluorescent reporter of ligand binding to the acylation site. *Journal of the American Chemical Society*, *130*(25), 7856–7861. https://doi.org/10.1021/ja7109822

Haymet, A. D. J., Ward, L. G., & Harding, M. M. (1999). Winter Flounder "Antifreeze" Proteins: Synthesis and Ice Growth Inhibition of Analogues that Probe the Relative Importance of Hydrophobic and Hydrogen-Bonding Interactions. https://doi.org/10.1021/JA9801341

Hempelmann, E., & Krafts, K. (2017). The mechanism of silver staining of proteins separated by SDS polyacrylamide gel electrophoresis. *Biotechnic & Histochemistry*, *92*(2), 79–85. https://doi.org/10.1080/10520295.2016.1265149

Herva, M. E., Zibaee, S., Fraser, G., Barker, R. A., Goedert, M., & Spillantini, M. G. (2014). Anti-amyloid Compounds Inhibit α-Synuclein Aggregation Induced by Protein Misfolding Cyclic Amplification (PMCA). *Journal of Biological Chemistry*, *289*(17), 11897–11905. https://doi.org/10.1074/jbc.M113.542340

Hew, C. L., Joshi, S., & Wang, N.-C. (1984). Analysis of fish antifreeze polypeptides by reversed-phase high-performance liquid chromatography. *Journal of Chromatography A*, *296*, 213–219. https://doi.org/10.1016/S0021-9673(01)96414-3

Hew, C. L., Slaughter, D., Fletcher, G. L., & Joshi, S. B. (1981). Antifreeze glycoproteins in the plasma of Newfoundland Atlantic cod ( *Gadus morhua* ). *Canadian Journal of Zoology*, *59*(11), 2186–2192. https://doi.org/10.1139/z81-296

Hirano, Y., Nishimiya, Y., Matsumoto, S., Matsushita, M., Todo, S., Miura, A., … Tsuda, S. (2008). Hypothermic preservation effect on mammalian cells of type III antifreeze proteins from notched-fin eelpout. *Cryobiology*, *57*(1), 46–51. https://doi.org/10.1016/J.CRYOBIOL.2008.05.006

Holmes, B. B., Furman, J. L., Mahan, T. E., Yamasaki, T. R., Mirbaha, H., Eades, W. C., … Diamond, M. I. (2014). Proteopathic tau seeding predicts tauopathy in vivo. *Proceedings of the National Academy of Sciences of the United States of America*, *111*(41), E4376–E4385. https://doi.org/10.1073/pnas.1411649111

Howie, A. J. (2015). "Green (or apple-green) birefringence" of Congo red-stained amyloid. *Amyloid : The International Journal of Experimental and Clinical Investigation : The Official Journal of the International Society of Amyloidosis*, *22*(3), 205–206. https://doi.org/10.3109/13506129.2015.1054026

Howie, A. J., & Brewer, D. B. (2009). Optical properties of amyloid stained by Congo red: history and mechanisms. *Micron (Oxford, England : 1993)*, *40*(3), 285–301. https://doi.org/10.1016/j.micron.2008.10.002

Iñaki Guijarro, J., Sunde, M., Jones, J. A., Campbelli, I. D., & Dobson, C. M. (1998). Amyloid fibril formation by an SH3 domain. *Proceedings of the National Academy of Sciences of the United States of America*, *95*(8), 4224–4228. https://doi.org/10.1073/pnas.95.8.4224

Jackson, M. P., & Hewitt, E. W. (2017). Why are Functional Amyloids Non-Toxic in Humans? *Biomolecules*, *7*(4). https://doi.org/10.3390/biom7040071

Jha, N. N., Kumar, R., Panigrahi, R., Navalkar, A., Ghosh, D., Sahay, S., … Maji, S. K. (2017). Comparison of α-Synuclein Fibril Inhibition by Four Different Amyloid Inhibitors. *ACS Chemical Neuroscience*, *8*(12), 2722–2733. https://doi.org/10.1021/acschemneuro.7b00261

Jimenez-Sanchez, M., Licitra, F., Underwood, B. R., & Rubinsztein, D. C. (2017). Huntington's Disease: Mechanisms of Pathogenesis and Therapeutic Strategies. *Cold Spring Harbor Perspectives in Medicine*, *7*(7). https://doi.org/10.1101/cshperspect.a024240

Jorov, A., Zhorov, B. S., & Yang, D. S. C. (2004). Theoretical study of interaction of winter flounder antifreeze protein with ice. *Protein Science : A Publication of the Protein Society*, *13*(6), 1524–1537. https://doi.org/10.1110/ps.04641104

Karuppagounder, S., Pinto, J., Xu, H., Chen, H., Beal, M., & Gibson, G. (2009). Dietary Supplementation With Resveratrol Reduces Plaque Pathology in a Transgenic Model of Alzheimer's Disease. *Neurochemistry International*, *54*(2). https://doi.org/10.1016/J.NEUINT.2008.10.008

Kawano, S., Inohana, Y., Hashi, Y., & Lin, J.-M. (2013). Analysis of keto-enol tautomers of curcumin by liquid chromatography/mass spectrometry. *Chinese Chemical Letters*, *24*(8), 685–687. https://doi.org/10.1016/J.CCLET.2013.05.006

Ke, D., Wang, X., Yang, Q., Niu, Y., Chai, S., Chen, Z., … Shen, W. (2011). Spectrometric Study on the Interaction of Dodecyltrimethylammonium Bromide with Curcumin. *Langmuir*, *27*(23), 14112–14117. https://doi.org/10.1021/la203592j

Kenward, K. D., Brandle, J., McPherson, J., & Davies, P. L. (1999). Type II fish antifreeze protein accumulation in transgenic tobacco does not confer frost resistance. *Transgenic Research*, *8*(2), 105–117. https://doi.org/10.1023/A:1008886629825

Kim, H. J., Lee, J. H., Hur, Y. B., Lee, C. W., Park, S.-H., & Koo, B.-W. (2017). Marine Antifreeze Proteins: Structure, Function, and Application to Cryopreservation as a Potential Cryoprotectant. *Marine Drugs*, *15*(2). https://doi.org/10.3390/md15020027

Kim, H. J., Shim, H. E., Lee, J. H., Kang, Y.-C., & Hur, Y. B. (2015). Ice-Binding Protein Derived from Glaciozyma Can Improve the Viability of Cryopreserved Mammalian Cells. *Journal of Microbiology and Biotechnology*, *25*(12), 1989–1996. https://doi.org/10.4014/jmb.1507.07041

Knight, C. A., Cheng, C. C., & DeVries, A. L. (1991). Adsorption of alpha-helical antifreeze peptides on specific ice crystal surface planes. *Biophysical Journal*, *59*(2), 409–418. https://doi.org/10.1016/S0006-3495(91)82234-2

Kondo, H., Hanada, Y., Sugimoto, H., Hoshino, T., Garnham, C. P., Davies, P. L., & Tsuda, S. (2012). Ice-binding site of snow mold fungus antifreeze protein deviates from structural regularity and high conservation. *Proceedings of the National Academy of Sciences of the United States of America*, *109*(24), 9360–9365. https://doi.org/10.1073/pnas.1121607109

Koronyo, Y., Salumbides, B. C., Black, K. L., & Koronyo-Hamaoui, M. (2012). Alzheimer's Disease in the Retina: Imaging Retinal Aß Plaques for Early Diagnosis and Therapy Assessment. *Neurodegenerative Diseases*, *10*(1–4), 285–293. https://doi.org/10.1159/000335154

Koushafar, H., Pham, L., Lee, C., & Rubinsky, B. (1997). Chemical adjuvant cryosurgery with antifreeze proteins. *Journal of Surgical Oncology*, *66*(2), 114–121. https://doi.org/10.1002/(SICI)1096-9098(199710)66:2<114::AID-JSO8>3.0.CO;2-G

Kroymann, J. (2011, June). Natural diversity and adaptation in plant secondary metabolism. *Current Opinion in Plant Biology*. https://doi.org/10.1016/j.pbi.2011.03.021

Kunnumakkara, A. B., Bordoloi, D., Padmavathi, G., Monisha, J., Roy, N. K., Prasad, S., & Aggarwal, B. B. (2017). Curcumin, the golden nutraceutical: multitargeting for multiple chronic diseases. *British Journal of Pharmacology*, *174*(11), 1325–1348. https://doi.org/10.1111/bph.13621

Kurien, B. T., Dorri, Y., & Scofield, R. H. (2012). Spicy SDS-PAGE gels: curcumin/turmeric as an environment-friendly protein stain. *Methods in Molecular Biology (Clifton, N.J.)*, *869*, 567–578. https://doi.org/10.1007/978-1-61779-821-4_51

Kurien, B. T., & Scofield, R. H. (2009). Increasing aqueous solubility of curcumin for improving bioavailability. *Trends in Pharmacological Sciences*, *30*(7), 334–335; author reply 335. https://doi.org/10.1016/j.tips.2009.04.005

Kurien, B. T., Singh, A., Matsumoto, H., & Scofield, R. H. (2007). Improving the Solubility and Pharmacological Efficacy of Curcumin by Heat Treatment. *ASSAY and Drug Development Technologies*, *5*(4), 567–576. https://doi.org/10.1089/adt.2007.064

Kyle, R. A. (2001). Amyloidosis: a convoluted story. *British Journal of Haematology*, *114*(3), 529–538. https://doi.org/10.1046/j.1365-2141.2001.02999.x

Laemmli, U. K. (1970). Cleavage of Structural Proteins during the Assembly of the Head of Bacteriophage T4. *Nature*, *227*(5259), 680–685. https://doi.org/10.1038/227680a0

Lee, C., Levin, A., & Branton, D. (1987). Copper staining: A five-minute protein stain for sodium dodecyl sulfate-polyacrylamide gels. *Analytical Biochemistry*, *166*(2), 308–312. https://doi.org/10.1016/0003-2697(87)90579-3

Lee, H. H., Lee, H. J., Kim, H. J., Lee, J. H., Ko, Y., Kim, S. M., … Kim, S. H. (2015). Effects of antifreeze proteins on the vitrification of mouse oocytes: comparison of three different antifreeze proteins. *Human Reproduction (Oxford, England)*, *30*(9), 2110–2119. https://doi.org/10.1093/humrep/dev170

Lee, J. K., Kim, Y. J., Park, K. S., Shin, S. C., Kim, H. J., Song, Y. H., & Park, H. (2011). Molecular and comparative analyses of type IV antifreeze proteins (AFPIVs) from two Antarctic fishes, *Pleuragramma antarcticum* and *Notothenia coriiceps*. *Comparative Biochemistry and Physiology. Part B, Biochemistry & Molecular Biology*, *159*(4), 197–205. https://doi.org/10.1016/j.cbpb.2011.04.006

Lee, J., Kim, S. K., Youm, H. W., Kim, H. J., Lee, J. R., Suh, C. S., & Kim, S. H. (2015). Effects of three different types of antifreeze proteins on mouse ovarian tissue cryopreservation and transplantation. *PloS One*, *10*(5), e0126252. https://doi.org/10.1371/journal.pone.0126252

LeVine, H. (1993). Thioflavine T interaction with synthetic Alzheimer's disease beta-amyloid peptides: detection of amyloid aggregation in solution. *Protein Science : A Publication of the Protein Society*, *2*(3), 404–410. https://doi.org/10.1002/pro.5560020312

LeVine, H. (1999). Quantification of beta-sheet amyloid fibril structures with thioflavin T. *Methods in Enzymology*, *309*, 274–284. https://doi.org/10.1016/s0076-6879(99)09020-5

Li, B., Fooksa, M., Heinze, S., & Meiler, J. (2018). Finding the needle in the haystack: towards solving the protein-folding problem computationally. *Critical Reviews in Biochemistry and Molecular Biology*, *53*(1), 1–28. https://doi.org/10.1080/10409238.2017.1380596

Lindow, S. E., Arny, D. C., & Upper, C. D. (1982). Bacterial ice nucleation: a factor in frost injury to plants. *Plant Physiology*, *70*(4), 1084–1089. https://doi.org/10.1104/pp.70.4.1084

Liu, J.-X., Zhai, Y.-H., & Gui, J.-F. (2009). Molecular characterization and expression pattern of AFPIV during embryogenesis in gibel carp(*Carassiu auratus gibelio*). *Molecular Biology Reports*, *36*(7), 2011–2018. https://doi.org/10.1007/s11033-008-9412-3

Liu, K. N., Lai, C. M., Lee, Y. T., Wang, S. N., Chen, R. P. Y., Jan, J. S., … Wang, S. S. S. (2012). Curcumin's pre-incubation temperature affects its inhibitory potency toward amyloid fibrillation and fibril-induced cytotoxicity of lysozyme. *Biochimica et Biophysica Acta - General Subjects*, *1820*(11), 1774–1786. https://doi.org/10.1016/j.bbagen.2012.07.012

Liu, Yang, Li, Z., Lin, Q., Kosinski, J., Seetharaman, J., Bujnicki, J. M., … Hew, C.-L. (2007). Structure and evolutionary origin of Ca(2+)-dependent herring type II antifreeze protein. *PloS One*, *2*(6), e548. https://doi.org/10.1371/journal.pone.0000548

Liu, Yujia, Cai, Y., Ying, D., Fu, Y., Xiong, Y., & Le, X. (2018). Ovalbumin as a carrier to significantly enhance the aqueous solubility and photostability of curcumin: Interaction and binding mechanism study. *International Journal of Biological Macromolecules*, *116*, 893–900. https://doi.org/10.1016/j.ijbiomac.2018.05.089

Low, W.-K., Lin, Q., & Hew, C. L. (2003). The Role of N and C Termini in the Antifreeze Activity of Winter Flounder ( *Pleuronectes americanus* ) Antifreeze Proteins. *Journal of Biological Chemistry*, *278*(12), 10334–10343. https://doi.org/10.1074/jbc.M300081200

Majhi, A., Rahman, G. M., Panchal, S., & Das, J. (2010). Binding of curcumin and its long chain derivatives to the activator binding domain of novel protein kinase C. *Bioorganic and Medicinal Chemistry*, *18*(4), 1591–1598. https://doi.org/10.1016/j.bmc.2009.12.075

Manolova, Y., Deneva, V., Antonov, L., Drakalska, E., Momekova, D., & Lambov, N. (2014). The effect of the water on the curcumin tautomerism: A quantitative approach. *Spectrochimica Acta Part A: Molecular and Biomolecular Spectroscopy*, *132*, 815–820. https://doi.org/10.1016/J.SAA.2014.05.096

Mao, M.-G., Chen, Y., Liu, R.-T., Lü, H.-Q., Gu, J., Jiang, Z.-Q., & Jiang, J.-L. (2018). Transcriptome from Pacific cod liver reveals types of apolipoproteins and expression analysis of AFP-IV, structural analogue with mammalian ApoA-I. *Comparative Biochemistry and Physiology. Part D, Genomics & Proteomics*, *28*, 204–212. https://doi.org/10.1016/j.cbd.2018.10.001

Marambaud, P., Zhao, H., & Davies, P. (2005). Resveratrol promotes clearance of Alzheimer's disease amyloid-beta peptides. *The Journal of Biological Chemistry*, *280*(45), 37377–37382. https://doi.org/10.1074/jbc.M508246200

Marshall, C. B., Chakrabartty, A., & Davies, P. L. (2005). Hyperactive Antifreeze Protein from Winter Flounder Is a Very Long Rod-like Dimer of α-Helices. *Journal of Biological Chemistry*, *280*(18), 17920–17929. https://doi.org/10.1074/jbc.M500622200

McDonald, D. G., & Milligan, C. L. (1992). *Fish Physiology, Volume XII, Part B, The Cardiovascular System*. (W. S. Hoar, D. J. Randall, & A. . Farrell, Eds.) (XII). Academic Press Inc.

Meister, K., DeVries, A. L., Bakker, H. J., & Drori, R. (2018). Antifreeze Glycoproteins Bind Irreversibly to Ice. *Journal of the American Chemical Society*, *140*(30), 9365–9368. https://doi.org/10.1021/jacs.8b04966

Merril, C. R. (1986). Development and mechanisms of silver stains for Electrophoresis. *Acta Histochemica et Cytochemica*, *19*(5), 655–667. https://doi.org/10.1267/ahc.19.655

Meyer, K., Keil, M., & Naldrett, M. J. (1999). A leucine-rich repeat protein of carrot that exhibits antifreeze activity. *FEBS Letters*, *447*(2–3), 171–178. https://doi.org/10.1016/s0014-5793(99)00280-x

Miao, M., Chan, S. L., Hew, C. L., & Gong, Z. (1998). The skin-type antifreeze protein gene intron of the winter flounder is a ubiquitous enhancer lacking a functional C/EBPalpha binding motif. *FEBS Letters*, *426*(1), 121–125. https://doi.org/10.1016/s0014-5793(98)00327-5

Miao, M. M. (2001). Transcriptional regulation of the antifreeze protein genes in winter flounder. Retrieved from https://tspace.library.utoronto.ca/handle/1807/15606

Middleton, A. J., Marshall, C. B., Faucher, F., Bar-Dolev, M., Braslavsky, I., Campbell, R. L., … Davies, P. L. (2012). Antifreeze Protein from Freeze-Tolerant Grass Has a Beta-Roll Fold with an Irregularly Structured Ice-Binding Site. *Journal of Molecular Biology*, *416*(5), 713–724. https://doi.org/10.1016/j.jmb.2012.01.032

Moussa, Z., Chebl, M., & Patra, D. (2017). Fluorescence of tautomeric forms of curcumin in different pH and biosurfactant rhamnolipids systems: Application towards on-off ratiometric fluorescence temperature sensing. *Journal of Photochemistry and Photobiology B: Biology*, *173*, 307–317. https://doi.org/10.1016/j.jphotobiol.2017.06.011

Mukherjee, A., & Soto, C. (2017, May 1). Prion-like protein aggregates and type 2 diabetes. *Cold Spring Harbor Perspectives in Medicine*. Cold Spring Harbor Laboratory Press. https://doi.org/10.1101/cshperspect.a024315

Muldrew, K., Rewcastle, J., Donnelly, B. J., Saliken, J. C., Liang, S., Goldie, S., … Sandison, G. (2001). Flounder antifreeze peptides increase the efficacy of cryosurgery. *Cryobiology*, *42*(3), 182–189. https://doi.org/10.1006/cryo.2001.2321

Mutsuga, M., Chambers, J. K., Uchida, K., Tei, M., Makibuchi, T., Mizorogi, T., … Nakayama, H. (2012). Binding of curcumin to senile plaques and cerebral amyloid angiopathy in the aged brain of various animals and to neurofibrillary tangles in Alzheimer's brain. *The Journal of Veterinary Medical Science*, *74*(1), 51–57. https://doi.org/10.1292/jvms.11-0307

Naiki, H, Higuchi, K., Hosokawa, M., & Takeda, T. (1989). Fluorometric determination of amyloid fibrils in vitro using the fluorescent dye, thioflavin T1. *Analytical Biochemistry*, *177*(2), 244–249. https://doi.org/10.1016/0003-2697(89)90046-8

Naiki, Hironobu. (2017). Thioflavin T: not an all-rounder, but a trustworthy friend for over 27 years. *Amyloid : The International Journal of Experimental and Clinical Investigation : The Official Journal of the International Society of Amyloidosis*, *24*(sup1), 9. https://doi.org/10.1080/13506129.2017.1278688

Nelson, K. M., Dahlin, J. L., Bisson, J., Graham, J., Pauli, G. F., & Walters, M. A. (2017). The Essential Medicinal Chemistry of Curcumin. *Journal of Medicinal Chemistry*, *60*(5), 1620–1637. https://doi.org/10.1021/acs.jmedchem.6b00975

Ono, K., Takahashi, R., Ikeda, T., & Yamada, M. (2012). Cross-seeding effects of amyloid β-protein and α-synuclein. *Journal of Neurochemistry*, *122*(5), 883–890. https://doi.org/10.1111/j.1471-4159.2012.07847.x

Oppenheimer, A. (1937). Turmeric (curcumin) in biliary diseases. *The Lancet*, *229*(5924), 619–621. https://doi.org/10.1016/S0140-6736(00)98193-5

Oskarsson, M. E., Paulsson, J. F., Schultz, S. W., Ingelsson, M., Westermark, P., & Westermark, G. T. (2015). In vivo seeding and cross-seeding of localized amyloidosis: a molecular link between type 2 diabetes and Alzheimer disease. *The American Journal of Pathology*, *185*(3), 834–846. https://doi.org/10.1016/j.ajpath.2014.11.016

Palhano, F. L., Lee, J., Grimster, N. P., & Kelly, J. W. (2013). Toward the molecular mechanism(s) by which EGCG treatment remodels mature amyloid fibrils. *Journal of the American Chemical Society*, *135*(20), 7503–7510. https://doi.org/10.1021/ja3115696

Pandey, N., Strider, J., Nolan, W. C., Yan, S. X., & Galvin, J. E. (2008). Curcumin inhibits aggregation of α-synuclein. *Acta Neuropathologica*, *115*(4), 479–489. https://doi.org/10.1007/s00401-007-0332-4

Patel, S. N., & Graether, S. P. (2010). Structures and ice-binding faces of the alanine-rich type I antifreeze proteins. *Biochemistry and Cell Biology = Biochimie et Biologie Cellulaire*, *88*(2), 223–229. https://doi.org/10.1139/o09-183

Pertaya, N., Marshall, C. B., DiPrinzio, C. L., Wilen, L., Thomson, E. S., Wettlaufer, J. S., … Braslavsky, I. (2007). Fluorescence microscopy evidence for quasi-permanent attachment of antifreeze proteins to ice surfaces. *Biophysical Journal*, *92*(10), 3663–3673. https://doi.org/10.1529/biophysj.106.096297

Pervin, M., Unno, K., Ohishi, T., Tanabe, H., Miyoshi, N., & Nakamura, Y. (2018). Beneficial Effects of Green Tea Catechins on Neurodegenerative Diseases. *Molecules (Basel, Switzerland)*, *23*(6). https://doi.org/10.3390/molecules23061297

Pham, L., Dahiya, R., & Rubinsky, B. (1999). An in vivo study of antifreeze protein adjuvant cryosurgery. *Cryobiology*, *38*(2), 169–175. https://doi.org/10.1006/cryo.1999.2158

Phan, H. T. T., Samarat, K., Takamur, Y., Azo-Oussou, A. F., Nakazono, Y., & Vestergaard, M. C. (2019). Polyphenols modulate alzheimer's amyloid beta aggregation in a structure-dependent manner. *Nutrients*, *11*(4). https://doi.org/10.3390/nu11040756

Porzoor, A., Alford, B., Hügel, H. M., Grando, D., Caine, J., & Macreadie, I. (2015). Anti-amyloidogenic properties of some phenolic compounds. *Biomolecules*, *5*(2), 505–527. https://doi.org/10.3390/biom5020505

Qiang, W., Yau, W. M., & Tycko, R. (2011). Structural evolution of Iowa mutant β-amyloid fibrils from polymorphic to homogeneous states under repeated seeded growth. *Journal of the American Chemical Society*, *133*(11), 4018–4029. https://doi.org/10.1021/ja109679q

Rabilloud, T., Vuillard, L., Gilly, C., & Lawrence, J.-J. (1994). Silver-staining of proteins in polyacrylamide gels: a general overview. Retrieved from https://hal.archives-ouvertes.fr/hal-00435208

Rath, A., Cunningham, F., & Deber, C. M. (2013). Acrylamide concentration determines the direction and magnitude of helical membrane protein gel shifts. *Proceedings of the National Academy of Sciences of the United States of America*, *110*(39), 15668–15673. https://doi.org/10.1073/pnas.1311305110

Raymond, J A, & DeVries, A. L. (1977). Adsorption inhibition as a mechanism of freezing resistance in polar fishes. *Proceedings of the National Academy of Sciences of the United States of America*, *74*(6), 2589–2593. https://doi.org/10.1073/pnas.74.6.2589

Raymond, James A., Fritsen, C., & Shen, K. (2007). An ice-binding protein from an Antarctic sea ice bacterium. *FEMS Microbiology Ecology*, *61*(2), 214–221. https://doi.org/10.1111/j.1574-6941.2007.00345.x

Raymond, James A., Janech, M. G., & Fritsen, C. H. (2009). Novel ice-binding proteins from a psychrophilic Antarctic alga (*Chlamydomonadaceae*, *Chlorophyceae*). *Journal of Phycology*, *45*(1), 130–136. https://doi.org/10.1111/j.1529-8817.2008.00623.x

Reddy, P. H., Manczak, M., Yin, X., Grady, M. C., Mitchell, A., Tonk, S., … Reddy, A. P. (2018). Protective Effects of Indian Spice Curcumin Against Amyloid-β in Alzheimer's Disease. *Journal of Alzheimer's Disease*, *61*(3), 843–866. https://doi.org/10.3233/JAD-170512

Ren, G., Okerberg, C. K., & Mathews, S. T. (2012). Ultrasensitive Protein Detection and Imaging: Comparison of Lumitein™, ProteoSilver™, SYPRO® Ruby, and Coomassie® Brilliant Blue Gel Stains (pp. 621–632). Humana Press, Totowa, NJ. https://doi.org/10.1007/978-1-61779-821-4_57

Rodrigues, D. F., & Tiedje, J. M. (2008). Coping with our cold planet. *Applied and Environmental Microbiology*, *74*(6), 1677–1686. https://doi.org/10.1128/AEM.02000-07

Rovnyagina, N. R., Sluchanko, N. N., Tikhonova, T. N., Fadeev, V. V, Litskevich, A. Y., Maskevich, A. A., & Shirshin, E. A. (2018). Binding of thioflavin T by albumins: An underestimated role of protein oligomeric heterogeneity. *International Journal of Biological Macromolecules*, *108*, 284–290. https://doi.org/10.1016/j.ijbiomac.2017.12.002

Sahu, A., Kasoju, N., & Bora, U. (2008). Fluorescence study of the curcumin-casein micelle complexation and its application as a drug nanocarrier to cancer cells. *Biomacromolecules*, *9*(10), 2905–2912. https://doi.org/10.1021/bm800683f

Salvadores, N., Shahnawaz, M., Scarpini, E., Tagliavini, F., & Soto, C. (2014). Detection of Misfolded Aβ Oligomers for Sensitive Biochemical Diagnosis of Alzheimer's Disease. *Cell Reports*, *7*(1), 261–268. https://doi.org/10.1016/j.celrep.2014.02.031

Sapan, C. V, Lundblad, R. L., & Price, N. C. (1999). Colorimetric protein assay techniques. *Biotechnology and Applied Biochemistry*, *29 ( Pt 2)*, 99–108. Retrieved from http://www.ncbi.nlm.nih.gov/pubmed/10075906

Scholander, P. F., Flagg, W., Walters, V., & Irving, L. (1953). Climatic Adaptation in Arctic and Tropical Poikilotherms. *Physiological Zoology*, *26*(1), 67–92. https://doi.org/10.1086/physzool.26.1.30152151

Schraufstatter, E., & Bernt, H. (1949). Antibacterial Action of Curcumin and Related Compounds. *Nature*, *164*(4167), 456–457. https://doi.org/10.1038/164456a0

Sharma, R. A., Gescher, A. J., & Steward, W. P. (2005). Curcumin: The story so far. *European Journal of Cancer*, *41*(13), 1955–1968. https://doi.org/10.1016/J.EJCA.2005.05.009

Sharp, K. A. (2011). A peek at ice binding by antifreeze proteins. *Proceedings of the National Academy of Sciences of the United States of America*, *108*(18), 7281–7282. https://doi.org/10.1073/pnas.1104618108

Shen, L., Ji, H., & Zhang, H. (2008). Why Is the C-terminus of Abeta(1-42) More Unfolded Than That of Abeta(1-40)? Clues From Hydrophobic Interaction. *The Journal of Physical Chemistry. B*, *112*(10). https://doi.org/10.1021/JP7108237

Sicheri, F., & Yang, D. S. C. (1995). Ice-binding structure and mechanism of an antifreeze protein from winter flounder. *Nature*, *375*(6530), 427–431. https://doi.org/10.1038/375427a0

Siemer, A. B., & McDermott, A. E. (2008). Solid-State NMR on a Type III Antifreeze Protein in the Presence of Ice. *Journal of the American Chemical Society*, *130*(51), 17394–17399. https://doi.org/10.1021/ja8047893

Silver Stain Protocol. (n.d.). Retrieved August 13, 2019, from Proteomics Resource Center, Rockefeller University. No longer available

Singh, P. K., Kotia, V., Ghosh, D., Mohite, G. M., Kumar, A., & Maji, S. K. (2013). Curcumin modulates α-synuclein aggregation and toxicity. *ACS Chemical Neuroscience*, *4*(3), 393–407. https://doi.org/10.1021/cn3001203

Singh, S., & DeMarco, M. L. (2020). In Vitro Conversion Assays Diagnostic for Neurodegenerative Proteinopathies. *The Journal of Applied Laboratory Medicine*, *5*(1), 142–157. https://doi.org/10.1373/jalm.2019.029801

Sipe, J. D., Benson, M. D., Buxbaum, J. N., Ikeda, S.-I., Merlini, G., Saraiva, M. J. M., & Westermark, P. (2010). Amyloid fibril protein nomenclature: 2010 recommendations from the nomenclature committee of the International Society of Amyloidosis. *Amyloid*, *17*(3–4), 101–104. https://doi.org/10.3109/13506129.2010.526812

Siviero, A., Gallo, E., Maggini, V., Gori, L., Mugelli, A., Firenzuoli, F., & Vannacci, A. (2015). Curcumin, a golden spice with a low bioavailability. *Journal of Herbal Medicine*, *5*(2), 57–70. https://doi.org/10.1016/J.HERMED.2015.03.001

Soto, C., Estrada, L., & Castilla, J. (2006). Amyloids, prions and the inherent infectious nature of misfolded protein aggregates. *Trends in Biochemical Sciences*, *31*(3), 150–155. https://doi.org/10.1016/j.tibs.2006.01.002

Sreerama, N., & Woody, R. W. (2004). Computation and Analysis of Protein Circular Dichroism Spectra. *Methods in Enzymology*, *383*, 318–351. https://doi.org/10.1016/S0076-6879(04)83013-1

Steensma, D. P. (2001). "Congo" Red Out of Africa? *Archives of Pathology & Laboratory Medicine*, *125*(2), 250–252. https://doi.org/10.1043/0003-9985(2001)125<0250:CR>2.0.CO;2

Steinberg, T. H. (2009). Chapter 31 Protein Gel Staining Methods: An Introduction and Overview. *Methods in Enzymology*, *463*, 541–563. https://doi.org/10.1016/S0076-6879(09)63031-7

Steinberg, T. H., Jones, L. J., Haugland, R. P., & Singer, V. L. (1996). SYPRO Orange and SYPRO Red Protein Gel Stains: One-Step Fluorescent Staining of Denaturing Gels for Detection of Nanogram Levels of Protein. *Analytical Biochemistry*, *239*(2), 223–237. https://doi.org/10.1006/ABIO.1996.0319

Sun, T., Lin, F.-H., Campbell, R. L., Allingham, J. S., & Davies, P. L. (2014). An Antifreeze Protein Folds with an Interior Network of More Than 400 Semi-Clathrate Waters. *Science*, *343*(6172), 795–798. https://doi.org/10.1126/science.1247407

Tapal, A., & Tiku, P. K. (2012). Complexation of curcumin with soy protein isolate and its implications on solubility and stability of curcumin. *Food Chemistry*, *130*(4), 960–965. https://doi.org/10.1016/j.foodchem.2011.08.025

Thapa, A., Jett, S. D., & Chi, E. Y. (2016). Curcumin Attenuates Amyloid-β Aggregate Toxicity and Modulates Amyloid-β Aggregation Pathway. *ACS Chemical Neuroscience*, *7*(1), 56–68. https://doi.org/10.1021/acschemneuro.5b00214

Toyama, B. H., & Weissman, J. S. (2011). Amyloid Structure: Conformational Diversity and Consequences. *Annual Review of Biochemistry*, *80*(1), 557–585. https://doi.org/10.1146/annurev-biochem-090908-120656

Trujillo, J., Chirino, Y. I., Molina-Jijón, E., Andérica-Romero, A. C., Tapia, E., & Pedraza-Chaverrí, J. (2013). Renoprotective effect of the antioxidant curcumin: Recent findings. *Redox Biology*, *1*(1), 448–456. https://doi.org/10.1016/j.redox.2013.09.003

Urbańczyk, M., Góra, J., Latajka, R., & Sewald, N. (2017). Antifreeze glycopeptides: from structure and activity studies to current approaches in chemical synthesis. *Amino Acids*, *49*(2), 209–222. https://doi.org/10.1007/s00726-016-2368-z

Vassar, P. S., & Culling, C. F. (1959). Fluorescent stains, with special reference to amyloid and connective tissues. *Archives of Pathology*, *68*, 487–498. Retrieved from http://www.ncbi.nlm.nih.gov/pubmed/13841452

Velander, P., Wu, L., Henderson, F., Zhang, S., Bevan, D. R., & Xu, B. (2017, September 1). Natural product-based amyloid inhibitors. *Biochemical Pharmacology*. Elsevier Inc. https://doi.org/10.1016/j.bcp.2017.04.004

Venketesh, S., & Dayananda, C. (2008). Properties, potentials, and prospects of antifreeze proteins. *Critical Reviews in Biotechnology*, *28*(1), 57–82. https://doi.org/10.1080/07388550801891152

Waddell, W. J. (1956). A simple ultraviolet spectrophotometric method for the determination of protein. *The Journal of Laboratory and Clinical Medicine*, *48*(2), 311–314. Retrieved from http://www.ncbi.nlm.nih.gov/pubmed/13346201

Wang, T., Zhu, Q., Yang, X., Layne, J. R., & Devries, A. L. (1994). Antifreeze Glycoproteins from Antarctic Notothenioid Fishes Fail to Protect the Rat Cardiac Explant during Hypothermic and Freezing Preservation. *Cryobiology*, *31*(2), 185–192. https://doi.org/10.1006/CRYO.1994.1022

Wen, D., & Laursen, R. A. (1993). Structure-function relationships in an antifreeze polypeptide. The role of charged amino acids. *The Journal of Biological Chemistry*, *268*(22), 16396–16400. Retrieved from http://www.ncbi.nlm.nih.gov/pubmed/8344924

Westermark, P., Andersson, A., & Westermark, G. T. (2011). Islet Amyloid Polypeptide, Islet Amyloid, and Diabetes Mellitus. *Physiological Reviews*, *91*(3), 795–826. https://doi.org/10.1152/physrev.00042.2009

Wolf, P. (1983). A critical reappraisal of Waddell's technique for ultraviolet spectrophotometric protein estimation. *Analytical Biochemistry*, *129*(1), 145–155. https://doi.org/10.1016/0003-2697(83)90062-3

Worrall, D., Elias, L., Ashford, D., Smallwood, M., Sidebottom, C., Lillford, P., … Bowles, D. (1998). A carrot leucine-rich-repeat protein that inhibits ice recrystallization. *Science (New York, N.Y.)*, *282*(5386), 115–117. https://doi.org/10.1126/science.282.5386.115

Xiao, Q., Xia, J.-H., Zhang, X.-J., Li, Z., Wang, Y., Zhou, L., & Gui, J.-F. (2014). Type-IV antifreeze proteins are essential for epiboly and convergence in gastrulation of zebrafish embryos. *International Journal of Biological Sciences*, *10*(7), 715–732. https://doi.org/10.7150/ijbs.9126

Xue, W.-F., Homans, S. W., & Radford, S. E. (2009). Amyloid fibril length distribution quantified by atomic force microscopy single-particle image analysis. *Protein Engineering, Design & Selection : PEDS*, *22*(8), 489–496. https://doi.org/10.1093/protein/gzp026

Yakupova, E. I., Bobyleva, L. G., Vikhlyantsev, I. M., & Bobylev, A. G. (2019). Congo Red and amyloids: history and relationship. *Bioscience Reports*, *39*(1). https://doi.org/10.1042/BSR20181415

Yam, A. Y., Wang, X., Gao, C. M., Connolly, M. D., Zuckermann, R. N., Bleu, T., … Salisbury, C. M. (2011). A universal method for detection of amyloidogenic misfolded proteins. *Biochemistry*, *50*(20), 4322–4329. https://doi.org/10.1021/bi200215j

Yamashita, Y., Miura, R., Takemoto, Y., Tsuda, S., Kawahara, H., & Obata, H. (2003). Type II Antifreeze Protein from a Mid-latitude Freshwater Fish, Japanese Smelt ( *Hypomesus nipponensis* ). *Bioscience, Biotechnology, and Biochemistry*, *67*(3), 461–466. https://doi.org/10.1271/bbb.67.461

Yang, D. S. C., Sax, M., Chakrabartty, A., & Hew, C. L. (1988). Crystal structure of an antifreeze polypeptide and its mechanistic implications. *Nature*, *333*(6170), 232–237. https://doi.org/10.1038/333232a0

Yang, Daniel S.C., Je Chung, Y., Chen, P., Rose, J. P., & Hew, C. L. (1986). Single crystals of a winter flounder antifreeze polypeptide. *Journal of Molecular Biology*, *189*(4), 725. https://doi.org/10.1016/0022-2836(86)90504-8

Yang, F., Lim, G. P., Begum, A. N., Ubeda, O. J., Simmons, M. R., Ambegaokar, S. S., … Cole, G. M. (2005). Curcumin Inhibits Formation of Amyloid β Oligomers and Fibrils, Binds Plaques, and Reduces Amyloid *in Vivo*. *Journal of Biological Chemistry*, *280*(7), 5892–5901. https://doi.org/10.1074/jbc.M404751200

Yang, T., Yang, H., Fan, Y., Li, B., & Hou, H. (2018). Interactions of quercetin, curcumin, epigallocatechin gallate and folic acid with gelatin. *International Journal of Biological Macromolecules*, *118*, 124–131. https://doi.org/10.1016/j.ijbiomac.2018.06.058

Yeh, C.-M., Kao, B.-Y., & Peng, H.-J. (2009). Production of a Recombinant Type 1 Antifreeze Protein Analogue by *L . lactis* and Its Applications on Frozen Meat and Frozen Dough. *Journal of Agricultural and Food Chemistry*, *57*(14), 6216–6223. https://doi.org/10.1021/jf900924f

Yeh, Y., & Feeney, R. E. (1996). Antifreeze Proteins: Structures and Mechanisms of Function. *Chemical Reviews*, *96*(2), 601–618. Retrieved from http://www.ncbi.nlm.nih.gov/pubmed/11848766

Yu, S. O., Brown, A., Middleton, A. J., Tomczak, M. M., Walker, V. K., & Davies, P. L. (2010). Ice restructuring inhibition activities in antifreeze proteins with distinct differences in thermal hysteresis. *Cryobiology*, *61*(3), 327–334. https://doi.org/10.1016/J.CRYOBIOL.2010.10.158

Zhang, M., Hu, R., Chen, H., Chang, Y., Ma, J., Liang, G., … Zheng, J. (2015). Polymorphic cross-seeding amyloid assemblies of amyloid-β and human islet amyloid polypeptide. *Physical Chemistry Chemical Physics : PCCP*, *17*(35), 23245–23256. https://doi.org/10.1039/c5cp03329b

Zhang, W., & Laursen, R. A. (1998). Structure-function relationships in a type I antifreeze polypeptide. The role of threonine methyl and hydroxyl groups in antifreeze activity. *The Journal of Biological Chemistry*, *273*(52), 34806–34812. https://doi.org/10.1074/jbc.273.52.34806

Zhao, Z., Deng, G., Lui, Q., & Laursen, R. A. (1998). Cloning and sequencing of cDNA encoding the LS-12 antifreeze protein in the longhorn sculpin, *Myoxocephalus octodecimspinosis*. *Biochimica et Biophysica Acta (BBA) - Protein Structure and Molecular Enzymology*, *1382*(2), 177–180. https://doi.org/10.1016/S0167-4838(97)00197-0

Ziegler, C. M., Zacharias, J. P., & Frisk, M. G. (2019). Migration diversity, spawning behavior, and habitat utilization of winter flounder. *Canadian Journal of Fisheries and Aquatic Sciences*, *76*(9), 1503–1514. https://doi.org/10.1139/cjfas-2018-0053